THERMOECONOMIC ANALYSIS OF COMBINED CYCLE POWER PLANTS

2023
MASTER THESIS
MECHANICAL ENGINEERING

Bashar Mohameed MAJEED

Thesis Advisor
Assist. Prof. Dr. Mutlu TEKIR

THERMOECONOMIC ANALYSIS OF COMBINED CYCLE POWER PLANTS

Bashar Mohameed MAJEED

Thesis Advisor
Assist. Prof. Dr. Mutlu TEKIR

T.C.
Karabuk University
Institute of Graduate Programs
Department of Mechanical Engineering

Prepared as
Master Thesis

KARABUK
December 2023

I certify that in my opinion the thesis submitted by Bashar Mohameed MAJEED titled "THERMOECONOMIC ANALYSIS OF COMBINED CYCLE POWER PLANTS" is fully adequate in scope and in quality as a thesis for the degree of Masters of Science.

Assist. Prof. Dr. Mutlu TEKIR .....

Thesis Advisor, Department of Mechanical Engineering

This thesis is accepted by the examining committee with a unanimous vote in the Department of Mechanical Engineering as a Master Degree thesis. 1/12/2023.

Examining Committee Members (Institutions)	Signature
Chairman : Prof. Dr. Kamil ARSLAN (KBU)	.....
Member : Assist. Prof. Dr. Mehmet GÜRDAL (KAU)	.....
Member : Assist. Prof. Dr. Mutlu TEKIR (KBU)	.....

The degree of Master of Science by the thesis submitted is approved by the Administrative Board of the Institute of Graduate Programs, Karabuk University.

Assoc. Prof. Dr. Zeynep ÖZCAN .....

Director of the Institute of Graduate Programs

"I declare that all the information within this thesis has been gathered and presented in accordance with academic regulations and ethical principles and I have according to the requirements of these regulations and principles cited all those which do not originate in this work as well."

Bashar Mohameed MAJEED

ABSTRACT

M. Sc. Thesis

THERMOECONOMIC ANALYSIS OF COMBINED CYCLE POWER PLANTS

Bashar Mohameed MAJEED

T.C.
Karabuk University
Institute of Graduate Programs
Department of Mechanical Engineering

Thesis Advisor:
Assist. Prof. Dr. Mutlu TEKIR
December 2023, 112 Pages

Integration of several power production technologies has shown promise in the search for effective and sustainable energy solutions. In this work, a unique power plant layout with three organic Rankine cycle (ORC) units and a Brayton cycle (GTC) is investigated. Utilizing a variety of heat sources and improving energy conversion efficiency are the goals of integrating these cycles. This study examines the performance analysis of the combined power plant via meticulous simulation. To clarify the complex interactions between the ORC units and the Brayton cycle, the simulation makes use of sophisticated thermodynamic models and fluid dynamics simulations. In Brayton cycle the gas turbine works by the energy generated by the burned fuel and this burned fuel will generate heat. This heat will be useful for boiled the water in Rankine cycle and generate the steam and generate the electricity. This combined cycle is simulated by software program energy equation solver (EES).

Carefully considered is the impact of altering ambient conditions, pressure ratios, and turbine and compressor efficiency. the models' findings highlight the complex interaction between the cycles' efficiencies, possibilities for heat recovery, and overall efficiency of energy conversion. Energy economic analysis of the gas turbine system is a combustion system capable of generating a high amount of heat that can be used in more than one organic Rankine cycle to obtain the greatest thermal efficiency. the interplay of the ORC units and waste heat recovery from the exhaust of the gas turbine shows a synergy that improves energy extraction and conversion. in order to find the best operating circumstances, performance of the system and component efficiency are compared. generating the largest amount of electrical energy through the combine power plane, where the originality lies in making great use of the heat generated from the exhaust of the system. the gas turbine. The knowledge base on combined power cycle topologies and their potential to sharply increase energy efficiency is being added to by this research. The results highlight how crucial it is to choose appropriate operating settings and maximize component efficiencies in order to get the maximum degree of overall system performance. The findings from this simulation-based analysis provide insightful advice for creating creative and sustainable energy systems that take use of the synergies between diverse power production technologies as the world's energy needs continue to change. The results show the entry temperature significantly impacts a system's efficiency and exergy, with the worst case being 51°C with 38.5% energy efficiency and the best being 15°C with 40.01% efficiency. It also affects cycle occupancy, Brayton cycle occupancy, and electricity costs, with the worst case being 51℃ and the best being 15℃. The pressure ratio also affects efficiency, with high-pressure ratios resulting higher efficiency. The cycle work net also affects the pressure ratio, with high-pressure ratios reducing total work and affecting Brayton cycle work. Compressor efficiency significantly impacts a system's overall efficiency, with the worst case being 70% with 35.5% energy efficiency. The best efficiency is achieved at 90%, with 41% exergy. The worst work is at 70%, with total work reaching 45 kJ. Electric energy costs increase with compressor efficiency, with the worst case at 90% and the best at 75%. The temperature of exhaust significantly impacts system efficiency, with 300 ℃ exhaust values resulting in 39.65% energy efficiency. The best efficiency is achieved at 210 ℃, with an exergy of 38.3%. The cycle work net and electrical energy cost also affect efficiency.

Key Words : Thermodynamic analysis,combined cycle,Brayton cycle
Science Code : 91436

ÖZET

Yüksek Lisans Tezi

KOMBİNE ÇEVRİM ENERJİ SANTRALLERİNİN TERMOEKONOMİK ANALİZİ

Bashar Mohameed MAJEED

Karabük Üniversitesi
Lisansüstü Eğitim Enstitüsü
Makine Mühendisliği Anabilim Dalı

Tez Danışmanı:
Dr. Öğr. Üyesi Mutlu TEKIR
Aralık 2023, 112 sayfa

Çeşitli enerji üretim teknolojilerinin entegrasyonu, etkili ve sürdürülebilir enerji çözümleri arayışında umut vaat ediyor. Bu çalışmada, üç Organik Rankine Çevrimi (ORC) ünitesi ve bir Gaz Türbin Çevrimi (GTC) içeren benzersiz bir enerji santrali yerleşimi incelenmiştir. Çeşitli ısı kaynaklarının kullanılması ve enerji dönüşüm verimliliğinin arttırılması, bu döngülerin entegre edilmesinin hedefleridir. Bu çalışma, kombine enerji santralinin performans analizini titiz bir simülasyon yoluyla incelemektedir. ORC birimleri ile gaz türbini çevrimi arasındaki karmaşık etkileşimleri açıklığa kavuşturmak için simülasyon, gelişmiş termodinamik modellerden ve akışkanlar dinamiği simülasyonlarından yararlanır. Değişen ortam koşullarının, basınç oranlarının ve türbin ve kompresör verimliliğinin etkisi dikkatle değerlendirilmektedir. Modellerin bulguları, çevrimlerin verimliliği, ısı geri kazanımı olanakları ve enerji dönüşümünün genel verimliliği arasındaki karmaşık etkileşimi vurgulamaktadır. ORC ünitelerinin etkileşimi ve gaz türbininin egzozundan atık ısı

geri kazanımı, enerji çıkarımını ve dönüşümünü geliştiren bir sinerji ortaya koyuyor. En iyi çalışma koşullarını bulmak için sistemin performansı ve bileşen verimliliği karşılaştırılır. Bu araştırma, birleşik güç döngüsü topolojileri ve bunların enerji verimliliğini keskin bir şekilde artırma potansiyeline ilişkin bilgi tabanına eklenmektedir. Sonuçlar, maksimum düzeyde genel sistem performansı elde etmek için uygun işletim koşullarını seçmenin ve bileşen verimliliğini en üst düzeye çıkarmanın ne kadar önemli olduğunu vurgulamaktadır. Bu simülasyona dayalı analizden elde edilen bulgular, dünyanın enerji ihtiyaçları değişmeye devam ederken, çeşitli enerji üretim teknolojileri arasındaki sinerjiden yararlanan yaratıcı ve sürdürülebilir enerji sistemleri oluşturmaya yönelik aydınlatıcı tavsiyeler sağlıyor. Sonuçlar, giriş sıcaklığının sistemin verimliliğini ve ekserjisini önemli ölçüde etkilediğini, en kötü durumun %38,5 enerji verimliliğiyle 51°C ve en iyi durumun %40,01 verimlilikle 15°C giriş sıcaklıklarında olduğunu gösteriyor. Aynı zamanda çevrim doluluğunu, gaz türbini çevriminin doluluğunu ve elektrik maliyetlerini de etkiler; en kötü durum 51°C ve en iyi durum 15°C'dir. Basınç oranı aynı zamanda verimliliği etkiler; yüksek basınç oranları daha yüksek verimlilik. Çevrim iş ağı aynı zamanda basınç oranını da etkiler; yüksek basınç oranları toplam işi azaltır ve gaz türbini çevrim işini etkiler. Kompresör verimliliği sistemin genel verimliliğini önemli ölçüde etkiler; en kötü durum %70 ekserji ve %35,5 enerji verimliliğidir. En iyi verim %41 ekserji ile %90'da elde edilir. En kötü iş %70'tir ve toplam iş 45 kJ'ye ulaşır. Elektrik enerjisi maliyetleri kompresör verimliliği arttıkça artar; en kötü durum %90, en iyi durum ise %75'tir. Egzoz sıcaklığı sistem verimliliğini önemli ölçüde etkiler; 300°C egzoz değerleri %39,65 enerji verimliliği sağlar. En iyi verim 210°C'de %38,3 ekserjiyle elde edilir. Çevrim iş ağı ve elektrik enerjisi maliyeti de verimliliği etkiler.

Anahtar Kelime : Termodinamik analiz, kombine çevrim, Brayton çevrimi

Bilim Kodu : 91436

ACKNOWLEDGMENT

I want to express my sincere gratitude to my thesis advisor, Dr. Mutlu TEKIR, for his unwavering support, guidance, and encouragement throughout my research.

I would also like to thank my thesis committee members for their insightful feedback and helpful suggestions. Their expertise and constructive criticism have been instrumental in shaping my research.

I want to thank my family, particularly my parents, for their unwavering love and support. Their encouragement and belief in me have been a constant source of strength and inspiration.

CONTENTS

Page

Page

Page

LIST OF FIGURES

Page

Page

LIST OF TABLES

Page

SYMBOLS AND ABBREVITIONS INDEX

SYMBOL

$\dot{E}$: Exergy flows

F_{AC} : Exergy efficiency Fuel.

h_{in} : Specific enthalpy per the mass entering the system

h_{out} : Specific enthalpy per mass leaving the system

I : interest rate (consider to be 10%)

$\dot{m}_{in}$: Total mass flow entering per unit time

$\dot{m}_{out}$: Total mass flow exiting per unit time

N : lifetime of the system

P : Pump

P_{AC} : Exergy efficiency Product

PEC : equipment's purchase cost in US dollar

s : Specific entropy of the mass emanating from the open system

s_0 : Specific entropy of the mass entering the open system

T_0 : Boundary temperature between the open system and the environment

Q : Heat transfer per unit time

$\dot{\mathrm{W}}$: Work done by the control volume per unit time

$\dot{Z}$: Cost performance

φ : maintenance factor

ψ : Specific exergy

ABBREVITIONS

AC : Air compressor

BC : Brayton cycle

CC : Combustion chamber

CON : Condenser

CRF : Capital Recovery Factor

EES : Engineering equation solver

GSO CC : Gas steam organic combined cycle

GT : Gas turbine

HE : Heat exchanger

HRB : Heat recovery boiler

HRSG : Heat recovery steam generation

ORC : Organic rankine cycle

ORT : Organic rankine turbine

RC : Rankine cycle

ST : Steam turbine

PART 1

INTRODUCTION

1.1. BACKGROUND

The greater part of modern cycle utilizes a ton of nuclear power by consuming petroleum product to deliver steam or intensity for the reason. After the cycle, heat is dismissed to the encompassing as waste. This waste intensity can be switched over completely to valuable refrigeration by utilizing an intensity worked refrigeration framework, for example, an ingestion refrigeration cycle [1]. Power bought from service organizations for ordinary fume pressure coolers can be diminished [2]. The utilization of intensity worked refrigeration frameworks assist with lessening issues connected with worldwide climate, for example, the alleged nursery impact from CO_2 emanation from the ignition of petroleum derivatives in utility power plants [2]. One more distinction between retention frameworks and ordinary fume pressure frameworks is the functioning liquid utilized. Most fume pressure frameworks regularly use chlorofluorocarbon refrigerants (CFCs), due to their thermos actual properties. It is through the confined utilization of CFCs, because of exhaustion of the ozone layer that will make ingestion frameworks more unmistakable [3,4] Notwithstanding, despite the fact that assimilation frameworks appear to give many benefits, fume pressure frameworks actually rule all market areas[5] to advance the utilization of ingestion frameworks, further advancement is expected to work on their exhibition and diminish cost[6]. To advance the utilization of ingestion frameworks, further advancement is expected to work on their exhibition and diminish cost.

Figure 1.1. CO_2 Emissions from power station [6].

As a choice to warm produced from power plants sun-oriented energy can be utilized in urbanized local area [7]. Be that as it may, for provincial networks in emerging nations it is the best wellspring of energy. There are a few significant purposes behind considering sunlight-based energy as an energy asset to address the issues of non-industrial nations [8].

- To start with, the greater part of the nations called creating are in or neighboring the jungles and have great sun powered radiation accessible.
- Besides, energy is a basic need of these nations yet they don't have broadly conveyed promptly accessible supplies of customary energy assets.
- Thirdly, the vast majority of the non-industrial nations are portrayed by dry environments, scattered and blocked off populaces and an absence of speculation capital and are in this manner confronted with basically insuperable impediments to the arrangement of energy by regular means, for instance, by zap. As opposed to this sun-based energy is promptly accessible and is as of now circulated to the likely clients.

- Fourthly, in view of the diffuse idea of sun powered energy the advancements all around the world have been in more modest units, which fit into the example of rustic financial aspects [9,10].

1.2. STEAM POWER

Coal is frequently used to fuel steam power plants, which are widely employed for electricity generation worldwide [11]. Even if there is currently enough coal in the globe to last for about 200 years, the innovation that is largely used to produce power from coal today has a significant detrimental impact on the environment [12]. In order to optimize the use of coal in power generation processes, efforts are often made to improve the efficiency and performance of current facilities through modifications and retrofits, as well as to promote advanced coal use [13].

Many electricity producing utilities are currently attempting to increase the productivity (or intensity rate) at their warm electric producing stations, many of which are over 25 years old. A couple percent increase in intensity rate is often attractive since it is thought that the costs and complexity of these interventions may be less expensive than other more expensive options [14].

Figure 1.2. Steam power plants [14].

1.2.1. Working Mechanism

A steam power plant's operating principle entails the use of steam to transform the thermal energy released during the burning of a fuel source into mechanical energy. For a variety of industrial activities and the production of electricity, steam power plants have been extensively used. here is a brief explanation of how a steam power plant function:

1. fuel combustion: In a combustion chamber, a fuel source, such as coal, natural gas, or oil, is burned to start the process. High-temperature gases are produced during this combustion, which releases thermal energy [15].
2. boiler: In a boiler, water is heated using high-temperature gases from the combustion chamber. A crucial part of the process by which heat energy is transmitted from the hot gases to the water is the boiler. High-pressure steam is produced from the heated water [15].
3. steam turbine: A steam turbine receives the high-pressure steam produced by the boiler. The steam turbine has several stages, each of which has a set of blades. High-pressure steam expands and loses pressure while supplying energy to the turbine blades as it passes over them. The turbine's rotor starts to turn as a result [16].
4. mechanical work: The mechanical work produced by the turbine rotor's revolution is normally employed to turn a generator. The mass flow rate of steam and the pressure drop across the turbine both affect how much mechanical effort is generated [17].
5. electrical generation: The generator, which is coupled to the turbine rotor, transforms mechanical energy into electrical energy. This is accomplished via the principles of electromagnetic induction, in which the spinning of the rotor produces a magnetic field that induces an electrical current in wire coils [17].
6. condenser: Low-pressure steam leaves the turbine and enters the condenser. By transferring heat to a cooling medium, frequently water from a cooling tower or a natural body of water, the steam is condensed back into water in the condenser. For the cycle to remain efficient, this procedure is essential [18].

7. feed water pump: The cycle is restarted by reheating the condensed water that was removed from the condenser and pumping it back into the boiler [15].
8. cooling system: A cooling system is employed to release the extra heat absorbed in the condenser. This could involve cooling ponds, towers, or some other kind of cooling system [18].

The Rankine Cycle, which is the cornerstone of steam power plants and a well-known thermodynamic process for converting heat into mechanical and electrical energy, is as previously explained.

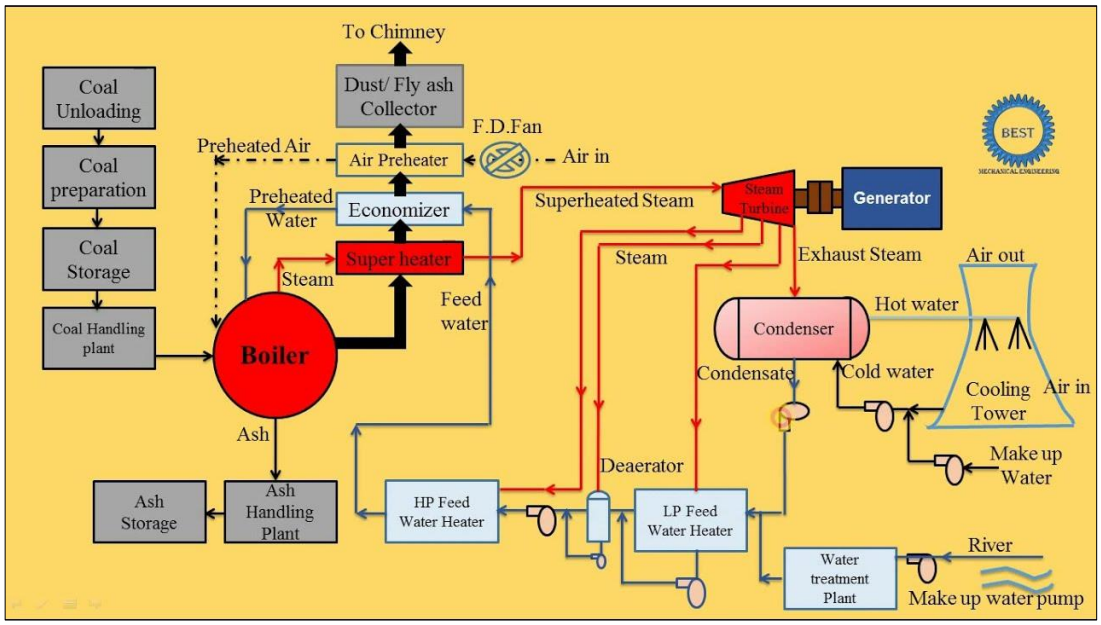

Figure 1.3. Layout of modern steam power plant [18].

1.2.2. Components

The major components of this power plant are boiler, steam turbine, condenser and feed water heater and super heater.

1.2.3. Boiler

An essential part of a steam power plant where water is boiled to produce high-pressure steam is the boiler. To ensure effective and secure boiler operation, several parts

cooperate. The combustion chamber of the furnace is where fuel is burned to produce heat energy. It offers the high-temperature gases necessary to heat the water in the boiler. Water walls are a ring of water-filled tubes or pipes that surround the furnace. They take in heat from the furnace gases, causing the water to warm up and produce steam. The high-temperature gases leaving the furnace pass through a series of tubes or coils that make up the super heater. Its goal is to raise the temperature and energy content of the steam by heating it further, past the point of saturation. The water is heated before it enters the boiler using an additional set of tubes or coils called an economizer. It increases overall thermal efficiency by transferring heat from the flue gas leaving the boiler to the incoming feed water. At the top of the boiler is a cylindrical container called the steam drum. Before the steam enters the super heater, it acts as a reservoir for the produced steam and assists in removing moisture from the steam. The boiler's water is continuously pumped through this system, which also consists of pipes and pumps. In order to avoid overheating and causing damage to the boiler tubes, it maintains the proper water level and circulation rate. Burners are in charge of the furnace's-controlled fuel combustion. They are made to offer stable, effective combustion while reducing emissions. In order to keep the boiler working in a safe manner, safety valves are essential. To avoid circumstances when there is too much pressure that could result in boiler explosions; they release the extra steam pressure. This pump is in charge of supplying water to the boiler and bridging the pressure gap between the boiler pressure and the feed water pressure. High-pressure steam exits the boiler through the steam outlet and is sent to the steam turbine to produce electricity. In a steam power plant, these parts work in unison to effectively transfer heat from the combustion process to water, resulting in the production of high-pressure steam that powers the steam turbine and, ultimately, generates electricity [19].

Figure 1.4. Boiler in steam power plants [19].

1.2.4. Steam Turbine

An essential part of a steam power plant is the steam turbine, which transforms the high-pressure steam produced in the boiler into mechanical energy. This mechanical energy can then be utilized to power a generator to produce electricity or carry out other mechanical tasks. The Rankine Cycle, a thermodynamic cycle that describes the transformation of heat into mechanical work using steam as the working fluid, underlies the operation of a steam turbine. Each stage of a steam turbine's design consists of a stationary nozzle and revolving blades or buckets. These processes expand the high-pressure steam, which rotates the rotor and drives a generator to generate energy. The core-revolving element of a steam turbine is the rotor. It transforms the kinetic energy of the steam into mechanical work and is connected to the generator. Depending on its capacity and design, steam turbines can have one or several rotors. The rotor is equipped with blades or buckets. They are made to effectively capture energy from the fast steam flow. A steam turbine normally has two different types of blades: stationary blades (nozzles) and moving blades (buckets). While the moving blades absorb energy from the steam as it flows over them, the fixed

blades direct the steam flow and regulate its direction. The turbine's stationary nozzles speed up and direct the flow of high-pressure steam onto the spinning blades. They are essential in regulating steam expansion and ensuring effective energy conversion. Steam leaves the turbine as low-pressure exhaust steam after entering the turbine through the steam inlet. In a closed-loop system, the exhaust steam is then condensed back into water in the condenser and returned to the boiler. The design of the blades and nozzles, the steam pressure and temperature, as well as the particular application, all affect how efficient a steam turbine is. In order to operate as efficiently as possible under those conditions, steam turbines are optimized for those settings [19].

Figure 1.5. Steam turbine [19].

1.2.4.1. Condenser

An essential part of a steam power plant is the condenser, which is in charge of condensing steam from the steam turbine's exhaust back into water. This procedure increases the power plant's overall efficiency and enables the boiler to reuse water effectively. At the steam turbine's exit, the condenser is normally a sizable, heat-exchanger-like component. Its main job is to turn the exhaust steam from the turbine into liquid water by reducing the pressure and temperature of the steam. The closed-loop cycle is subsequently finished by returning the condensed water to the boiler for warming [15].

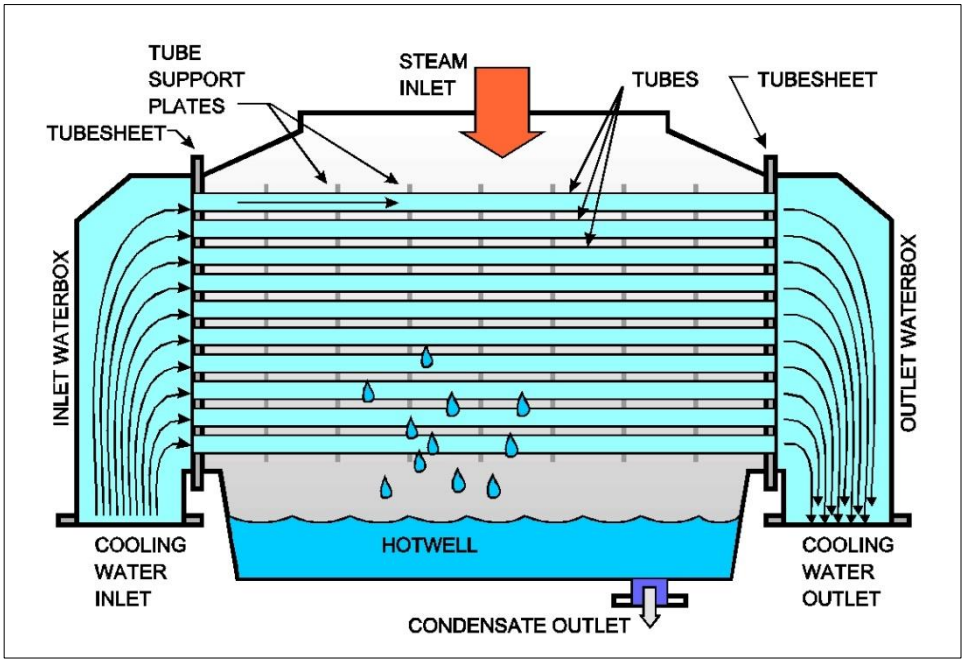

Figure 1.6. Condenser in steam power plants [15].

1.2.4.2. Feed Water Heater

By preheating the water before it enters the boiler, feed water heaters, which are significant parts of steam power plants, significantly increase the plant's total efficiency. A feed water heater is a type of heat exchanger that is commonly installed in a steam power plant's feed water system. The cold water (feed water) that is provided to the boiler is preheated as its main job. Feed water heaters aid in lowering the amount of heat energy needed to turn feed water into steam by utilizing the leftover heat from the exhaust steam leaving the turbine, increasing the thermal efficiency of the power plant [15].

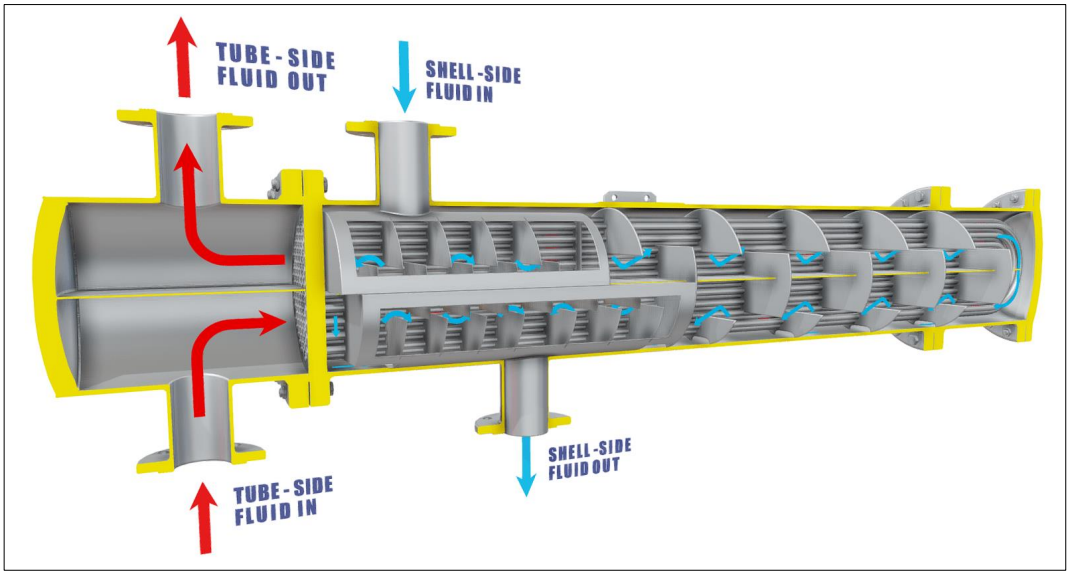

Figure 1.7. Feed water heater in steam power plants [15].

1.2.4.3. Super Heater

In order to raise the temperature of saturated steam over its saturation point, the super heater, a crucial part of a steam power plant, must be used. The steam turbine then receives this superheated steam for improved performance and efficiency. The Super heater is usually made up of a number of coils or tubes and is positioned in the steam stream following the boiler. Its major job is to maintain pressure while increasing the temperature of the steam to a point above its saturation temperature. By providing higher-temperature steam for expansion, superheating the steam increases the steam turbine's efficiency and work output [19].

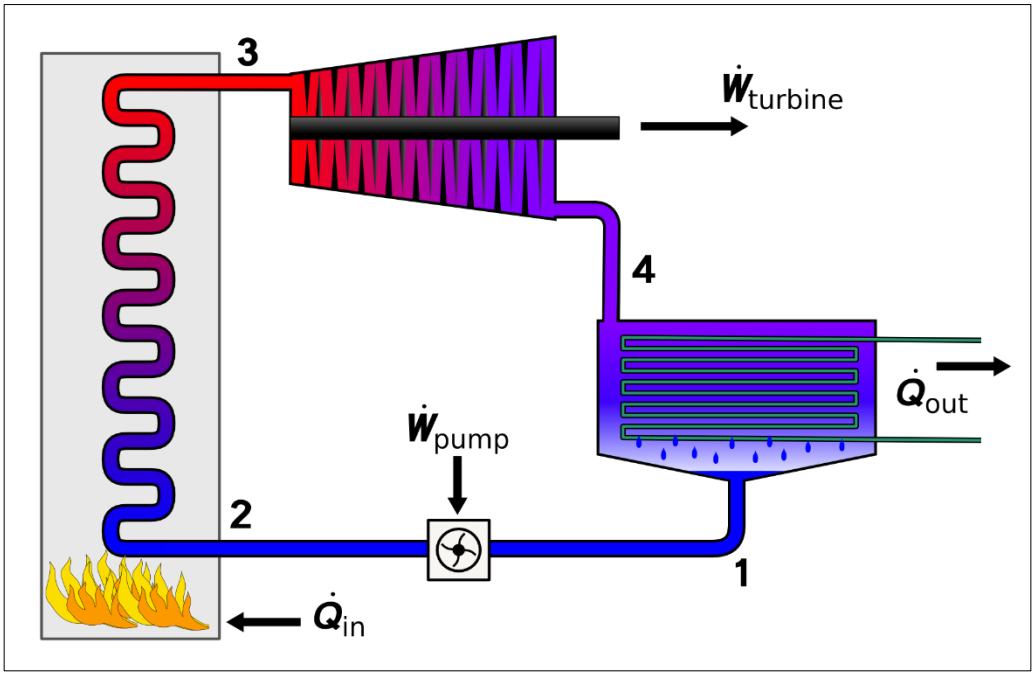

Figure 1.8. Super heater in steam power plants [19].

1.3. COMBINED CYCLE POWER PLANT

In order to increase total efficiency and energy production, a combined cycle power plant combines two different thermodynamic cycles, namely the Brayton Cycle (a gas turbine) and the Rankine Cycle (a steam turbine). The main energy source in a combined cycle power plant is often natural gas or another clean-burning fuel. There are two primary parts to the plant; the first part is a gas turbine, also referred to as a combustion turbine. It uses the Brayton cycle, which involves compressing air, combining it with fuel, and burning the resulting mixture to create high-pressure, high-temperature gases. Through the expansion of these gases in a turbine, mechanical energy is produced, which powers a generator to provide electricity. The second component is a steam turbine that uses the Rankine Cycle to run. It generates steam using the gas turbine's exhaust heat. After passing through a steam turbine, where it expands and produces more mechanical power, the steam is then used to power a second generator. Compressor, combustion chamber, and turbine are examples of parts found in a gas turbine. The heat recovery steam generator (HRSG) harnesses waste heat from the gas turbine's exhaust gases to create high-pressure steam. The steam turbine is in charge of turning the high-pressure steam's thermal energy into mechanical work. To turn mechanical energy into electricity, generators are connected

to both the gas turbine and the steam turbine. to remove extra heat from the steam turbine's condenser, a cooling system is often used. Efficiency and benefits: when compared to traditional power plants, combined cycle power plants are noted for their great efficiency. Combination cycle plants can achieve thermal efficiencies of up to 60% by turning the gas turbine's waste heat into steam and additional electricity, making them more economical and environmentally benign [20].

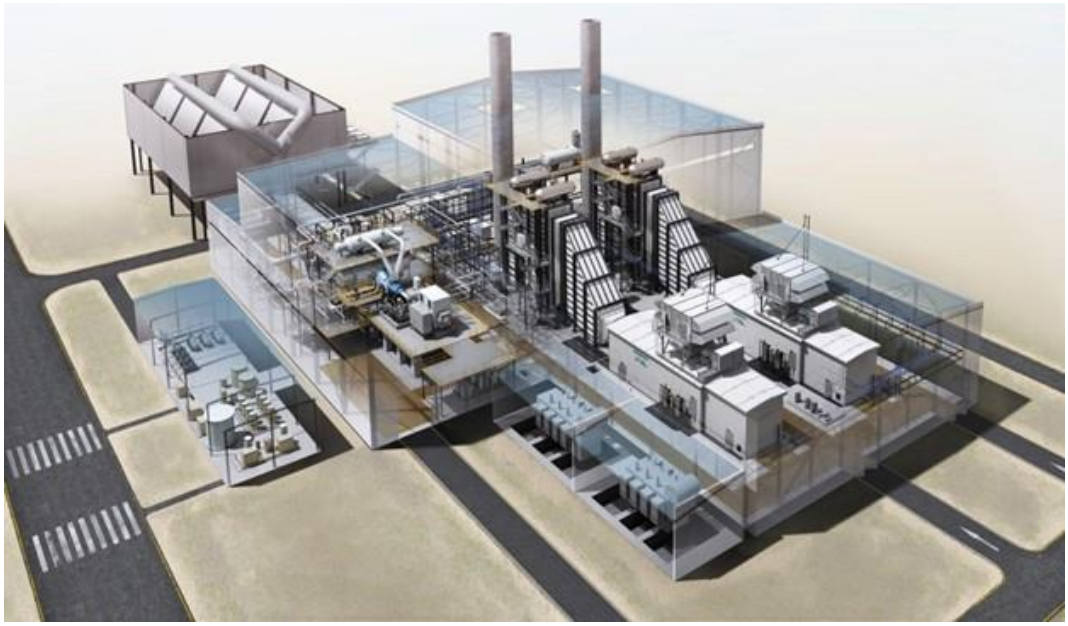

Figure 1.9. A combined cycle power plant [20].

1.4. BASIC OF A COMBINED CYCLE

Two power plant cycles make up the essential consolidated cycle's thermodynamic cycle. one is a steam turbine cycle called the Rankine Cycle, and the other is a gas turbine cycle called the Joule or Brayton Cycle. The gas turbine power plant cycle, which is 1-2-(3.4-1, is the garnish cycle. It shows how intensity and work are moved in a space with high temperatures.

At a lower temperature, the Rankine steam cycle, addressed by the letters a-b-c-d-e-f-a, is known as the lining cycle. In a waste intensity recuperation evaporator, the lining cycle is when heat energy from the high-temperature fumes gas is moved to water and steam. Gas turbine fumes rejects heat during the steady tension cycle 4-1. In the cycles

a-b, b-c, and c-d, a portion of this intensity is consumed by the feed water, wet steam, and superheated steam.

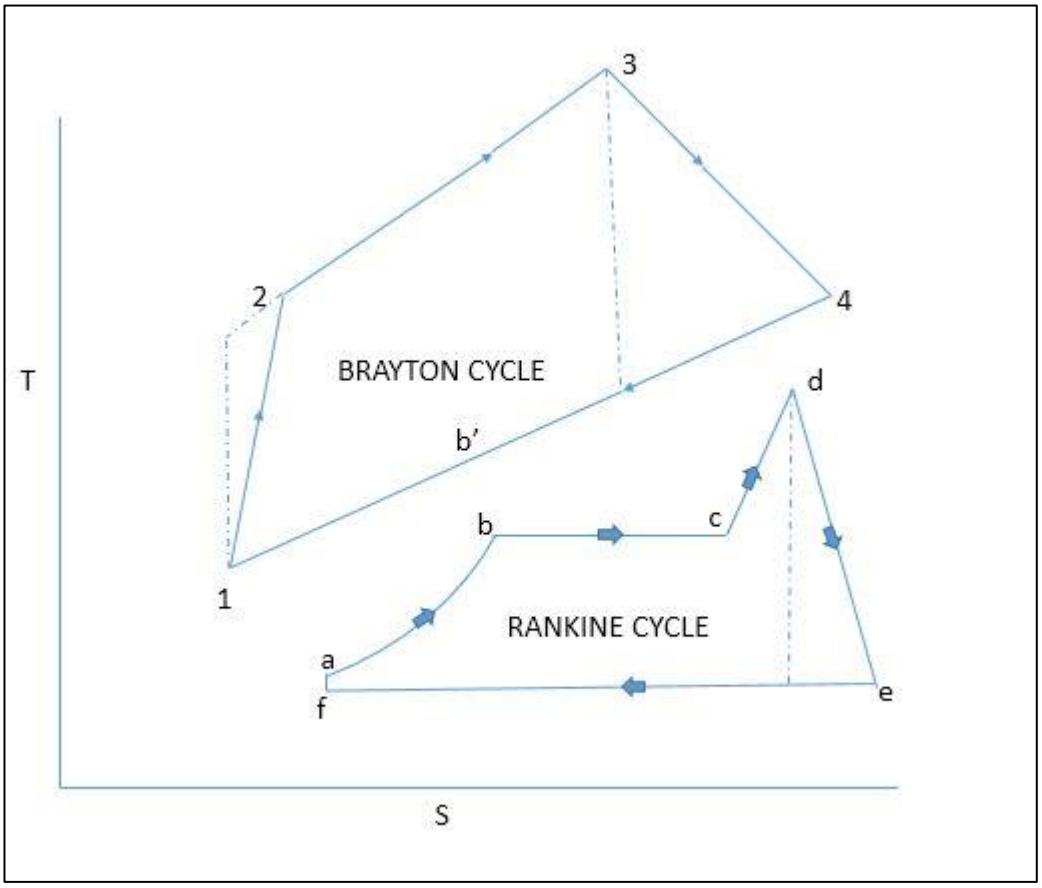

Figure 1.10. Cycle of a combined cycle power plant.

1.5. DESIGN PRINCIPLES OF A COMBINED CYCLE POWER PLANT

In order to increase energy efficiency and electricity output, combined cycle power plants combine two distinct thermodynamic cycles, usually a steam turbine cycle and a baryton cycle. A combined cycle power plant's design must take into account a number of important factors. The following design tenets are listed with the sources that back them up:

1. efficiency optimization: The primary goal of a combined cycle power plant is to maximize efficiency. This is achieved by integrating the gas turbine and steam turbine cycles to extract as much energy as possible from the fuel. This

integration minimizes waste heat. For detailed information on efficiency optimization [21].

2. gas turbine selection: Selecting the right gas turbine is crucial for the plant's performance. Factors such as the turbine's size, efficiency, and fuel flexibility should be considered. Modern gas turbines are designed to operate at high temperatures and pressures to increase efficiency [22].
3. heat recovery steam Generator (HRSG) Design: The HRSG captures waste heat from the gas turbine exhaust to produce steam for the steam turbine. Proper HRSG design is essential to efficiently transfer heat [23].
4. steam turbine selection: The choice of a steam turbine should complement the gas turbine and HRSG. Factors such as steam pressure, temperature, and capacity should be considered [24].
5. heat integration: Efficient heat integration between the gas and steam cycles is essential. Heat exchangers and other components should be strategically placed to optimize heat transfer [25].
6. control and automation: The control system should be designed to operate both the gas and steam cycles efficiently. advanced control strategies are essential for maintaining stable operation and load-following capabilities.
7. environmental considerations: Compliance with environmental regulations is crucial. Emissions control technologies such as selective catalytic reduction (SCR) and flue gas desulfurization (FGD) may be required. Refer to environmental engineering books for details on emissions control.
8. safety and reliability: Safety measures should be incorporated into the design to ensure the protection of personnel and equipment. Additionally, a focus on reliability and redundancy is essential for uninterrupted power generation.
9. grid integration: The power plant must be designed to seamlessly integrate with the electrical grid, including synchronization and load-following capabilities.
10. life cycle cost analysis: consider a life cycle cost analysis that takes into account not only the initial capital investment but also operational and maintenance costs over the plant's lifetime.

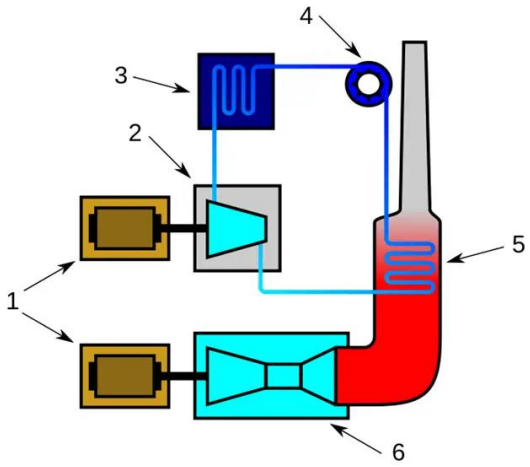

1. Electric Generators, 2. Steam Turbine, 3. Condenser, 4. Water Feed Pump
5. Heat Recovery Steam Generators or Boiler, 6. Gas Turbine

Figure 1.11. Working principle of a combined cycle power plant.

1.6. EFFICIENCY OF A COMBINED CYCLE POWER PLANT

Combining the steam and gas cycle will produce low outcome temperatures and high info temperatures. A comparable fuel source increases the combined productivity of the cycle. As a result, the high termination temperature of the gas turbine and the waste intensity temperature from the condensers of the steam cycle form the thermodynamic cycle of a connected cycle plant. this broad reach demonstrates the excellent carnot productivity of the cycle. The true productivity is more than the efficacy of any plant on its own, even though it is not precisely the carnot proficiency.

In perfect conditions, when operating at maximum efficiency and with no aging, a combined cycle power plant's electric effectiveness can exceed 60%. This is because the reduced warming value of the fuel used results in the creation of electric energy. Similar to single cycle warm units, combined cycle warm units provide the delivery of low-temperature heat energy for contemporary chores, space heating, and other uses. Combined heat and power (CHP) plants are the term used to refer to these power offices, and cogeneration is the cycle in question.

In lower warming worth and gross result scenarios, help's whole cycle efficiencies are sometimes greater than half. The apex, continuous state LHV proficiency of 55 to 59%

is exhibited by the majority of consolidated cycle units, particularly the larger ones [21].

1.7. PROBLEM STATEMENT

The energy sector in Iraq encounters notable obstacles as a result of the nation's escalating energy requirements and the imperative to effectively exploit its enormous fossil fuel reserves. The primary power generation systems in Iraq are largely reliant on basic cycles. However, these systems, despite their extensive utilization, lack optimization for efficiency, resulting in significant energy wastage and elevated operational expenses. moreover, the significant environmental consequences associated with these systems, namely in relation to the release of greenhouse gases, are substantial and contradict the objectives of global environmental sustainability. The resolution of these concerns could be achieved through the use of enhanced power production technology, such as the combined Brayton - Organic Rankine Cycle nonetheless, the implementation of these technologies necessitates a comprehensive comprehension of their thermodynamic characteristics and financial feasibility under the specific circumstances of Iraq's distinct climate, economic situation, and technological framework [26].

The thermodynamic efficiency of power generation systems plays a pivotal role in the arid and high-temperature conditions prevalent in Iraq. The integration of a brayton - ORC system, which utilizes waste heat from the exhaust of a gas turbine to produce supplementary power, has promise in substantially augmenting the overall efficiency of power plants. However, there is a dearth of extensive research about the performance of the system in the specific climatic circumstances of Iraq, which can have an impact on the condensation processes that are vital to the Organic Rankine Cycle (ORC). Furthermore, the investigation of suitable working fluids, which necessitate optimization based on local ambient temperatures to enhance the efficiency of the cycle, has not been thoroughly examined within the Iraqi context. This highlights a knowledge gap in understanding how the integrated Brayton - ORC system might be customized for optimal performance in the specific environmental conditions of Iraq [27].

The assessment of the feasibility of implementing the combined brayton - ORC system in Iraq necessitates the consideration of both economic factors and thermodynamic studies as equally significant components. Given the significant dependence of the nation's economy on the oil and gas industry, it is imperative to assess the potential justification of the substantial upfront expenses linked to the implementation of combined cycle technology. This evaluation is necessary to ascertain the long-term advantages in terms of enhanced efficiency and diminished fuel consumption. Furthermore, it is crucial to consider the potential economic advantages in light of the volatile energy market in Iraq and the fiscal interests of the government. An in-depth energy economic analysis is required to assess the economic viability of implementing the combined brayton - ORC system in Iraq's power generation sector. This analysis should take into account many factors such as local fuel prices, maintenance costs, and potential government incentives. By considering these aspects, a comprehensive evaluation may be conducted to establish the economic attractiveness of this system [28].

1.8. AIM AND OBJECTIVES

To address the expansion of energy use and the environmental pollution associated with its construction, the overall goal of continuing Innovation is to provide a basic and convincing methodology for rapidly heating a steam turbine during the start-up of a combined cycle power plant. The previously owned common cycle will be applied to an EES programming project to explore the efficiency of the Rankine cycle.

1.9. THESIS LAYOUT

This thesis consists of five chapters as follows:

Chapter 1: Introduction: contains background about steam power plants, and the issue faced steam power plants and benefits. Moreover, give basic information about solar energy.

Chapter 2: Review the literature related to steam power plants, the differences between

traditional methods of generating electricity and the combined cycle engine for steam power, and previous studies related to the subject of the study.

Chapter 3: This chapter explains the study's design and techniques. The Brayton and Organic Rankine Cycle designs, working fluid selection, and thermodynamic and economic analysis are covered. The chapter covers data collecting, simulation tools including the engineering equation solver (EES) software program, and analytical methodologies.

Chapter 4: Represents the results obtained from the modelling software and the discussion of the results.

Chapter 5: Conclusions and recommendations for the future work

PART 2

LITERATURE REVIEW

A complex and extremely effective system for producing electricity or mechanical power is a combined cycle engine, sometimes known as a combined cycle power plant or simply a CCE. combining two different thermodynamic cycle a gas turbine cycle and a steam turbine cycle to improve energy conversion and overall efficiency constitutes a tremendous achievement in power production technology. Based on the Brayton Cycle principle, the gas turbine cycle generates high-velocity exhaust gases by compressing and combining fuel and air before lighting it on fire. These gases power a gas turbine, which can be used to power a generator or perform other mechanical tasks. However, the Brayton Cycle efficiency is constrained, particularly when trying to convert thermal energy into electricity. a combined cycle engine, which uses a steam turbine to power the Rankine Cycle, incorporates a second thermodynamic cycle to get around this restriction. The gas turbine's exhaust heat is caught and used to warm water, which in turn creates steam. once inside a steam turbine, this steam is used to power a generator, which can subsequently be used to generate more energy or carry out mechanical tasks. when compared to conventional single-cycle power plants, the overall efficiency can be significantly increased because to this clever combining of the two cycles. The remarkable efficiency of a combined cycle engine, which frequently exceeds 60% is one of its main benefits. because of its great efficiency, it is an environmentally benign method of producing electricity because it uses less fuel and emits less greenhouse gases per unit of energy produced. Large-scale power plants, particularly those built for baseload or peak-load electricity generation, as well as industrial settings requiring both energy and process heat frequently employ combined cycle engines. In conclusion, a combined cycle engine is a state-of-the-art power generation technology that maximizes energy conversion by utilizing the advantages of both steam and gas turbine cycle. It is an essential part of

the infrastructure for modern power generation due to its exceptional efficiency, positive effects on the environment, and adaptability.

2.1. ORGANIC RANKINE CYCLE

One possible way to turn low-grade heat sources into electrical power is through the Organic Rankine cycle (ORC). The commercialization of ORC power plants in the KW range has not attained high maturity despite the construction of multiple MW-scale power plants around the world. This is because small-scale facilities are plagued by design issues, high specific costs, and potential customers who are SMEs. With a focus on working fluid selection and expander design, this review paper delves into the scientific and financial status of ORC technology. Additionally, it includes an analysis of the European market to inform future developments. [29]

Lee et al. [30] analyzed the heat exchanger and radial-inflow turbine of the organic Rankine cycle (ORC) system using one-dimensional analysis technique. By building an ORC system for industrial waste heat recovery, it is able to produce 534 KW of power overall with a 13.5% thermal efficiency. The study shows that the system's performance is highly dependent on the temperatures of the cooling water input and the heat source. As the temperature of the heat source input rises, the mass flow rate, net power output, and heat utilization ratio all increase, but thermal efficiency decreases as the temperature of the cooling water inflow rises.

Tumen Ozdil et al. [31] studied subcritical pressure zones, the Organic Rankine Cycle (ORC), organic flash cycle with two-phase expander (OFCT), and organic flash cycle (OFCB) in this work. The working fluids consist of o-xylene, R123, and R245fa. According to the study, an organic flash cycle is an efficient way to recover low-grade energy sources, and the optimal cycle type or working fluid is determined by the temperature of the source.

An Organic Rankine Cycle (ORC) in a power plant in southern Turkey is thermodynamically analyzed. An evaporator, turbine, condenser, pump, and generator make up the system. According to the study Yu et al. [32], there is a relationship

between energy efficiency and the pinch point, with energy efficiency rising as the pinch point temperature decreases. For saturated liquid form, the ORC's energy and exergy efficiencies are computed to be 9.96% and 47.22%, respectively. Exergy efficiency for various water phases is also calculated in the study, and the results demonstrate that the evaporator has a major impact on the system's exergy rate efficiency. In order to increase the efficiency of the system, the evaporator is precisely assessed.

Yu et al. [33] investigated the Organic Rankine Cycle (ORC) which is a useful technology that operates autonomously and requires little maintenance to convert low temperature heat into electricity. New ORC architectures are being developed as a result of the necessity for cost-effectiveness despite its widespread usage. Though they have been studied recently, ORC architectures have not gotten much attention because of problems with system complexity, thermodynamic potential, limited experimental data, and handling different boundary conditions. An overview of ORC architectures is given in this article, together with information on accessible experimental data, performance evaluation standards, and boundary conditions.

Wang et al. [34] proposes a simulation model that recovers waste heat from engine exhaust gas and jacket water using the Organic Rankine Cycle (ORC) bottoming mechanism of a diesel engine. Waste heat absorption, expansion power, system efficiency, exergy loss, and exergy efficiency are all evaluated by the model. Findings indicate that between 75% and 9.5% of waste heat may be recovered under high to moderate load engine settings, with expansion power of up to 14.5 kW, recovery efficiency of up to 9.2%, and energy efficiency of up to 21.7%. The thermal efficiency of a diesel engine can be increased by 6.1% by combining a bottoming ORC system.
Using R123, R245fa, and isobutene, this study examines the effects of thermodynamic design factors on the net power output and surface areas of the HRVG and condenser. The study's performance evaluation criterion is the ratio of net power generation to total heat transfer area. The system's performance is optimized by the use of a genetic algorithm. The HRVG and condenser's surface areas and net power generation are found to be highly influenced by the following factors: pinch temperature difference,

approach temperature difference, turbine intake pressure, and turbine inlet temperature. In parametric optimization, isobutene outperforms R123 or R245fa.

Li et al. [35] looks into how the efficacy of the regenerative Organic Rankine Cycle (ORC) on R123, a low boiling point heat source, is affected by varying the regenerator and working fluid mass flow rate. Leakage issues were resolved, and the turbine was safeguarded by the use of a throttle valve. An first test using a geothermal source operating at 130°C produced 6 k_W of electricity and a regenerative ORC efficiency of 7.98%, which was 1.83% greater than the ORC's basic efficiency.

Quoilin et al. [36] examined the one promising heat conversion technology for a sustainable energy source which is the Organic Rankine cycle (ORC). It is applicable to decentralized power plants and has the ability to recover low-grade heat. An overview of ORC usage, market analysis, technological challenges, and optimization strategies are given in this publication. it also covers current advancements in research and development for the future generation of ORC, as well as technological limitations. The market and manufacturers for commercial ORC modules are also covered.

Aghahossein et al. [37] compares the effectiveness of the Organic Rankine Cycle (ORC) with different working fluids in order to assess its suitability for low-grade heat sources. Sensitivity studies are used to compare CO_2 emissions, environmental attributes, and operational features. The following are possible working fluids: R404a, R407c, R600a, R134a, R123, and R245fa. The results offer recommendations for choosing working fluids that maximize power output while reducing adverse environmental effects, presenting a more environmentally friendly option than fuel combustion systems.

Wang et al. [38] looks at a novel technology that combines a gasoline engine with a dual loop Organic Rankine Cycle (ORC), in order to recycle heat lost by an internal combustion engine. While the high temperature loop solely recovers exhaust heat, the low temperature loop recovers heat from the coolant as well as the high temperature loop. The research calculates a gasoline engine's performance map and contrasts the

amount of heat lost by the coolant and exhaust systems over the engine's operating range. The results demonstrate that the low temperature loop has a higher net power than the high temperature loop, and in the small load zone, the relative output power rises from 14% to 50%.

Wang et al. [39] looked at the performance of nine pure organic working fluids in particular settings using a thermodynamic model in Matlab and REFPROP in one technique for recovering low-grade waste heat from engines is the Organic Rankine cycle (ORC). The findings indicated that R245fa and R245ca were the least environmentally hazardous, while R11, R141b, R113, and R123 had somewhat better thermodynamic performances. The best control concept for the transient ORC process was also found by the investigation.

Rayegan et al. [40] use the Refprop 8.0 database to compare the working fluid capacities in solar Rankine Cycle under the same operating conditions. Based on chemical composition, temperature-entropy diagram, and fluid effects on cycle exergy efficiency, vapor expansion ratio, thermal efficiency, and net power generated, the study compares ORC working fluids. It is suggested that eleven different fluids be used in solar ORCs with medium- or low-temperature solar collectors. The study discovered that utilizing regenerating ORC and raising collector efficiency could lower irreversibility and improve energy efficiency. The cycle exergy efficiency is dependent on regeneration, although it is independent of fluid when collector efficiency is increased. At the studied temperature ranges, more complex molecules result in more effective regenerative cycle.

Sun et al. [41] study R134a as the working fluid to investigate an organic Rankine Cycle (ORC) heat recovery power plant. In order to enhance the plant's performance, mathematical models and algorithms are created with an emphasis on thermal efficiency and net power generation. The optimization method ROSENB together with the penalty function approach are suggested to optimize either net power production or thermal efficiency. The findings demonstrate that, in order to maximize system net power output and thermal efficiency, the correlations between controlled and uncontrolled variables are almost identical to the liner function

The main goal of this research is to employ a unique thermodynamic analysis to match a stationary internal combustion Engine (ICE) to a vapor cycle. three primary categories of fluids are identified by the study: overhanging, nearly isentropic, and bell-shaped. Parametric analysis is used to find each fluid's ideal evaporation pressures. three cycle configurations are examined: regenerated cycle, simple cycle with engine cooling water and exhaust gases, and simple cycle with engine cooling water and exhaust gases. to find the optimal fluid and cycle design, important thermodynamic cycle parameters, and overall power system efficiency, a second law analysis is performed.

Solar thermal energy-driven reverse osmosis desalination is a viable renewable energy method, especially when water resources are limited. Reverse osmosis (RO), which consumes less energy, is frequently employed in conjunction with the organic Rankine cycle (ORC). However, in order to assess the effectiveness of new technologies, thorough theoretical research is required. Vaja et al. [42] the objective of this work is to extend the theoretical analysis to solar ORCs that are heated by stationary solar collectors. Twelve separate compounds and four distinct models are thought to be the ORC's operating fluids. In order to minimize the aperture area needed for each unit of mechanical power generation, the ideal operating parameters for the solar ORC are determined. The results have applications in system sizing, techno-economic analysis, working fluids of Rankine cycles, and solar power cycle architecture assessment.

Delgado et al. [43] examined the Organic Rankine cycle for low-grade waste using different working fluids, heat recovery. Exergy efficiency is the goal of an evolutionary algorithm that optimizes theoretical factors that impact ORC performance. water cycle are outperformed by organic working fluids, with R236EA cycle offering the highest energy efficiency. under waste heat conditions, internal heat exchangers are unable to enhance ORC performance. For working fluids with a non-positive slope for the saturation vapor curve, the cycle also operates optimally when there is saturated vapor at the turbine inlet.

Dai et al. [44] create a dynamic model for an Organic Rankine Cycle (ORC) for control and diagnostic systems, the study suggests two methods. Modeling was done

with Madelia, and simulation was done with Dymola. When compared to experimental data, both models exhibit respectable accuracy; however, the moving boundary model exhibits faster performance.

Wei et al. [45] talks about employing exhaust heat and HFC-245fa to enhance the efficiency of an Organic Rankine Cycle (ORC) system. It implies that while reducing sub-cooling at the condenser outlet, boosting exhaust heat can boost output net power and efficiency. Elevated room temperature has the potential to reduce output net power and efficiency by more than 30%. It is advised to select an appropriate nominal state depending on the operating environment in order to increase performance.

An innovative use of cogeneration in small-scale biomass power and heat plants is the ORC, which modifies the architecture of the power plant and influences the working fluid selection process. A program has been developed to identify fluids that are acceptable thermodynamically, such as alkyl benzenes, which have the highest efficiency [46].

low-grade heat sources are used in an environmentally friendly technique called the "Organic Ranking cycle" (ORC) to generate a turbine system. The working fluid in the system is HCFC-123, which has a low boiling point and low latent heat. to find the optimal operating conditions, an experimental tool and a numerical simulation model were developed. According to Drescher et al. [47] the HCFC-123 greatly improves cycle performance, and the turbine designed for testing functioned well.

Non-isothermal phase shift advantage of organic fluid mixes is highlighted when Yamamoto et al. [48] assesses their application in Rankine power cycle. Stan Mix is a commercial product that utilizes the mixing principles of Wong and Sandler for analysis and optimization. the study also emphasizes how crucial it is to choose the ideal working-fluid composition in order to create an efficient ORC design.

2.2. BRAYTON CYCLE

The supercritical CO_2 (S-CO_2) Brayton cycle has been extensively employed in a variety of heat sources due to its efficiency and compact size. A 2000–2019 study that looked at 724 academic papers on the S–CO_2 Cycle analyzed data from 55 nations, 543 institutes, and 1378 authors. According to the data, South Korea, China, and the United States are the top three countries in S-CO_2 studies. Five viewpoints were considered in the evaluation of current research: application, cycle configurations, modeling, CO_2-based mixtures, system components, and trials. It is recommended that future research be done to hasten the S-CO_2 power system's commercialization [49].

Supercritical Carbon dioxide (S-CO_2) Brayton Cycle, with its high-power conversion efficiency, compact design, ease of use, and low efficiency loss through dry cooling, is a promising alternative for nuclear reactor applications. It can be utilized in fusion reactors, compact modular reactors, generation IV reactors, and other nuclear power plants. The S-CO_2 power cycle functions as a self-sustaining and self-propelled decay heat removal system, which can further improve the safety of commercial nuclear power reactors. Wu et al. [50] examines the literature on nuclear applications based on the S-CO_2 power cycle, examining its features, experimental studies, and different research domains. The S-CO_2 Brayton Cycle is a viable substitute for increasing nuclear energy uses, the study says.

Yang et al. [51] investigates the part-load performance of four common S-CO2 Brayton cycles: the intercooling, reheating, recompression, and simple recuperative cycles. The reheating cycle is found to be more efficient than the simple recuperative cycle, although under part-load conditions, the reheating cycle is outperformed by the recompression and intercooling cycles. On the other hand, the intercooling cycle responds best to wide-range load change when the load is more than 60%. When actual total power generation is less than 62.5% of maximum total electricity generation, the recompression cycle performs better; when this ratio is greater than 68.3%, the intercooling cycle performs better.

Chen et al. [52] A promising heat recovery method for raising cycle thermodynamic efficiency and reducing pollutants in Brayton Cycle is the Maisotsenko cycle. This work uses the idea of finite time thermodynamics to build the open Maisotsenko-

Brayton cycle model while taking plant size constraints into account. The model takes into account heat transfer losses to the ambient, irreversible losses in the compressor and turbine, and irreversible combustion losses in the combustor. It also takes into account pressure drop losses in the intake, compression, expansion, and discharge operations. Power output and efficiency can be optimized by adjusting the working fluid's mass flow rate and pressure drop loss distribution. The study also establishes the maximum power output, the ideal relative inlet pressure drop at the compressor intake, and the compressor's ideal pressure ratio for the cycle. The power and efficiency performances of the open Maisotsenko-Brayton cycle are found to be superior to those of the standard open regenerated Brayton cycle.

The supercritical CO_2 Brayton Cycle (SCBC) is a viable way to increase power production technology's efficiency and cost-effectiveness. In the moderate temperature range (450-750°C), it offers excellent efficiency and small equipment sizes, but it also has material difficulties because of the high temperature and pressure. Solar energy, nuclear power, waste heat sources, and high-temperature fuel cells can all be utilized with SCBC. The structural forms, applications, thermodynamics, optimization, and design of the SCBC. Liu et al. [53] recommends boosting the efficiency of turbomachinery, creating small heat exchangers, constructing expansive testing facilities, refining SCBC designs, and enhancing control methods. Further research on commercialization is required.

Mecheri et al. [54] uses industrial modeling hypotheses and a thermodynamic approach to investigate the performance of supercritical CO_2 cycle in coal power plants. It recommends starting with the design of a power cycle when putting the technology into practice. The primary findings indicate that even with low temperature heat in the flue gas from coal combustion, a recompression cycle is required for this application; with an efficiency differential larger than 4.5%pt. With efficiency gains of 1.5% points, the single reheat arrangement is an efficient one. Efficiency is increased by 0.3 to 0.5%pt by using modern flue gas economizer setups and double reheat and recompression cycles.

Ho et al. [55] evaluates the cost and performance of various closed-loop Brayton Cycle

designs for supercritical carbon dioxide (s-CO_2) in comparison to a concentrated solar heat source. There is consideration of cascaded, simple, recompression, and partial cooling cycles. Temperature variations and the lowest cost of power-block components are made possible by the fundamental cycle. cycle topologies with narrower temperature differentials result in lower costs for solar collectors and receivers as well as improved efficiency. Improved cycle efficiencies lead to the lowest total cost of solar and power-block components.

Due to its high temperatures and financial savings, concentrated solar power, or CSP, is becoming more and more popular. To make this technology commercially viable, research has concentrated on solar field, solar receiver, energy storage, and power block. Because of its better thermal efficiency and compactness, supercritical CO_2 Brayton cycles have emerged as a competitive alternative for power blocks with central receiver tower systems. Padilla et al. [56] studied four distinct supercritical CO_2 Brayton Cycle configurations in this paper: partial cooling with recompression, simple Brayton Cycle, recompression Brayton cycle, and recompression with main compression intercooling. According to the study, the recompression cycle with main compression intercooling achieves the optimum thermal performance, with the thermal efficiency of the supercritical CO_2 Brayton Cycle rising monotonically with cycle temperature. With a bell-shaped curve, the exergy efficiency peaks between 700 and 750°C, depending on the cycle design.

Al-Sulaiman et al. [57] explain five supercritical carbon dioxide Brayton cycles coupled with a solar power tower were compared. A differential evolution method and a mathematical code were employed in the analysis to create and improve a heliostat field pattern. The heliostat field's optical performance was enhanced prior to its merger with the supercritical CO_2 Brayton Cycle. At a maximum of 52%, the recompression Brayton cycle had the highest thermal efficiency. While having a simpler configuration, the regenerative Brayton Cycle functioned similarly. The research was carried out at Saudi Arabia's Dhahran.

Ahn et al. [58] closed Brayton Cycle such as the supercritical CO_2 cycle, helium cycle, and nitrogen cycle have replaced the steam Rankine Cycle, which was formerly

employed in sodium-cooled fast reactors (SFRs) due to worries about sodium water reactions. the physical dimensions and performance of these gas Brayton cycle are compared for small modular SFR applications, taking system volume and turbomachinery architecture into account.

research on the solar thermal Brayton Cycle and Brayton cycle has demonstrated its potential in power plants in sun-drenched locations. minimizing pressure losses and maximizing heat transfer, however, come at a cost. Because of heat loss, the receiver must function at high temperatures, which presents difficulties. To maximize solar thermal power. Le Roux et al. [59] advise applying the Gouy-Stodola theorem, turbine modeling, various modeling vantage points, and the total entropy generation minimization approach. In order to advance solar thermal research generally, they hope to offer guidance to future investigators on how to best forecast and optimize the solar thermal Brayton cycle.

Despite of the high development costs, supercritical CO_2 Brayton cycle are a viable way to increase the efficiency of solar-thermal power plants These cycle have applications beyond the generation of solar energy and can become more attractive when the operating temperature rises. Iverson et al. [60] simulates short-term transients in solar environments by showing how Brayton turbomachinery reacts to varying heat input. The system's thermal mass permits the cycle to continue for brief intervals until the input stabilizes, despite fluctuations. These transients can be lessened by storage, and the effects of short- and long-term storage options on system efficiency are contrasted. Additionally, the study benchmarks computer modeling using a data collection for robust supercritical CO_2 Brayton Cycle operation, investigating how cycle upgrades affect efficiency and loss mechanisms.

For applications involving concentrated solar power, Garg et al. [61] contrasts three different kinds of carbon dioxide-based Brayton cycle. At 85 bar, the supercritical cycle has the best thermal efficiency, growing linearly with decreasing side pressure. Despite a larger turbine inlet pressure, it can still generate electricity with over 30% thermal efficiency at lower source temperatures. Irreversibility evaluations of the compressor, regenerator, turbine, and gas cooler show reduced efficiency compared to

ideal cycles. High-pressure drawbacks can be mitigated by the supercritical cycle low volumetric flow rates and minimal source temperature sensitivity.

Conboy [62] study the performance of important power cycle components as well as expected operating limits while approaching greater speeds and temperatures.
supercritical CO_2 (S-CO_2) power cycle have he advantage of superior plant economics because of their small size, high power conversion efficiency, and ability to employ conventional building materials. The United States and Sandia national labs. A megawatt-scale supercritical CO_2 split-flow recompression Brayton Cycle, one of the first and only in the world to manufacture S-CO_2, is being built and operated by the department of energy. More heaters, a second recuperating printed circuit heat exchanger (PCHE), greater waste heat removal capability, larger capacity load banks, higher temperature piping, and better scavenging pumps to lessen wind age within the turbomachinery are some of the major improvements made to the Sandia-DOE test loop. In terms of turbine intake temperature, shaft speed, pressure ratio, flow rate, and electrical power generated, the loop has broken previous records.

Sarkar [63] investigates how operational parameters affect the ideal pressure ratio, energetic efficiency, and irreversibility of the components in an S-CO_2 recompression cycle. It is discovered that the ideal pressure ratio and cycle efficiencies are more significantly impacted by the minimum operating temperature than by the maximum operating temperature. The study also shows that the irreversibility of heat exchangers is larger than that of turbomachinery, and that the irreversibility is more strongly influenced by the working characteristics of recuperations. The high temperature recuperation's efficacy is twice as crucial as the low temperature recuperation's, and the turbine's isentropic efficiency is more important than compressors. The second law efficiency reduction is more significantly impacted by the reactor's pressure drop.

Supercritical carbon dioxide (S-CO_2) Brayton cycle performance is frequently examined using the recompression supercritical cycle, usually referred to as the Feher cycle. For sodium-cooled fast reactors (SFRs) running at low core output temperatures, it might not be the ideal arrangement. Alternative cycle configurations for an S-CO_2 Brayton cycle coupled to the advanced burner test reactor (ABTR) SFR prototype

design have been studied by researchers. Since there were no benefits discovered, the recompression supercritical cycle was improved. compared to earlier evaluations that fixed the minimum temperature and pressure randomly. Moisseytsev et al. [64] indicated that an optimal combination of minimum cycle temperature and pressure might generate gains in cycle efficiency of at least 1%. nevertheless, depending on the climate of the plant site, larger coolers for heat rejection and lower heat sink temperatures at minimum temperatures below critical temperatures can be required.

Zhang et al. [65] investigates pressure drops and power plant size constraints into account while building a thermodynamic model for open mixed Brayton and inverse Brayton cycle using finite time thermodynamics. there are eleven flow resistances in the gas stream, four of which are associated with isentropic efficiency. the airflow rate and net power output are impacted by the residual flow resistances, which are caused by variations in the flow cross-section at different locations. the pressure drops related to flow through different cross-sectional regions are found using the compressor inlet relative pressure drop. the power output, thermal conversion efficiency, and compressor pressure ratio of the top cycle are calculated analytically. the model cycle performance is optimized by adjusting the compressor input pressure, air mass flow rate, and pressure losses throughout the flow channel. An additional maximum is reached in respect to the top cycle compressor pressure ratio, and power output is optimized in relation to the bottom cycle compressor inlet pressure, air mass flow rate, or other pressure drop.

Due to the potential for higher efficiency than conventional steam cycles, research on high temperature, direct cycle gas cooled reactors has garnered attention. The Brayton cycle helium/helium recuperate must function in extreme environments with respect to pressure, temperature, and differential in pressure. the heatric Printed circuit heat exchanger and the norman plate fin concept were two of the promising tiny recuperate technologies that were the subject of the research. At CEA's claire loop, a prototype of the heatric printed circuit heat exchanger was built and tested, subjected to recuperate-typical thermal shocks. The thermal and mechanical properties of the mock-ups were analyzed using finite element and computational fluid dynamics models. Pra et al. [66] conducted between the experimental and numerical results, and suggestions were

given for full-size recuperates employing the selected technologies.

Alabdoadaim et al. [67] examines the functionality of a theoretical thermal power system made up of inverse and developed Brayton Cycle. By applying varied input pressures for a range of expansion pressure values, the study modified the Brayton cycle pressure ratio. The system performed better when it was run at high pressure ratios, according to the results. The regeneration system has the smallest work output and the shortest component sizes, whereas the base system outperformed the simple Brayton Cycle .

Agnew et al. [68] using the commercial process modeling program IPSE Pro, this work presents an optimization analysis of combined Brayton and reversed Brayton cycle. In order to achieve the best outcomes, the study recommended raising the bottom cycle intake pressure and adjusting the upper cycle pressure ratio, bottom cycle expansion pressure, and bottom cycle inlet pressure.

2.3. COMBINED POWER PLANE

This study uses thermodynamic studies of each system component to examine the operation of a combined cycle power plant (CCPP). The combustion chamber was found to be the source of the most energy destruction, with the condenser suffering the greatest energy losses. because of the surrounding temperature, the gas turbine generated less power. According to the study, exergy analysis is a useful method for assessing the performance of the CCPP since it can be used to find more fuel-efficient designs that emit fewer emissions of air pollution and use less fuel [69]

Kotowicz et al. [70] looks at closed air cooling, closed steam cooling, open air cooling, and sequential combustion both with and without cooling air coolers.increase electrical efficiency, the study assesses different gas turbine upgrades in a contemporary combined cycle power plant. Among the plant's machinery are a subcritical heat recovery steam generator and a 200 MW gas turbine. The study also emphasizes how gas turbine efficiency and the power plant are affected by increased allowed metal

blade temperatures. The paper proposes that industry-standard methods can raise net electric efficiency to 0.63–0.65.

Ibrahim et al. [71] uses simulation models to discover features and optimal operating conditions for combined cycle gas turbine (CCGT) systems, with the goal of increasing efficiency and lowering pollution in power-producing facilities. Simulation models, including thermal analysis, optimization strategies, error analysis, and performance metrics evaluation, are generated using the MATLAB 10A program. ANOVA is used to examine the data, and the resultant coefficient of determination (R2) is 0.985. The accuracy of the model is demonstrated by extracting performance and operating data from the MARAFIQ CCGT plant in Saudi Arabia. A 0.8104% mistake is found by doing an error analysis utilizing the records of the actual plant. An optimization technique called adaptive neuro-fuzzy system (ANFIS) is utilized. At 1540 MW and 61%, respectively, the maximum power output and thermal efficiency are attained. It is discovered that the most important element for optimal performance is the turbine inlet temperature. The models developed in this work serve as a useful stand-in for expensive and time-consuming experimental attempts to evaluate and improve CCPP.

Power Plant subsystems and components are essential for effective operation, however because of financial limitations, operators struggle with asset management and maintenance scheduling. Sabouhi et al. [72] focuses on combined cycle power plants (CCPP) dependability modeling in order to make techno-economic decisions about equipment maintenance. For both gas turbine power plants (GTPP) and steam turbine power plants (STPP), reliability models are developed that pinpoint the critical elements that have the biggest impact on system reliability and availability objectives. This aids in the selection of efficient maintenance schedules, enabling effective planning and the allocation of techno-economic resources.

Kotowicz et al. [73] addresses how to use heat from the cooling air and change gas turbine characteristics to increase efficiency in combined cycle power plants. It proves that the only method to raise efficiency without consuming heat is to improve the turbine's features. Efficiency can be increased by two to three percentage points with an additional steam cycle, and the compression ratio likewise rises. According to the

economic study, if the expenses associated with investing in gas turbines can be kept reasonable, the suggested development path might be feasible.

Conventional steam turbine is expected to be replaced by the gas turbine and its combined cycle (CCGT) in the world's power generation. To predict the characteristics and operational parameters of the CCGT system, a simulation system was created. Tajik Mansouri et al. [74] suggested that performance be enhanced by raising the cycle peak compression and temperature ratios. Using the MATLAB tool, the CCGT power plant performance model demonstrated higher cycle peak temperature and compression ratios along with a high overall thermal efficiency of 58%. At lower ambient temperatures and higher turbine inlet temperatures, the best efficiency was attained at greater compression ratios. The models employed in this work are useful instruments for CCGT power plant performance estimation.

Energy supply-demand imbalance is growing, which calls for the creation of new energy sources and the effective use of already-existing resources. Power plants with combination cycle are a useful way to use energy resources. Ersayin et al. [75] analyzes an operating power plant to determine energy and energy efficiencies using thermodynamics and real-world data. The energy efficiency of the combined cycle power plant is 56% and 50.04%, respectively, with the combustion chamber exhibiting the highest rate of energy destruction. Ideas for alterations and improvements are provided in light of the results.

Combination cycle power plants (CCPPs) are essential for power generation because of their efficiency. But because they have to start and stop frequently, they need to use sophisticated methods like model-based procedures. Precise large-scale model implementation is facilitated by modeling languages and libraries. Strong algorithms are required to solve these models-based optimization problems.Ticâ et al. [76] presents a technique to improve start-up performance by transforming a CCPP physical model into an optimization-oriented model. continuous approximations of the heaviside function are used in the process to show the model's consistency and applicability for control and optimization.

Sarkar et al. [77] examines the effects of water mass flow rates and entrance temperatures on system COP, water output temperatures, cooling and heating capacities, and evaporator and gas cooler systems. Heating and cooling are done at the same time with Tran's essential CO_2 heat pumps. The water mass flow rate and the inlet temperature have a substantial impact on system performance, according to the results. Performance and outlet temperatures are more significantly impacted by the gas cooler's inlet temperature. The study offers suggestions for choosing the ideal water mass flow rate to achieve the best outcomes.

Conventional energy-based methods detect irreversible components and processes, but they are limited in their ability to understand energy destruction because of technological or financial constraints. The goal of cutting-edge exergy-based research is to go over these limitations and comprehend plants better. Petrakopoulou et al. [78] investigated combined cycle power plant using both conventional and innovative energetic methodologies. with the exception of gas turbine expanders and high-pressure steam turbines, most energy destruction is unavoidable. Unavoidable components are limited by internal technological restrictions, and endogenous exergy degradation suggests that component interactions are not a primary factor in thermodynamic inefficiencies. This improved analysis shows new strategies for improvement.

Ibrahim et al. [79] examines the performance implications of different configurations as well as the thermodynamics of combined cycle gas turbines. The study finds that regenerative gas turbines are more efficient at lower compression ratios through simulation using MATLAB software. For the purpose of producing power, the basic gas turbine arrangement is preferable. The study highlights the important impact of ambient temperature and compression ratios on combined cycle performance and proposes that regenerative additions to the topping cycle can lead to a higher overall efficiency.

gas turbines are a major source of electricity for combined cycle power plants (CCPP), and as a result, their dynamics are becoming more and more significant. Precise gas turbine models have been created to explore these dynamics. In order to address power

system concerns, this research Fraidenraich et al. [80] attempts to comprehend, model, and analyze the behavior of gas turbine-based facilities. Three different dynamic models were thoroughly simulated with Matlab/Simulink by comparing their responses. The efficiency and precision of the results are comparable to those found in pertinent literature, demonstrating the effectiveness of the comprehensive and using low temperature organic Rankine cycle, this paper explores the bottoming cycle for medium- and large-scale combined cycle power facilities. It seeks to illustrate the possibilities of these alternative cycles using heavy-duty, highly efficient gas turbines, including recuperative gas turbines. In this study, organic fluids such as R113, R245, isobutene, toluene, cyclohexane, and pentane are examined. High global efficiencies and competitive performances have been obtained for the combined ORC cycle of toluene and cyclohexane. The economic implications of ORC usage in combined cycle are also examined in this research.

Application of static and dynamic simulation models to enhance combined cycle power plant startup is covered in this paper Polyzakis et al. [81] clear the Powerful computers can be used to perform dynamic simulation models, which are useful tools for comprehending the features of power plants. with the use of advanced process simulation software (APROS), the heat recovery steam generator (HRSG) model has a high degree of precision, particularly during powerful transients. The simulation is able to predict operational activities and precisely estimate the dynamic behavior of the real HRSG. It is possible to reduce the start-up time and lifespan consumption of highly stressed components through parametric research.

Basic cycle, the intercooled cycle, the reheated cycle, and the intercooled and reheated cycle are the four distinct Brayton cycle that will be compared in this study in order to optimize a combined cycle power plant. With 200 MW coming from the gas turbine and 100 MW from the steam turbine, the projected combined cycle plant will produce 300 MW of electricity. Because of its high bottoming steam cycle thermal efficiency and high exhaust gas temperature, the reheated gas turbine is the most recommended option. A combined cycle power plant that is more efficient and less expensive can be produced by an optimum Brayton cycle. examining every possible cycle for a combined power plant running at base load, Koch et al. [82] concentrates on reliability,

efficiency, installation and running costs, and maintainability. The simple cycle, intercooled cycle, reheated cycle, and intercooled and reheated cycle designs are only a few of the systems that are examined in this study.

Cihan et al. [83] Uses an evolutionary algorithm to lower the product cost of advanced combined cycle power plants. Simultaneous optimization of the process variables and design configuration (process structure) is achieved. Numerous gas turbine systems on the market, three different pressure levels for steam generation in the heat-recovery steam generator, supplementary firing, steam reheat, parallel configuration of heat exchangers in the gas path, and steam injection into the gas turbine are just a few of the superstructure design options that the optimization algorithm may choose from for the power plant. Economically speaking, for the assumptions and simplifications made in this analysis, a 240 MW combined cycle power plant with a big gas turbine (150 MW), a two-pressure heat recovery steam generator with a reheated, but without additional firing, is selected. The final ideal design and a detailed exergy investigation of chosen intermediate solutions reveal the extent, location, and causes of the thermodynamic inefficiencies.

Thorough energy and exergy analysis of a combined-cycle power plant was carried out, with an emphasis on energy and exergy flows and losses. According to Hosseini et al. [84] more than 85% of irreversible energy losses are caused by combustion chambers, gas turbines, and heat recovery steam generators (HRSG). thermal and useful recommendations were given for these components in order to improve system efficiency.

Arrieta et al. [85] investigates the technical and financial review concluded that the integrated solar combined cycle System with 67 MW e Solar Field (ISCCS-67) is the best design for Iran's first solar power plant. Over the course of its 30-year operational life, the ISCCS-67 saves 59 million dollars in fuel costs and eliminates CO_2 emissions by 2.4 million tons. Moreover, it boosts steam turbine capacity by 50% and total efficiency by 4%. With the same capacity factor, the LEC of ISCCS-67 is between 10% and 33% less expensive than combined cycle and gas turbine.

Because of its adaptability and the accessibility of natural gas, thermal power is essential for the production of electricity. Building thermal power plants is Brazil's top priority as it transitions from a hydraulic-based to a hydrothermal energy system. The performance of these plants is greatly influenced by the surrounding conditions, such as air pressure, relative humidity, and ambient temperature. Franco et al. [86] makes use of a multiple-shaft plant that has a steam turbine for auxiliary firing and two Siemens AG 501F gas turbines coupled to three HRSGs for re-heating. Understanding the effects of ambient temperature and further firing on generated power, heat rate, and thermal efficiency requires knowledge of the outcomes of a thermodynamic simulation performed with gate cycle software version 5.51.0.r.

Chiesa et al. [87] investigates the usage of fuels and biomass for energy, proposing an economic analysis based on energy loss. It implies that plants with thermodynamic efficiencies higher than minimum values can employ biomass. The use of biomass as an auxiliary fuel in combined cycle power plants in addition to natural gas is covered in the paper. It offers two technical solutions: using current gas turbine models, it is possible to achieve plant efficiencies of up to 57% and 60%.

Franco et al. [88] looks into three possible ways to get net electric efficiency in combined cycle applications for big power gas turbines to be higher than 60%. Three methods are examined: two independent closed-loop circuits, closed-loop steam cooling for rotor blades and vanes, and conventional open-loop air cooling. An improved version of the thermodynamic algorithm GS is used to assess performance, with a focus on large-scale single-shaft machines. Thermodynamic research reveals that efficiency levels exceeding 61% are achievable with existing technology, even when dependability, capital cost, and environmental challenges are disregarded.

Bolland et al. [89] suggests boosting combined cycle plant efficiency to over 60% without new gas turbine technology. This can be achieved by optimizing the heat recovery steam generator (HRSG) using parallel sections and limiting subcritical conditions. combining HRSG optimization with gas turbine reheat and gas-to-gas recuperation can increase plant efficiency to 65%. HRSG optimization alone can achieve efficiencies of around 60%.

Closed-loop combustion (CC) system, two CO_2 removal techniques are compared in this work (Bolland and Mathieu, 1998). In the first, pure oxygen is burned in a semi-closed Brayton cycle with CO_2 as the working fluid, producing zero emissions. The second approach entails partially recirculating the heat recovery boiler of a CC flue gas, with the remaining flow going to a CO_2 scrubber. According to Dubey et al. [90] the CC cycle performance is unaffected by the heat recovery boiler arrangement, and it is only slightly impacted by the recirculation ratio. In similar circumstances, the system efficiency with partial recirculation and a CO_2 scrubber is 2-3% greater than the CO_2-based CC efficiency.

Energy economic analysis of the gas turbine system is a combustion system capable of generating a high amount of heat that can be used in more than one organic Rankine cycle to obtain the greatest thermal efficiency. generating the largest amount of electrical energy through the combine power plane, where the originality lies in making great use of the heat generated from the exhaust of the system gas turbine.

PART 3

METHODOLOGY

3.1. INTRODUCTION

This study has been arranged for the natural gas consolidated cycle (NGCC) consistent state examination. It comprises of two fundamental parts, the initial segment is the Brayton Cycle, which comprises of a gas turbine (GT), combustion chamber (CC), and an air compressor (AC), and the subsequent part addresses the natural rankine cycle, which comprises of an heat exchanger (HE), a Organic Rankine Turbine (ORT), condenser (CON2), siphon (P), and heat recovery boiler (HRB) (see Fig. 3.1). The working guideline of the installed framework can be summed up as follows.

At the point when air enters an air compressor (AC), it is compacted to working tension and warmed. The air is then shipped to a controller place where it responds with gaseous petrol fuel to shape high-pressure, high-temperature exhaust gases. Through the GT, the exhaust gases grow to deliver mechanical power. HRB changes over compressed water into steam at high temperatures utilizing the temperature of the exhaust gases. To create more mechanical energy, the fume is extended as it goes through the OFT. The water is compressed through the siphon after it enters the condenser which changes over the entire fume into a soaked fluid This development goes on through the three periods of the natural rankine cycle.

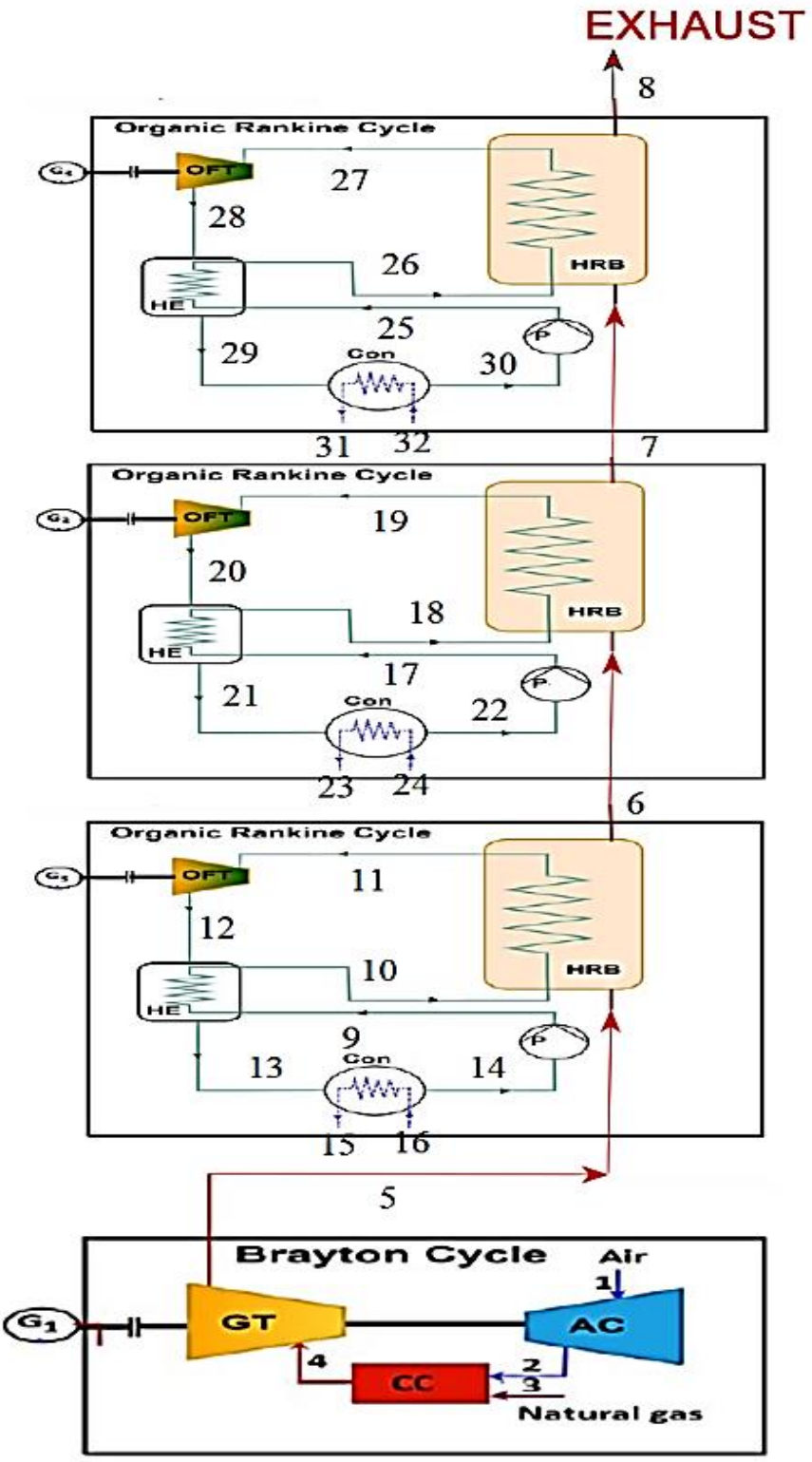

Figure 3.1. Schematic diagram of the NGCC and ORC.

3.2. GENERAL MASS, ENERGY AND EXERGY EQUATIONS

Both the organic rankine cycle (ORC) and the natural gas combined cycle (NGCC) are separate thermodynamic power-generation technologies. It is necessary to use fundamental thermodynamic principles, which are stated through generic mass, energy, and exergy equations, in order to comprehend how they function and how efficient they are. certain equations provide the theoretical framework for evaluating the effectiveness and performance of certain power generation systems. For the generation of significant amounts of electricity, NGCC power stations are frequently chosen. To get the most energy out of a given volume of natural gas, they combine two thermodynamic cycle, the Brayton cycle (a gas turbine) and the Rankine cycle (a steam turbine). We use the following equations to understand how an NGCC functions: This equation guarantees the steady-state operation essential presumption that the mass flow rates into and out of the system remain constant. The energy equation takes into consideration the work done by the gas turbine, the change in enthalpy of the working fluid, and the heat input (from the burning of natural gas). It measures the system's internal energy transfer. Exergy is a measure of a system's capacity for beneficial work. Exergy input (through fuel combustion), exergy output (via exhaust gases and work output), and exergy change are all tracked by the exergy equation. It sheds light on the losses and irreversibility's that occur during the NGCC cycle. When low-temperature heat sources, such geothermal or waste heat, are available, ORC systems are employed to generate electricity. Organic fluids with lower boiling points than water are used in these cycles. The mass equation assures that mass flow rates are conserved for steady-state operation, just like in the NGCC. The ORC's energy equation takes the heat input (from the heat source), the work done by the turbine, and the change in enthalpy of the organic working fluid into consideration. The energy transmission inside the ORC system is quantified. The ORC system's exergy equation keeps track of the exergy input which comes from the heat source exergy output which comes from work output and exhaust and the change in exergy. It gives an indication of the thermodynamic effectiveness of the system and the likelihood that usable work may be extracted from the low-temperature heat source. The general mass, energy, and exergy equations are crucial instruments for assessing the effectiveness and efficiency of NGCC and ORC power generation systems, in conclusion. These equations give engineers and researchers the ability to

evaluate how well these systems transform input energy into usable work and pinpoint areas for process development and optimization.

The conservation of mass equation for SSSF open system :[91]

$$\sum \dot{m}_{in} = \sum \dot{m}_{out} \quad (3.1)$$

where:

$\sum \dot{m}_{in}$: the total mass flow entering per unit time. , $\sum \dot{m}_{out}$: the total mass flow exiting per unit time. The energy balance for every part depends on the primary law of thermodynamics for SSSF open framework [1].:

$$\dot{Q} + \dot{W} = \sum \dot{m}_{out} h_{out} - \sum \dot{m}_{in} h_{\text{in}} \quad (3.2)$$

where:

$\dot{Q}$: The heat transfer per unit time. ,$\dot{W}$ Work done by the control volume per unit time, h_{in} : Specific enthalpy per the mass entering the system and h_{out} Specific enthalpy per mass leaving the system. dissimilar to mass and energy, entropy isn't monitored in open and shut frameworks, as entropy is delivered because of irreversibility. In open frameworks, the entropy equilibrium can be communicated as :[91]

$$\dot{E} = \dot{m}\psi \quad (3.3)$$

$$\psi = (h - h_0) - T_0(s - s_0) \quad (3.4)$$

where;

s_0: Specific entropy of the mass entering the open system. s: Specific entropy of the mass emanating from the open system. T_0 : The boundary temperature between the open system and the environment, $\dot{E}$: the exergy flows. ψ : the specific exergy.

Energy investigation doesn't give data about framework irreversibility because of entropy age and exergy obliteration. Subsequently, the thermodynamic presentation of NNCC frameworks ought to be finished by thinking about the second regulation proficiency. Exergy will be helpful to exploit the framework when you get a firsthand last routine with the climate.

3.3. THERMODYNAMIC ANALYSIS FOR BC MODEL

Most gas turbine power generation uses the Brayton Cycle (BC) model, a thermodynamic power cycle foundation. Optimising power plant performance under different working conditions requires BC model thermodynamic analysis. The cycle isentropic compression, constant pressure combustion, expansion, and heat rejection mechanisms are examined in detail. in the BC model, air is compressed, heated, and expanded to work on the turbine, which is directly connected to a generator. The BC model's efficiency depends on the compressor-turbine pressure ratio, gas temperature at the turbine input, and heat rejection at the conclusion of the cycle. These parameters are carefully calculated to maximize thermal energy to mechanical work conversion. under thermodynamic analysis, the BC model's thermal efficiency is a function of compressor and turbine efficiencies and cycle temperature restrictions. In actual life, non-isentropic compression and expansion, combustion chamber pressure decreases, and incomplete heat recovery reduce Brayton cycle efficiency. To accurately measure the cycle efficiency, the analysis integrates these practical considerations. The cycle energy output and efficiency depend on the working fluid and its constant pressure specific heat capacity. Variating the compressor pressure ratio, which affects net work production and cycle efficiency, and choosing an ideal turbine inlet temperature that the building materials can sustain without deterioration maximize the BC model's working condition. Operationally, the BC model's thermodynamic analysis evaluates load response, stability, and part-load performance. Power plants' ability to fulfill variable energy demands depends on these operational elements. The BC model's thermodynamic analysis additionally considers ambient temperature changes and component wear, which can dramatically impact cycle performance. by rigorously thermodynamically analyzing the BC model under various working conditions, engineers can develop strategies to reduce inefficiencies, extend the power plant's

lifespan, and maintain energy output, ensuring operational reliability and economic viability [49].

3.3.1. Compressor Model

air compressor, machines that utilization ability to make dynamic energy, pack and compress air and may deliver it in short explodes. Rotating air compressor are expected because of the huge stream paces of turbines and their relatively low-pressure proportions. Fiery connection for the air compressor model is changed as follow [2]:

Energy balance:

$$\dot{W}_{AC} = \dot{m}_{\text{air}} (h_2 - h_1) \tag{3.5}$$

Isentropic efficiency:

$$\eta_{AC} = \frac{\dot{W}_{AC,S}}{\dot{W}_{AC}} \tag{3.6}$$

Exegetic relations for the air compressor model are altered as follow:

Exergy balance:

$$\dot{E}_{D,AC} = \left(\dot{E}_1 - \dot{E}_2\right) + \dot{W}_{AC} \tag{3.7}$$

Exergy efficiency:

$$P_{\text{AC}} = \dot{E}_2 - \dot{E}_1 \tag{3.8}$$

$$F_{\text{AC}} = \dot{W}_{\text{AC}} \tag{3.9}$$

$$\varepsilon_{\text{AC}} = \frac{P_{\text{AC}}}{F_{\text{AC}}} = 1 - \frac{\dot{E}_{\text{D,AC}}}{F_{\text{AC}}} \tag{3.10}$$

Where;

P_{AC} : Product.
F_{AC} : Fuel.
$\varepsilon_{\mathrm{AC}}$: Exergy efficiency.

3.3.2. Combustion Chamber Model

The ignition chamber is the region of the gas turbine where energy is presented. The combustor is the wellspring of energy for the gas turbine cycle. It takes in air, adds fuel, joins the two, and afterward permits the blend to consume. This methodology is in many cases completed under ceaseless tension (albeit little strain misfortunes are by and large present). Temperature is a vital trademark during burning; it is normally limited by material characteristics. The materials should be impervious to outrageous temperatures and temperature angles. any other way, the gas turbine might come up short [92]

Exegetic connection for the ignition chamber model is altered as follow:

Energy balance:

$$\dot{m}_2 h_2 + \eta_{CC} \dot{m}_3 \mathrm{LHV} = \dot{m}_4 h_4 \tag{3.11}$$

Exergetic relations for the ignition chamber model are changed as follow:

Exergy balance:

$$\dot{E}_{\mathrm{D,CC}} = \dot{E}_2 + \dot{E}_3 - \dot{E}_4 \tag{3.12}$$

Exergy efficiency:

$$P_{\mathrm{CC}} = \dot{E}_4 \tag{3.13}$$

$$F_{CC} = \dot{E}_2 + \dot{E}_3 \tag{3.14}$$

$$\varepsilon_{CC} = \frac{P_{CC}}{F_{CC}} = 1 - \frac{\dot{E}_{D,CC}}{F_{CC}} \tag{3.15}$$

3.3.3. Gas Turbine Model

All gas turbines are planned as a joined conduit, where vaporous energy isn't provided nor eliminated, yet rather changed from strain and temperature to speed. As air moves from a major admission to a more modest leave, the speed of the air increments. At higher velocities, influence pressure rises. The general tension in the framework stays consistent, and since no energy is provided or removed, static strain drops. This might be seen as static tension being changed over completely to affect pressure, with the end goal that an expansion in static strain is joined by a progression of air by means of a united pipe and extension. any development brings about a comparing temperature decline. The gas turbine model involves creating a detailed mathematical representation or computer simulation of a gas turbine system, which is a type of internal combustion engine used for power generation and propulsion. This model aims to capture the complex interactions and thermodynamic processes within the gas turbine, allowing researchers, to analyze its behavior under various operating conditions. The model considers key parameters such as inlet temperature, pressure ratios, compressor and turbine efficiencies, combustion characteristics, and the specific design of the components. These tools enable a virtual representation of the gas turbine's components, such as the compressor, combustion chamber, and turbine, as well as the flow of air and gases throughout the system. By inputting different variables and scenarios into the model, researchers can simulate the performance of the gas turbine and evaluate how changes in design or operating conditions impact factors like efficiency, power output, and emissions [92].

Exergetic connection for the gas turbine model is altered as follow:

Energy balance:

$$\dot{W}_{GT} = \dot{m}_{gas}(h_4 - h_5) \quad (3.16)$$

Isentropic efficiency:

$$\eta_{GT} = \frac{\dot{W}_{GT,s}}{\dot{W}_{GT}} \quad (3.17)$$

Exegetic relations for the gas turbine model are altered as follow:

Exergy balance:

$$\dot{E}_{D,GT} = \left(\dot{E}_4 - \dot{E}_5\right) - \dot{W}_{GT} \quad (3.18)$$

Exergy efficiency:

$$P_{\mathrm{GT}} = \dot{W}_{GT} \quad (3.19)$$

$$F_{\mathrm{GT}} = \dot{E}_4 - \dot{E}_5 \quad (3.20)$$

$$\varepsilon_{\mathrm{GT}} = \frac{P_{\mathrm{GT}}}{F_{\mathrm{GT}}} = 1 - \frac{\dot{E}_{\mathrm{D,GT}}}{F_{\mathrm{GT}}} \quad (3.21)$$

3.4 THERMODYNAMIC ANALYSIS FOR ORC MODEL

The concept delineates the fundamental principles and constituent elements of the organic rankine cycle (ORC) model, which is a pivotal concept in the examination and enhancement of energy conversion processes via thermodynamic analysis. The ORC model comprises four fundamental components: an expander (turbine), a pump, an evaporator, and a condenser. ORC systems differ from traditional rankine cycle in that they employ organic fluids with lower boiling points as the working fluid. The choice of organic fluid is determined by the specific application and the temperature of the heat source. The decision is pivotal in guaranteeing efficient energy conversion. The ORC model functions by employing four essential processes: isentropic compression,

isothermal heat addition, isentropic expansion, and heat release in the condenser. during isentropic compression, a pump elevates both the pressure and temperature of the working fluid. The evaporator enables isothermal heat transfer by absorbing thermal energy from a heat source operating at a lower temperature, resulting in the evaporation of the fluid at a consistent temperature. The turbine undergoes isentropic expansion, converting high-pressure, high-temperature vapor into mechanical work. The condenser facilitates the conversion of the working fluid from a gaseous state to a liquid state by transferring heat to a cooling medium maintained at a consistent temperature. The temperature of the heat source has a substantial impact on the efficiency of the ORC system. The text emphasizes the significance of thermodynamic analysis in comprehending the process by which the ORC model converts low-temperature heat into practical work. The analysis allows engineers and scientists to tailor ORC systems for specific uses, choose suitable working fluids, and improve overall energy efficiency. It highlights the ORC model as a vital tool for efficient and sustainable energy conversion [48].

The organic rankine cycle model, with its unique utilization of organic fluids and isentropic processes, represents a sophisticated and versatile approach to energy conversion. Through thermodynamic analysis, engineers gain insights into the intricacies of the ORC system, allowing for tailored designs, improved efficiency, and a more sustainable harnessing of low-temperature heat sources. As the quest for effective and environmentally friendly energy solutions continues, the ORC model stands out as a valuable tool contributing to the advancement of sustainable energy conversion technologies.

3.4.1. HRB Model

The temperature of the steam delivered in the waste intensity recuperation heater is firmly connected with the temperature of the fume’s gas. on the off chance that the temperature of the fumes gas is inadequate to create the ideal steam temperature, augmentations, for example, helper burners are made into the heater. [93] Lively connection for the HRSG model is adjusted as follow:

Energy balance:

$$\dot{m}_6 + \dot{m}_{18} = \dot{m}_7 + \dot{m}_{19} \quad (3.22)$$

$$\dot{Q}_{HRB} = \dot{m}_{18}(h_{19} - h_{18}) \quad (3.23)$$

Exergetic relations for the HRSG model are modified as follow:

Exergy balance:

$$\dot{E}_{\mathrm{D},HRB} = \dot{E}_6 - \dot{E}_7 + \dot{E}_{18} - \dot{E}_{19} \quad (3.24)$$

Exergy efficiency:

$$P_{HRB} = \dot{E}_{19} - \dot{E}_{18} \quad (3.25)$$

$$F_{HRB} = \dot{E}_6 - \dot{E}_7 \quad (3.26)$$

$$\varepsilon_{HRB} = \frac{P_{HRB}}{F_{HRB}} = 1 - \frac{\dot{E}_{\mathrm{D},HRB}}{F_{HRB}} \quad (3.27)$$

3.4.2. ORT Model

The steam turbine's motivation is to change the steam's nuclear power into mechanical energy. The steam is conveyed from the primary extension region of the turbine to the edges on the rotor and grows to the gathering pressure. The spoiled steam passes from the turbine body to the condenser. [92] Lively connection for the steam turbine model is altered as follow:

Energy balance:

$$\dot{W}_{\mathrm{OFT}} = \dot{m}_{19}(h_{20} - h_{19}) \quad (3.28)$$

Isentropic efficiency:

$$\eta_{\mathrm{OFT}} = \frac{\dot{W}_{\mathrm{OFT},s}}{\dot{W}_{\mathrm{OFT}}} \quad (3.29)$$

Exergetic relations for the steam turbine model are modified as follow:

Exergy balance:

$$\dot{E}_{\mathrm{D,OFT}} = \left(\dot{E}_{19} - \dot{E}_{20}\right) - \dot{W}_{\mathrm{OFT}} \quad (3.30)$$

Exergy efficiency:

$$P_{\mathrm{OFT}} = \dot{E}_{19} - \dot{E}_{20} \quad (3.31)$$

$$F_{\mathrm{OFT}} = \dot{W}_{\mathrm{OFT}} \quad (3.32)$$

$$\varepsilon_{\mathrm{OFT}} = \frac{P_{\mathrm{OFT}}}{F_{\mathrm{OFT}}} = 1 - \frac{\dot{E}_{\mathrm{D,OFT}}}{F_{\mathrm{OFT}}} \quad (3.33)$$

3.4.3. Condenser Model

The condensers are the kind of intensity exchanger, and their motivation is to change over the spoiled steam from the turbine body into the water by consolidating it with the assistance of cooling water. The water-cooled condensers are liked in the fume power plants in view of lower gathering pressure contrasted with the air-cooled framework, simpler control of consolidating pressure, higher intensity move because of the great intensity limit of water. [92] The enthusiastic connection for the condenser model is adjusted as follow:

Energy balance:

$$\dot{m}_{21} + \dot{m}_{24} = \dot{m}_{22} + \dot{m}_{23} \quad (3.34)$$

$$\dot{Q}_{COND2} = \dot{m}_{21}(h_{22} - h_{21}) \quad (3.35)$$

Exergetic relations for the condenser model are modified as follow:

Exergy balance:

$$\dot{E}_{\mathrm{D},\,COND2} = \left(\dot{E}_{21} - \dot{E}_{22}\right) + \left(\dot{E}_{23} - \dot{E}_{24}\right) \tag{3.36}$$

Exergy efficiency:

$$P_{COND2} = \dot{E}_{24} - \dot{E}_{23} \tag{3.37}$$

$$F_{COND2} = \dot{E}_{21} - \dot{E}_{22} \tag{3.38}$$

$$\varepsilon_{COND2} = \frac{P_{COND2}}{F_{COND2}} = 1 - \frac{\dot{E}_{\mathrm{D},COND2}}{F_{COND2}} \tag{3.39}$$

3.4.4. Pump Model

The obligation of the feedwater siphon is to assimilate the compressed water required for steam creation from the feed tank and send it to the framework. air compressor and siphons are equivalent in that the two of them help strain in a liquid and push it through a line. compressible gases will be diminished in volume when they are compacted by the air compressor. Fluids are difficult to pack; while some are more straightforward to compress, siphons for the most part work to compress and move fluids. [92,94] Fiery relations for the siphon model are altered as follow:

Energy balance:

$$\dot{W}_{\mathrm{Pump3}} = \dot{m}_{22}(h_{17} - h_{22}) \tag{3.40}$$

Isentropic efficiency:

$$\eta_{\mathrm{Pump2}} = \frac{\dot{W}_{\mathrm{Pump2},s}}{\dot{W}_{\mathrm{Pump2}}} \tag{3.41}$$

Exergetic relations for the pump are modified as follow:

Exergy balance:

$$\dot{E}_{\text{D, Pump2}} = \left(\dot{E}_{22} - \dot{E}_{17}\right) + \dot{W}_{\text{Pump2}} \tag{3.42}$$

Exergy efficiency:

$$P_{\text{Pump3}} = \dot{E}_{17} - \dot{E}_{22} \tag{3.43}$$

$$F_{\text{Pump3}} = \dot{W}_{\text{Pump3}} \tag{3.44}$$

$$\varepsilon_{\text{Pump3}} = \frac{P_{\text{Pump3}}}{F_{\text{Pump3}}} = 1 - \frac{\dot{E}_{\text{D,Pump3}}}{F_{\text{Pump3}}} \tag{3.45}$$

3.4.5. HE Model

The temperature of the steam delivered in the waste intensity recuperation boilers is firmly connected with the temperature of the fume's gas. In the event that the temperature of the fumes gas is deficient to deliver the ideal steam temperature, augmentations, for example, assistant burners are made into the evaporator. [93]
Vivacious connection for the HRSG model is adjusted as follow:

Energy balance:

$$\dot{m}_{17} + \dot{m}_{20} = \dot{m}_{18} + \dot{m}_{21} \tag{3.46}$$

$$\dot{Q}_{HE} = \dot{m}_{17}(h_{18} - h_{17}) \tag{3.47}$$

Exergetic relations for the HE model are modified as follow:

Exergy balance:

$$\dot{E}_{\mathrm{D,HE}} = \dot{E}_{17} - \dot{E}_{18} + \dot{E}_{20} - \dot{E}_{21} \quad (3.48)$$

Exergy efficiency:

$$P_{\mathrm{HE}} = \dot{E}_{21} - \dot{E}_{20} \quad (3.49)$$

$$F_{\mathrm{HE}} = \dot{E}_{17} - \dot{E}_{18} \quad (3.50)$$

$$\varepsilon_{\mathrm{HE}} = \frac{P_{\mathrm{HE}}}{F_{\mathrm{HE}}} = 1 - \frac{\dot{E}_{\mathrm{D,HE}}}{F_{\mathrm{HE}}} \quad (3.51)$$

3.5. ECONOMIC ANALYSIS

The chief expenses of a warm framework are the capital venture, the activity and upkeep, and the fuel costs. In light of the capital recuperation factor (CRF) an improved on financial model can be applied. [90] The complete capital venture (TCI) in a plant is given by the amount of all the bought gear costs (PEC) duplicated by a steady component. The all-out capital interest in a plant is in this way given by:

$$\dot{Z}_k = \frac{Z_k \times CRF \times \phi}{N \times 3600} \quad (3.52)$$

Where;

PEC: the equipment's purchase cost in US dollar. φ: the maintenance factor (1.06). CRF: the Capital Recovery Factor, which can be calculated as:

$$\mathrm{CRF} = \frac{i(1+i)^n}{(1+i)^n - 1} \quad (3.53)$$

Where i: the interest rate (consider to be 10%) n: lifetime of the system (consider to be 20 years). The buy gear cost (PEC) for the NGCC parts is as per the following:

Brayton cycle part costs : [92]

Based on variables including the system's size, application, and the standard of the materials and components employed, the cost of the components in a Brayton Cycle varies considerably. Some of the important factors that can affect the overall cost include compressors, combustor, turbines, heat exchangers, power electronics, fuel delivery systems, control and monitoring systems, materials, size and capacity, emissions and environmental controls, maintenance and operating costs, and research and development costs. The entire cost of a Brayton Cycle may be affected by the material choice, size and capacity, emissions and environmental controls, maintenance and operating expenses, and research and development expenditures. When determining the cost of a Brayton cycle for a particular application, it is essential to do a thorough cost analysis and take particular needs into account.

Air compressor

$$\dot{Z}_{Ac} = (71.1m40.9 - \eta_{Ac})(P_5 P_4)\mathrm{Ln}\,(P_5 P_4) \tag{3.54}$$

Combustion chamber

$$\dot{Z}cc = (46.08m40.995 - P_7 P_5)(1 + \exp - (0.018T_7 - 26.4)) \tag{3.55}$$

Gas turbine

$$\dot{Z}_{GT} = (479.34m70.92 - \eta_T)\mathrm{Ln}\,(P_7 P_8)(1 + \exp - (0.036T_7 - 54.4)) \tag{3.56}$$

Steam turbine

$$\dot{Z}_{ST} = 6000(\dot{W}_{ST})0.7 \tag{3.57}$$

Heat recovery steam generation

$$\dot{Z}_{HRSG} = 130(AB0.093)0.78 \tag{3.58}$$

Condenser

$$Z_{Cond} = 1773m \quad (3.59)$$

Pump

$$Z_{FC} = (71.1m10.9 - \eta_{FC})(P_2P_1)Ln\ (P_2P_1) \quad (3.60)$$

Deaerator

$$Z_{Deaerator} = 52000m \quad (3.61)$$

Organic Steam turbine

$$Z_{OST} = (71.1m10.9 - \eta_{FC})(P_2P_1)Ln\ (P_2P_1) \quad (3.62)$$

Organic Pump

$$Z_{FC} = (2100m10.9 - \eta_{FC})(P_2P_1)Ln\ (P_2P_1) \quad (3.63)$$

Organic Condenser

$$Z_{Cond} = 1773m \quad (3.64)$$

Organic Evaporator

$$Z_{EV} = 235(Q)0.75 \quad (3.65)$$

Organic Heat exchanger

$$Z_{HE} = 235(Q)0.75 \quad (3.66)$$

3.6. COST PERFORMANCE

The framework all out cost rate, barring fuel costs (Ż) is the summation over all parts of $\left(\dot{Z}_{\mathrm{k}}^{\mathrm{M}}\right)$ from following condition: [95]

$$\dot{Z}_{\mathrm{T}} = \sum_k \dot{Z}_{\mathrm{k}} = \sum_k \left(\dot{Z}_{\mathrm{k}}^{\mathrm{N}} + \dot{Z}_{\mathrm{k}}^{\mathrm{OM}}\right) = \frac{\sum_{\mathrm{k}} \mathrm{CRF}\ \beta(1+\gamma)\mathrm{PEC}_{\mathrm{k}}}{\tau} \tag{3.67}$$

3.7. ASSUMPTIONS AND INPUT PARAMETER TO THE COMBINED SYSTEM

The overall presumptions made for the recreation of the joined framework are recorded as follows:

All part of the joined framework works under consistent state conditions compositions of air at the channel of AC are 79% N_2 and 21% O_2

1. Natural gas is totally oxidized in the CC.
2. Ideal gas standards apply to the fume's gases.
3. The CC is protected totally

The info information for NGCC examination enlisted in table 3.1.

Table 3.1. Operation conditions used for the NGCC [96].

Parameter	Value
Compression ratio	12
Mass flow rate of fuel, kg/s	2.4
Mass flow rate of exhaust gases, kg/s	145
Exhaust gases temperature, K	400
Ambient temperature, K	288
Boiler pressure, bar	100
Condenser pressure, bar	0.5
Steam turbine inlet temperature, K	750
Turbine efficiency, %	90
Compressor efficiency, %	86
Pump efficiency, %	85

3.8. COMBINED SYSTEM INTEGRATION IN EES

EES program is utilized in the reenactment of the NGCC. The program offers basic arrangements, advancement, and charting. Mass equilibrium, energy balance, exergy balance examination of every part has been finished by utilizing the EES program. Also, various examinations were finished by utilizing EES to find the impact of the information boundaries on the NGCC, for example, work net, warm effectiveness, exergy proficiency, and energy cost. These are summed up in table 3.2. The consequences of the recreation will be analyzed in the accompanying section. Figure 3.2 presents the stream graph for the EES programming in light of numerical demonstrating of the NGCC.

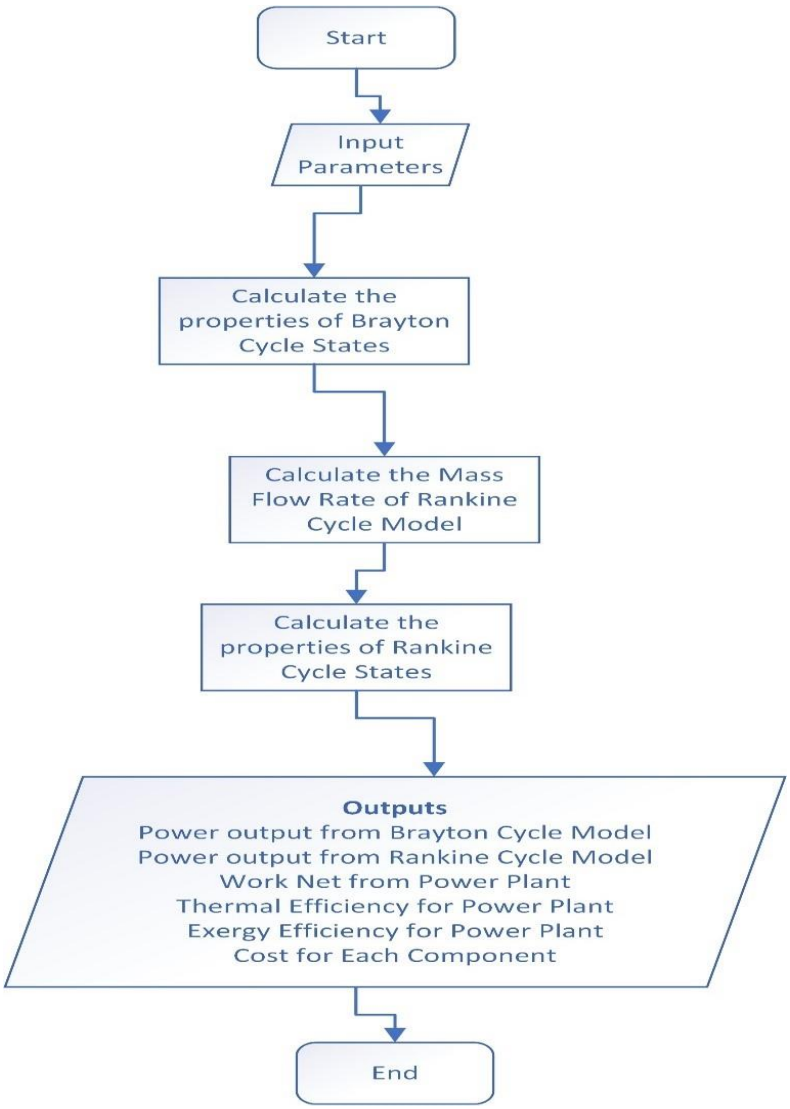

Figure 3.2. Flow chart of the NGCC.

Table 3.2. NGCC performance [96].

Array Sequence	Parameter	Unit
1	Net output power	MW
2	Overall exergy efficiency	%
3	Overall thermal efficiency	%
4	Input exergy	MW
5	Exergy destruction	MW
6	Total cost of brayton cycle components	USD/h
7	Total cost of rankine cycle components	USD/h
8	Total cost of the combined system	USD/h
9	Electricity cost of brayton cycle	USD/h
10	Electricity cost of rankine cycle	USD/h
11	Electricity cost of the combined system	USD/h

PART 4

RESULTS AND DISCUSSION

A potential strategy to improve the effectiveness and overall performance of energy systems is to combine different power producing technologies. Three Organic Rankine cycle (ORC) units and one gas turbine cycle (GTC) are coupled in a single power plant in one novel arrangement. This setup attempts to increase overall energy conversion efficiency and maximize the use of various heat sources. The organic Rankine cycle is a thermodynamic process that converts low-temperature heat sources into electricity by using organic fluids with lower boiling temperatures than water. The gas turbine cycle, on the other hand, is renowned for its high-power output and efficiency in turning fuel energy into electricity. It is powered by burning natural gas or other fuels. The power plant may use both low- and high-temperature heat sources by integrating various technologies, optimizing the use of available energy. while the gas turbine cycle effectively transforms fuel energy into electricity, the three ORC units may collect energy from a variety of waste heat sources. An improved and more reliable power generating system that can adjust to various heat sources and demand changes is made possible by the integration of these cycle. Complex thermodynamic calculations, heat transport analysis, and fluid dynamics models go into the simulation of this integrated power plant. The behavior of each component within the power plant is simulated, and sophisticated modeling tools and software are utilized to forecast the performance of the whole system. engineers and scientists may improve a system's efficiency, power production, and environmental effect by analyzing numerous operating factors, heat source fluctuations, and load situations. This hybrid power plant structure exemplifies a cutting-edge strategy for energy production that combines many technologies to provide a more effective and sustainable energy source. Such integrated power production systems show tremendous potential in assisting in the development of a cleaner and more sustainable energy future as the globe searches for solutions to lower greenhouse gas emissions and increase energy efficiency.

4.1. VALIDATION

The impact of isentropic efficiency (AC) on air compressor performance and overall cost rate. The data showed that a rise in AC corresponds to an increase in net and GSO CC system efficiency. Increasing the AC will result in a decrease in the power needed to run the compressor, which will increase the power output of the gas turbine if the airflow rates remain constant. Total net increases from 215.6 MW to 275 MW with a change in AC from 70% to roughly 88%. The cycle first- and second-law efficiencies would increase if AC was boosted. The findings suggest that raising AC is necessary to achieve improved efficiency. But this is not cost-effective. Based on these results, a reduced cycle's overall cost is obtained by boosting AC from 70% to roughly 84%. however, increasing AC further will increase the cycle overall cost beyond 84% superfast. From Figure 4.1, it is evident that the similarities in the results obtained through the computational simulation process are that the error rate does not exceed 10%, which is a good percentage for comparison with previous research.

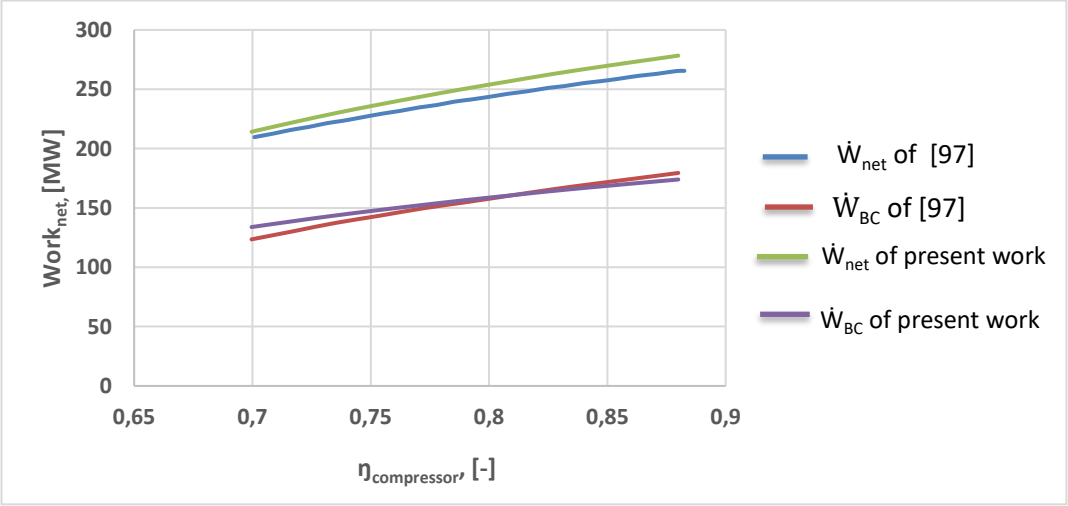

Figure 4.1. Variation of $\dot{W}_{net}$ with η_{AC}.

Also a simulation was made for the present work and the previous work [97] regarding the input temperature and pressure ratio of the brayton cycle and because of the Brayton cycle is a similar part, the results were with regard to temperature, the difference ratio is 2.5 % and with regard to the pressure ratio it was 2.6% These are very similar results.

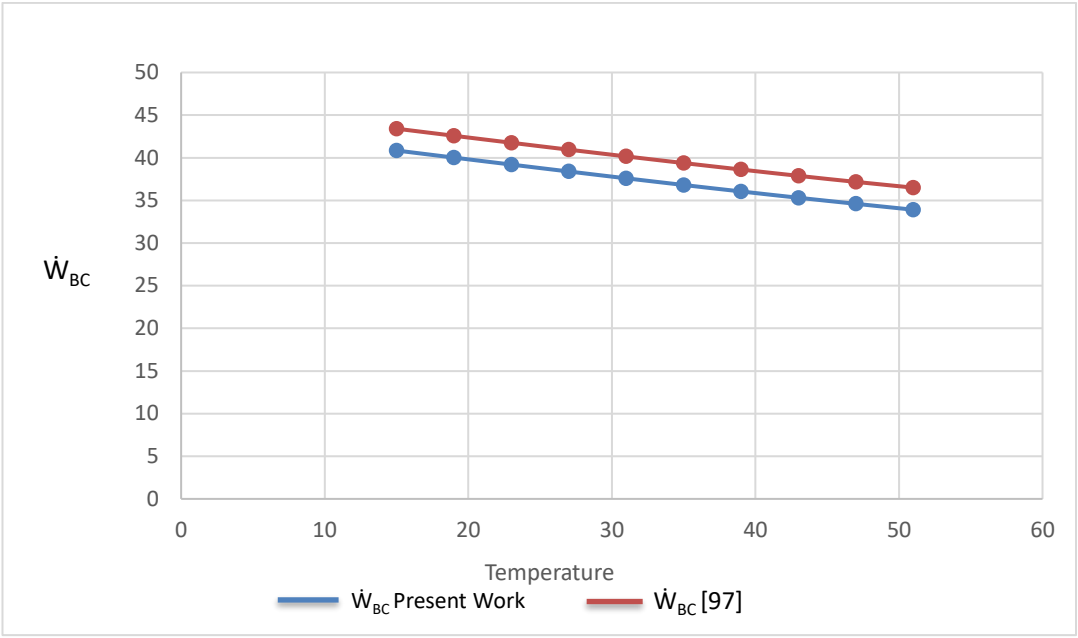

Fiqure 4.2. Compression $\dot{W}_{BC}$ with temperature.

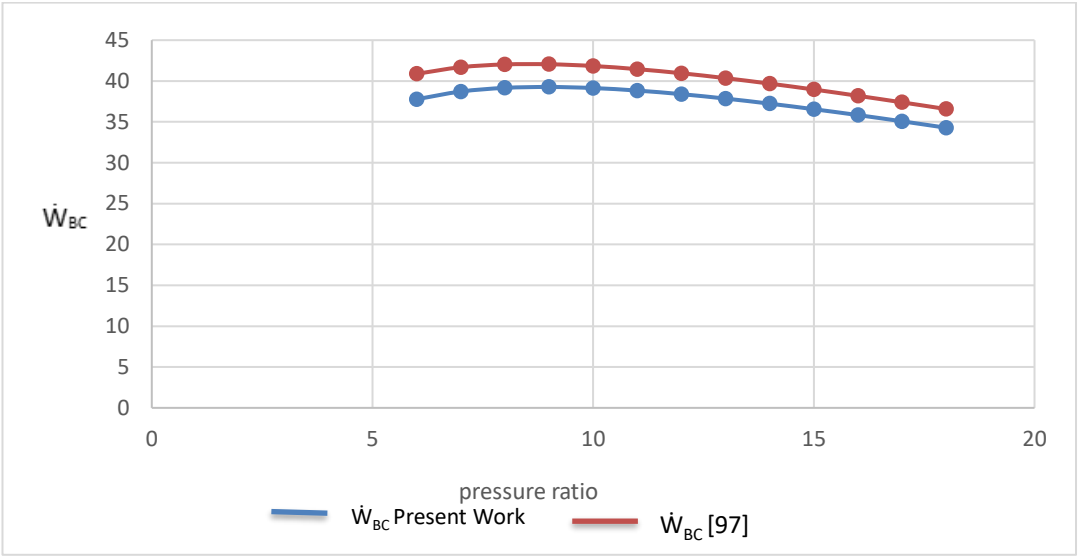

Fiqure 4.3. Compression $\dot{W}_{BC}$ with pressure ratio.

4.2. EFFECT THE AMBIENT TEMPERATURE ON COMBINES CYCLE PERFORMANCE

The performance of combined power cycles, such as those that combine organic rankine cycle (ORC) units with gas turbine cycles (GTC), is greatly influenced by the ambient temperature. understanding how the temperature of the environment affects these cycles' performance is crucial for increasing the combined power plant's output

and efficiency. the temperature of the air entering the compressor has a significant impact on the efficiency of a gas turbine cycle. reduced air density brought on by higher ambient temperatures has an impact on the compressor's operation. Reduced cycle efficiency results from the compressor having to work more to obtain the necessary compression ratio as the air gets less dense. the "compressor stall" phenomenon may lead to a reduction in power production and an increase in fuel consumption. the temperature differential between the heat source and the cooling medium affects ORC systems. The temperature at which heat is supplied and the temperature at which heat is rejected define the ORC cycle efficiency. the effectiveness of the ORC units may decline as a result of lower temperature differences brought on by higher ambient temperatures. Temperature fluctuations may also have an impact on how well the ORC working fluid performs, which might modify the fluid's properties and how it transfers heat. the waste heat from the gas turbine's exhaust may be used as a heat source for the ORC units in a combined cycle setup. the energy available for the ORC cycle may be improved by higher exhaust gas temperatures, which may result from higher ambient temperatures. The decreased efficiency of the gas turbine cycle owing to warmer input air temperatures, however, may cancel out the efficiency increase. to sustain peak performance, the ORC cycle and gas turbine both need cooling. the efficacy of both cycles may be impacted by higher ambient temperatures, which may also have an effect on the effectiveness of cooling systems. In order to keep components from overheating and performing poorly, adequate cooling becomes essential. these temperature-related interactions have an impact on the combined cycle overall efficiency and power production. The efficiency of the combined system at various ambient temperatures must be carefully considered when individual cycle efficiencies are being optimized. Engineers must take into account these temperature-related effects while constructing and running a combined cycle power plant that consists of both ORC units and a gas turbine to enhance overall performance and efficiency. For the best results, operational parameters and heat source consumption may be fine-tuned by using simulation and modeling to forecast the system behavior under various ambient temperature circumstances.

Figure 4.4 shows the effect of entry temperatures on the total efficiency of the system, as the increase in the entry temperature reduces the efficiency of the system, and therefore the entry temperature value of 51℃ was the worst case, as the energy efficiency reached 38.5%, while the best temperature reached is at the temperature is 15°C, as the efficiency reached 40.01%.

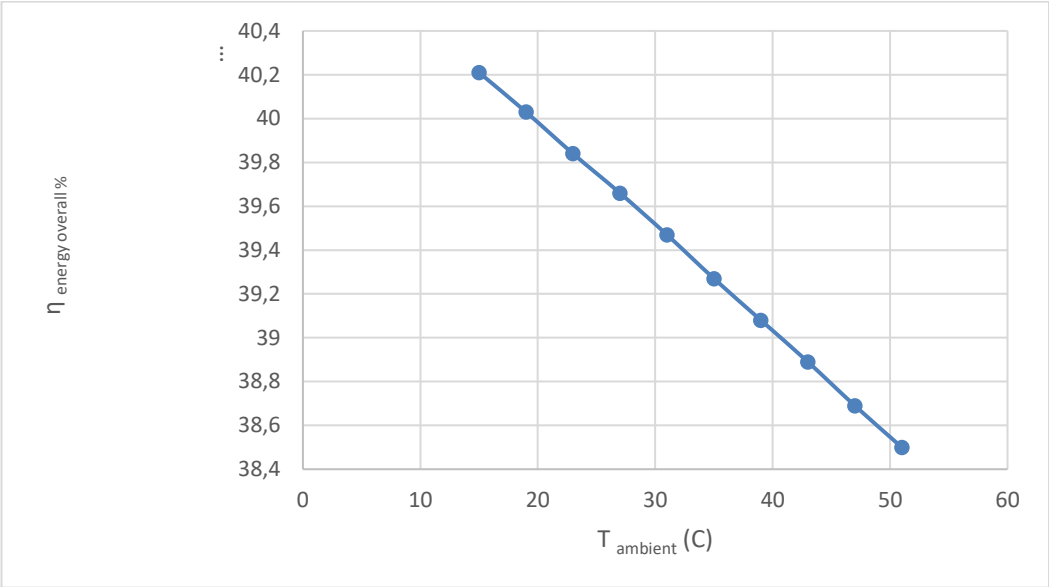

Figure 4.4. Variation of η energy overall with ambient temperature.

Figure 4.5 shows the effect of entry temperatures on the exergy of the system, where the increase in the entry temperature reduces the exergy of the system, and therefore the entry temperature value of 51°C was the worst case, as the exergy reached 37.1%, while the best temperature was reached at temperature 15℃ , where the efficiency reached 38.9%.

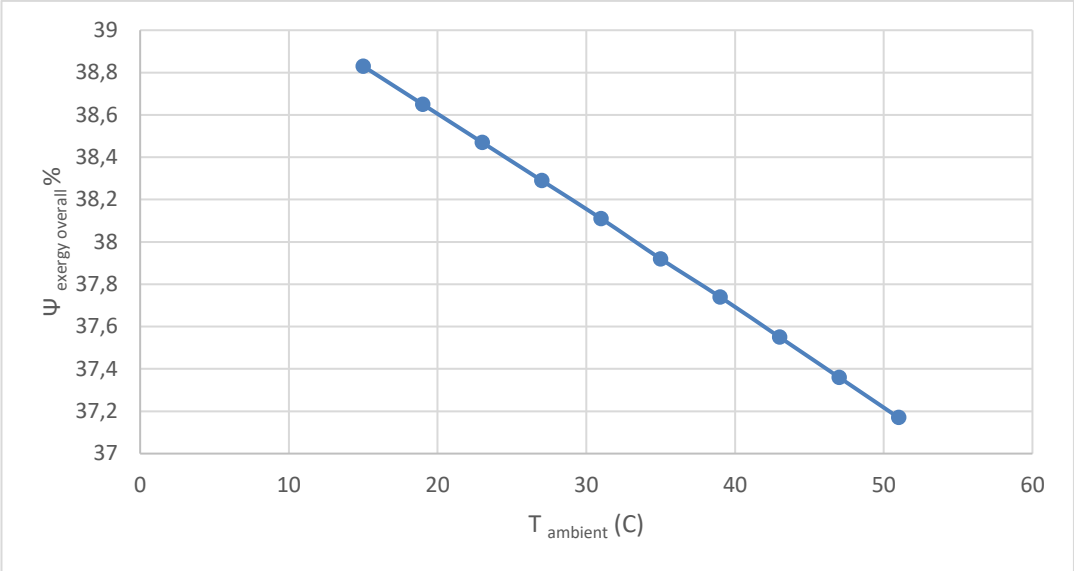

Figure 4.5. Variation of Ψ_{exergy} overall with ambient temperature.

Figure 4.6 shows the effect of entry temperatures on the cycle occupancy, as the increase in the entry temperatures reduces the cycle occupancy, and therefore the entry temperature value of 51°C was the worst case, as the total occupancy reached 50.8 kJ, while the best temperature reached is at the 15°C, where the total work was 57.8 kJ.

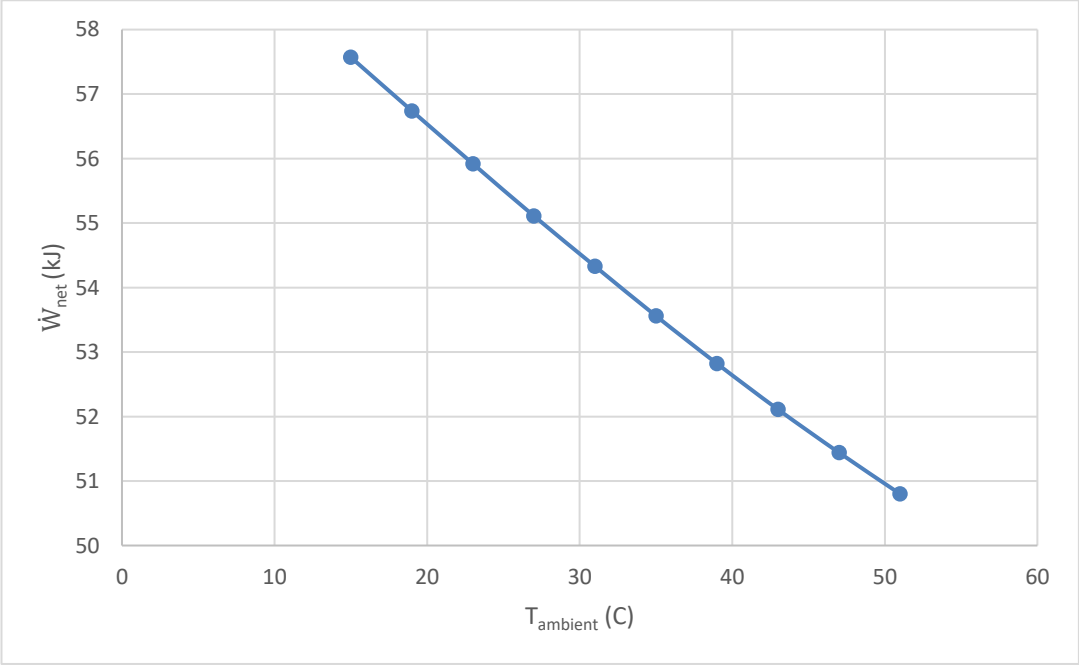

Figure 4.6. Variation of $\dot{W}_{net}$ with ambient temperature.

Figure 4.7 shows the effect of entry temperatures on the occupancy of the gas turbine cycle, as the increase in the entry temperatures reduces the occupancy of the gas turbine cycle. Therefore, the entry temperature value of 51 ℃ was the worst case, as the total occupancy reached 36.5 kJ, while the best temperature was reached. It is at a temperature of 15℃ , where the gas turbine cycle occupancy reached 43.5 kJ.

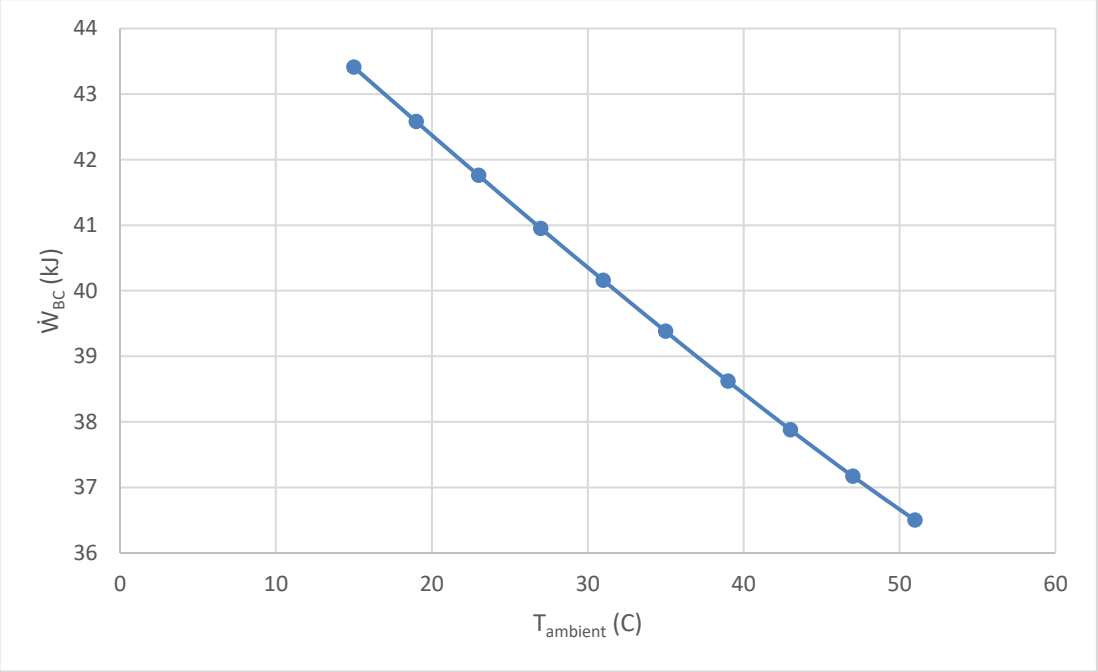

Figure 4.7. Variation of $\dot{W}_{BC}$ with ambient temperature.

Figure 4.8 shows the effect of entry temperatures on the cost of electric energy, as the increase in entry temperatures increases the cost of electrical energy. Therefore, the entry temperature value of 51°C was the worst case, as the cost of electrical energy reached 2.14 USD/MWh, while the best cost of electrical energy was It is reached at a temperature of 15°C, where the cost of electric energy reached 1.86 USD/MWh.

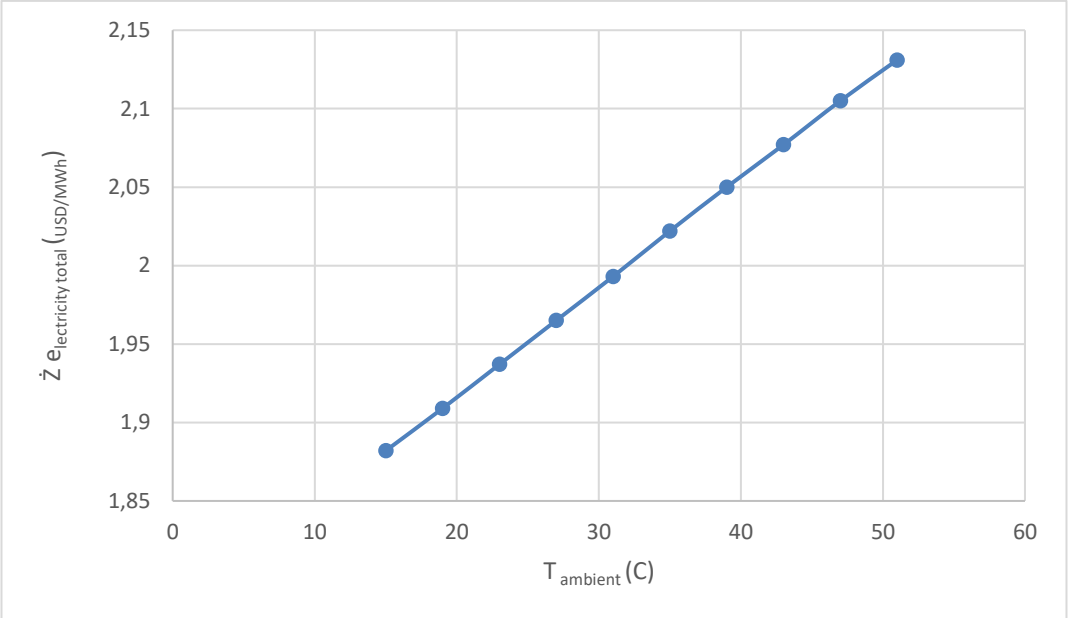

Figure 4.8. Variation of Ż electricity total with ambient temperature.

4.3. EFFECT THE PRESSURE RATIO ON COMBINES CYCLE PERFORMANCE

The performance of combined power cycles, which contain both Organic Rankine cycle (ORC) units and gas turbine cycles (GTC), is greatly influenced by the pressure ratio. The pressure ratio affects different elements of the cycle thermodynamic behavior by measuring the relationship between a cycle peak and lowest pressures. The efficiency and power output of a gas turbine cycle are directly impacted by the pressure ratio. higher-pressure ratios need greater work input since the compression process in the gas turbine's compressor uses a large amount of labor. Due to rising labor demands and increased losses, the compression process becomes less effective as the pressure ratio rises. The pressure ratio has an impact on the working fluid's evaporating and condensing phases in an ORC system. higher pressure ratios may improve the cycle's capacity to reject heat to the cooling medium and remove heat from the heat source. As a consequence, the ORC units may operate more efficiently and perform better at transferring heat. The temperature of the exhaust gases is influenced by the pressure ratio of the gas turbine cycle, which in turn impacts the heat supply to the ORC units. Increased exhaust gas temperatures brought on by higher pressure ratios may provide more heat energy to the ORC units for greater power

output. the overall effectiveness of the gas turbine cycle itself may be adversely impacted by the rise in pressure ratio, which would reduce the total benefit of the combined system. the combined cycle total efficiency and power production are significantly influenced by the pressure ratio. To maximize the performance of the combined system, the pressure ratios of the gas turbine and ORC cycles must be balanced. Although a larger pressure ratio in one cycle may boost the possibility for heat recovery, it may also result in higher cycle losses, which would reduce the efficiency of the whole system. The power plant's unique requirements, such as the available heat sources, the capacity for cooling, and the intended production of power, must be carefully considered when choosing the pressure ratio as a design parameter. An ideal pressure ratio guarantees that the energy sources that are now accessible are used effectively while maintaining a fair component efficiency. In conclusion, the efficiency, power production, and overall effectiveness of combined power cycle are greatly impacted by the pressure ratio. the pressure ratios for both the gas turbine and ORC cycles need to be carefully considered by engineers and researchers, taking into consideration the trade-offs between greater heat recovery potential and possible efficiency losses. the design and operation of effective combined power plants may be guided by simulation and modeling tools, which can be used to evaluate the impact of various pressure ratios on cycle performance.

Figure 4.9 shows the effect of pressure ratio on the total efficiency of the system, as the increase in the pressure ratio increase the efficiency of the system, and therefore the pressure ratio value of 6 was the worst case, as the energy efficiency reached 35.9%, while the best efficiency reached is at pressure ratio is 15, as the efficiency reached 40.01%.

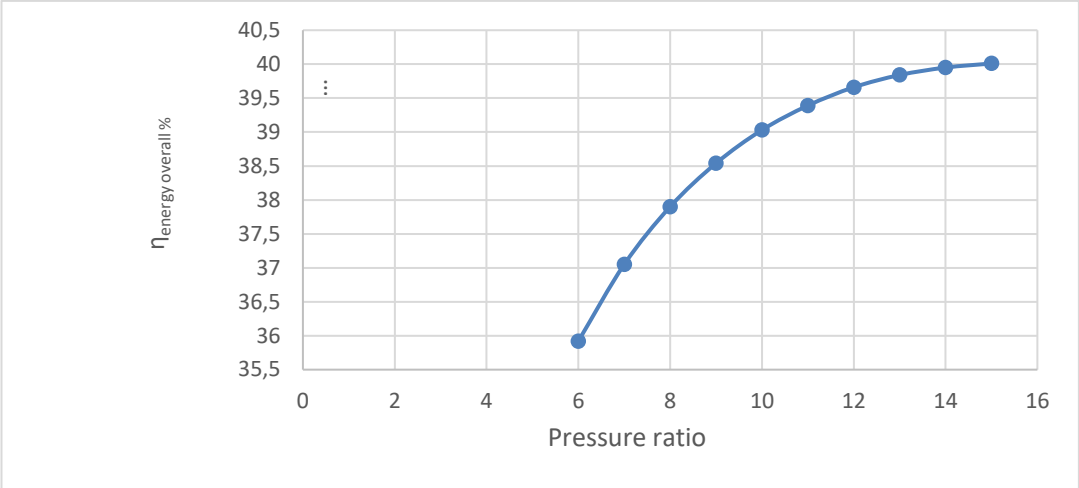

Figure 4.9. Variation of η_{energy} overall with pressure ratio.

Figure 4.10 shows the effect of pressure ratio on the exergy of the system, where the increase in the pressure ratio increases the exergy of the system, and therefore the pressure ratio value of 6 was the worst case, as the exergy reached 34.6%, while the best exergy was reached at pressure ratio 15, where the efficiency reached 38.7%.

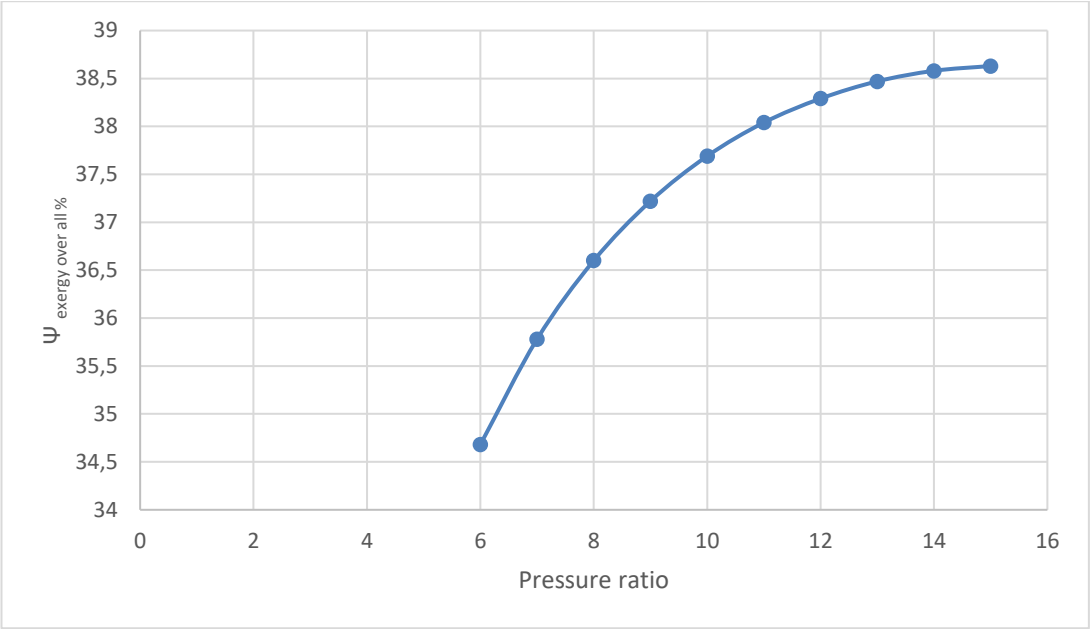

Figure 4.10. Variation of Ψ_{exergy} overall with pressure ratio.

Figure 4.11 shows the effect of pressure ratio on the cycle work net, as the increase in the pressure ratio reduces the cycle work net, and therefore the pressure ratio 7 was the worst case, as the total work reached 58.5 kJ, while the best work reached is at the 15,

where the total work was 52.2 kJ.

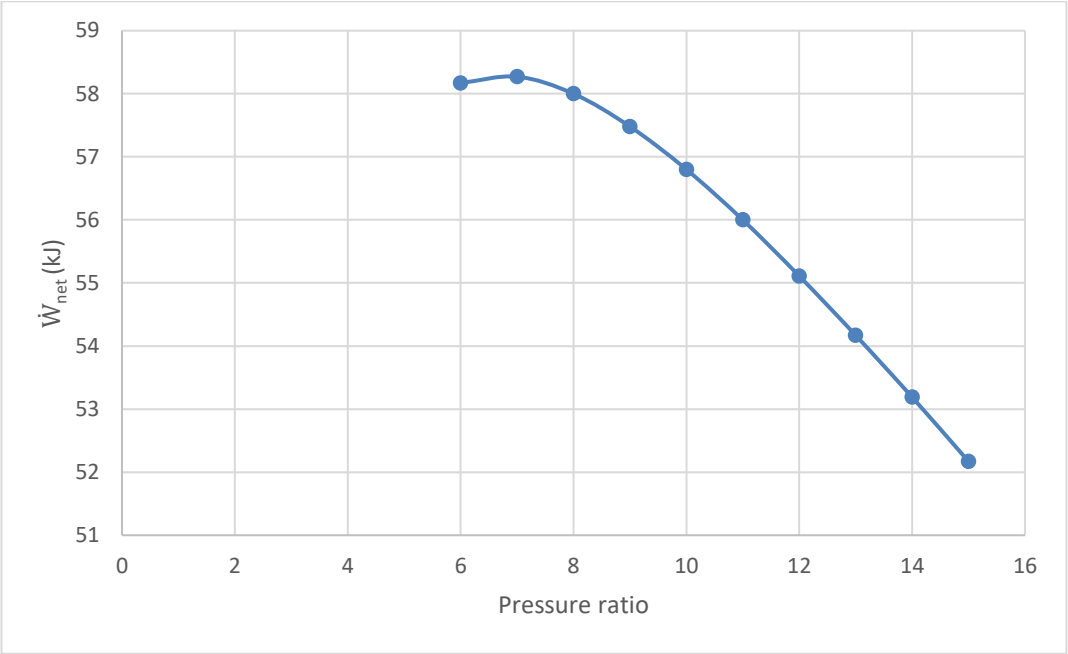

Figure 4.11. Variation of $\dot{W}_{net}$ with pressure ratio.

Figure 4.12 shows the effect of pressure ratio on the work of the gas turbine cycle, as the increase in the pressure ratio reduces the work of the gas turbine cycle. Therefore, the pressure ratio value of 15 was the worst case, as gas turbine cycle work reached 38.8 kJ, while the best work of the gas turbine cycle was reached. It is at a pressure ratio of 9, where the gas turbine cycle work reached 42.2 kJ.

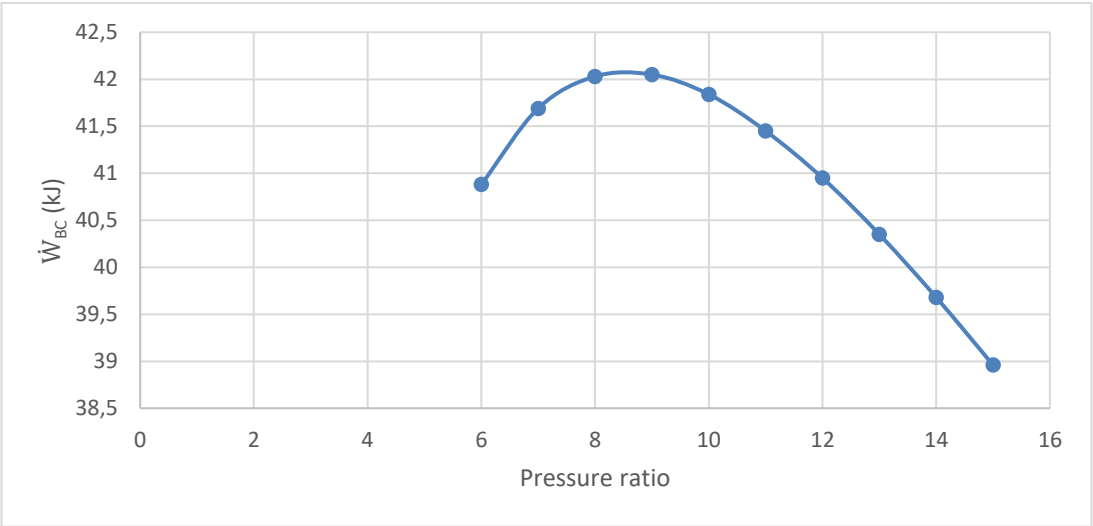

Figure 4.12. Variation of $\dot{W}_{BC}$ with pressure ratio.

Figure 4.13 shows the effect of pressure ratio on the cost of electric energy, as the increase in pressure ratio increases the cost of electrical energy. Therefore, the pressure ratio value of 15 was the worst case, as the cost of electrical energy reached 2.4 USD/MWh, while the best cost of electrical energy was It is reached at a pressure ratio of 6, where the cost of electric energy reached 1.25 USD/MWh.

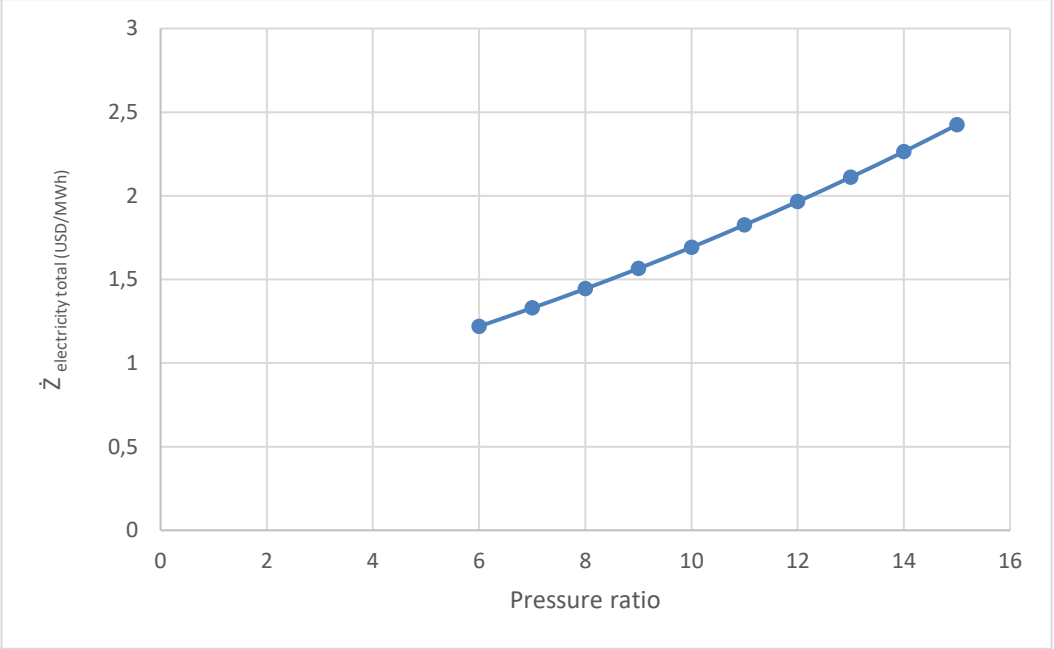

Figure 4.13. Variation of $\dot{Z}_{electricity}$ total with pressure ratio.

4.4. EFFECT THE COMPRESSOR EFFICIENCY ON COMBINED CYCLE PERFORMANCE

Compressor efficiency has a substantial influence on the overall performance of combined power cycles, such as those using both Organic Rankine Cycle (ORC) units and gas turbine cycle (GTC). The effectiveness of a compressor is measured by how well it can raise the pressure of the working fluid or air without incurring too many energy losses. Prior to combustion, the incoming air must be compressed in a gas turbine cycle by the compressor. Less energy is wasted as heat during compression due to a higher compressor efficiency, which implies there is more energy available for combustion and subsequent power production. A larger mass flow rate of air entering the combustion chamber improves combustion efficiency, which may result in a higher output of power and improved cycle efficiency. In combined cycle, the

ORC units may be powered by waste heat from the gas turbine's exhaust. More waste heat is available for the ORC cycle due to the gas turbine cycle better compressor efficiency, which may lead to greater heat recovery potential and improved ORC efficiency. this makes greater use of the available energy sources, improving the performance of the combined cycle as a whole. the gas turbine cycle compressor efficiency has an impact on both its own performance as well as the efficiency of the overall combined cycle. A more efficient compressor increases the gas turbine's total cycle efficiency, raising the temperature of the exhaust gases and increasing the amount of heat available for the ORC units. This interaction may result in increased energy conversion efficiency and increased power output. The total effectiveness and power output of the gas turbine and combined cycles are directly influenced by compressor efficiency. Increased power output and greater total cycle efficiency are the results of improved compressor efficiency, which lowers the amount of energy needed to compress the air. This is crucial in combined cycles since increasing energy conversion is one of the main goals. For combined cycles to operate as efficiently as possible, a high-efficiency compressor design is essential. The trade-offs between compressor efficiency, system complexity, cost, and total cycle efficiency must be considered by engineers. The total system setup and operating characteristics are influenced by the compressor's design and efficiency. In conclusion, the efficiency of the compressor has a big impact on the effectiveness, output, and overall performance of combined power cycles. Engineers can make combined power plants more effective and efficient by increasing compressor efficiency, which will also increase the efficiency of the gas turbine and ORC cycle. In order to get the best results, the compressor design and how it affects cycle performance must be carefully taken into account.

Figure 4.14 shows the effect of compressor efficiency on the total efficiency of the system, as the increase in the compressor efficiency increase the efficiency of the system, and therefore the compressor efficiency value of 70% was the worst case, as the energy efficiency reached 35.5%, while the best efficiency reached is at compressor efficiency is 90%, as the efficiency reached 42.4%.

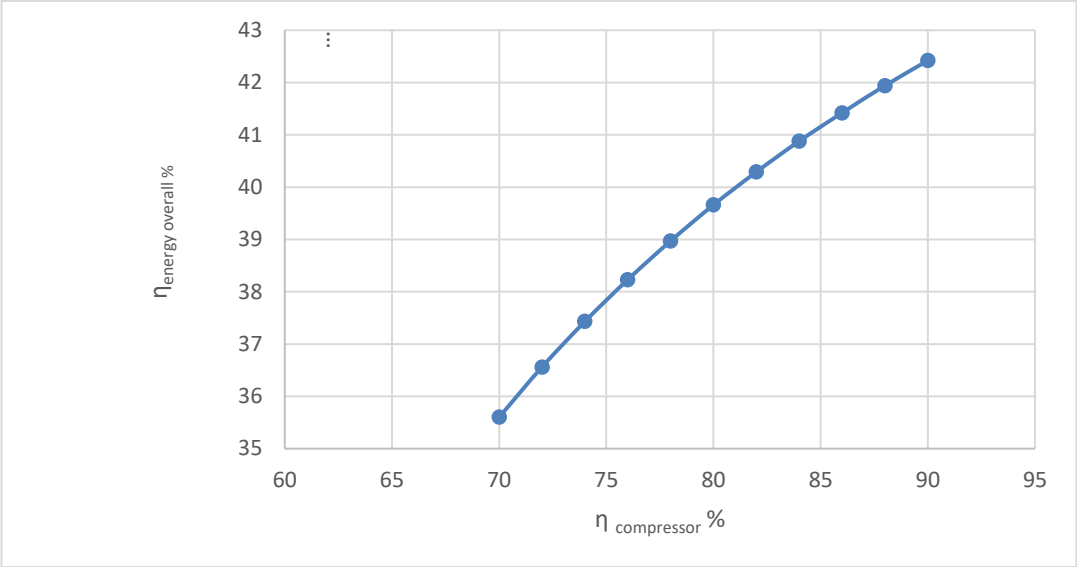

Figure 4.14. Variation of η_{energy} overall with compressor efficiency.

Figure 4.15 shows the effect of compressor efficiency on the exergy of the system, where the increase in the compressor efficiency increases the exergy of the system, and therefore the compressor efficiency value of 70% was the worst case, as the exergy reached 34.5%, while the best exergy was reached at compressor efficiency 90%, where the efficiency reached 41%.

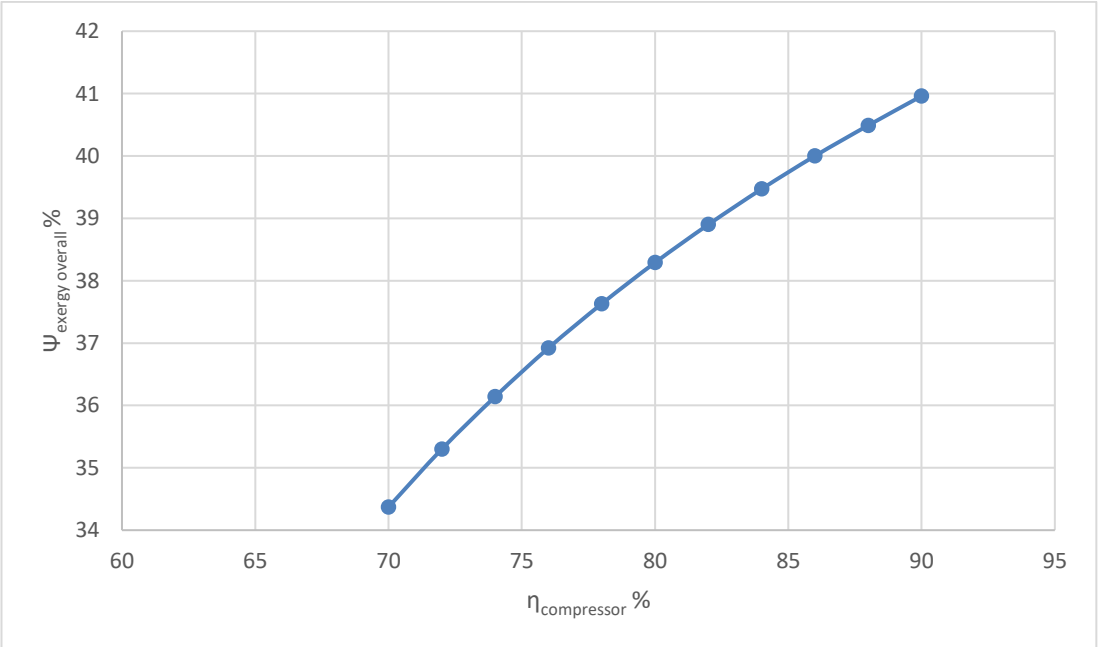

Figure 4.15. Variation of Ψ_{exergy} overall with compressor efficiency.

Figure 4.16 shows the effect of compressor efficiency on the cycle work net, as the increase in the compressor efficiency increase the cycle work net, and therefore the compressor efficiency 70 %was the worst case, as the total work net reached 45 kJ, while the best work reached is at the 90%, where the total work was 62 kJ.

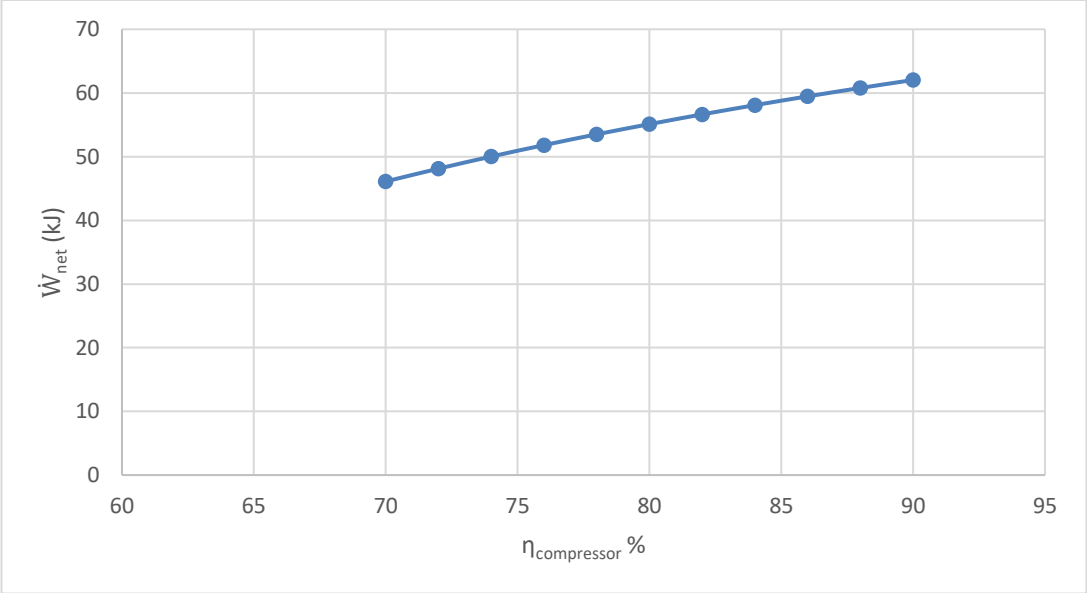

Figure 4.16. Variation of $\dot{W}_{net}$ with compressor efficiency.

Figure 4.17 shows the effect of compressor efficiency on the work of the gas turbine cycle, as the increase in the compressor efficiency increase the work of the gas turbine cycle. Therefore, the compressor efficiency value of 70 % was the worst case, as the total work BC reached 32 kJ, while the best work of the gas turbine cycle was reached. It is at a compressor efficiency of 90 %, where the gas turbine cycle work reached 48 kJ.

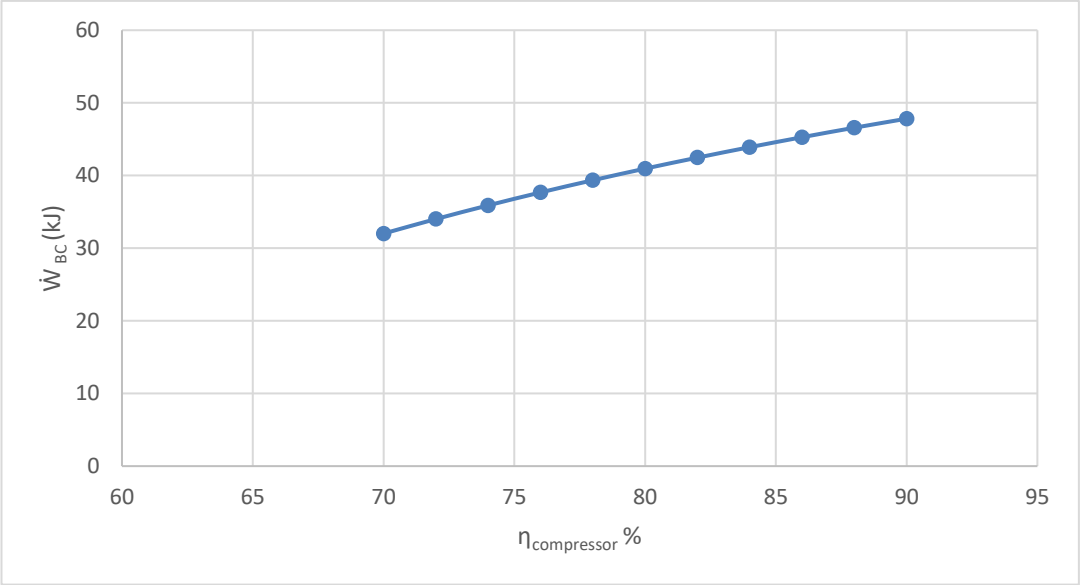

Figure 4.17. Variation of $\dot{W}_{BC}$ with compressor efficiency.

Figure 4.18 shows the effect of compressor efficiency on the cost of electric energy, as the increase in compressor efficiency increases the cost of electrical energy. Therefore, The compressor efficiency value of 90 %was the worst case, as the cost of electrical energy reached 5 USD/MWh, while the best cost of electrical energy was It is reached at a compressor efficiency 75%, where the cost of electric energy reached 1.9 USD/MWh.

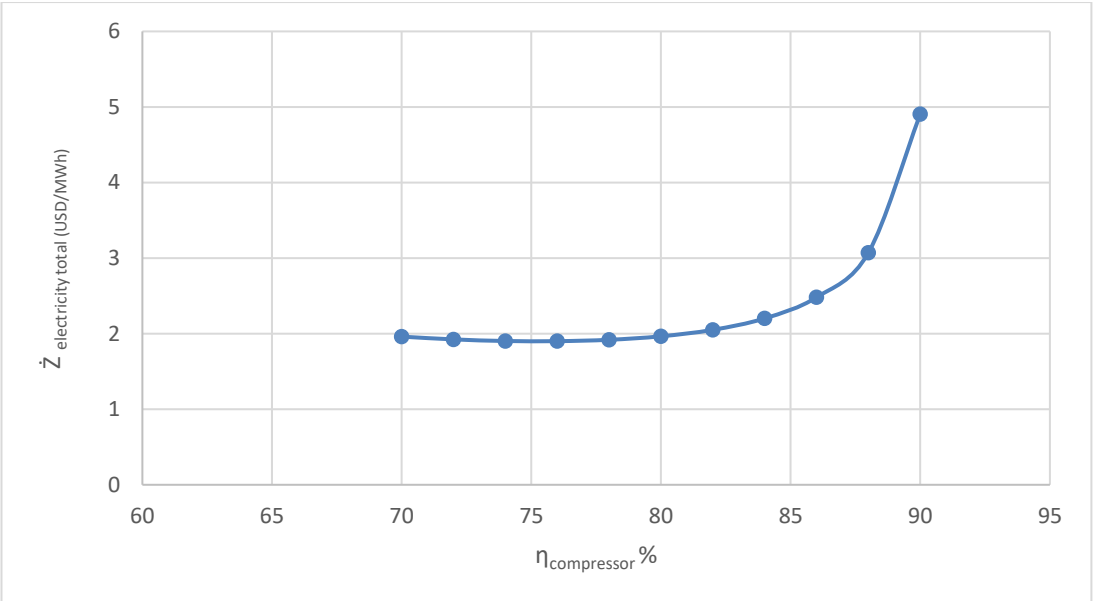

Figure 4.18. Variation of $\dot{Z}$ electricity total with compressor efficiency.

4.5. EFFECT THE TURBINE EFFICIENCY ON COMBINED CYCLE PERFORMANCE

The performance of combined power cycles, which include both Organic Rankine Cycle (ORC) units and gas turbine cycle (GTC), is significantly influenced by the turbine efficiency. The capacity of the turbine to efficiently transform the energy of the expanding fluid into meaningful mechanical work is referred to as turbine efficiency. In a gas turbine cycle, the turbine is in charge of drawing power from the expanding combustion gases and transforming it into mechanical power to operate the compressor and generator. greater mechanical power production for the cycle results from more energy being successfully collected from the expanding gases due to higher turbine efficiency. As a result, power production is boosted as well as cycle efficiency. In combined cycles, the ORC units may be powered by waste heat from the gas turbine's exhaust. More waste heat is available for the ORC cycle when the gas turbine cycle's turbine efficiency is greater. This enhances the ORC units' total performance and capacity for heat recovery, enhancing efficiency and increasing power production. The gas turbine cycle's turbine efficiency affects both its own performance and that of the ORC units. Higher exhaust gas temperatures are made possible by more effective gas turbines, which increases the amount of heat that can be used in the ORC cycle. This interaction improves the combined cycle overall efficiency and the way waste heat is used. The total effectiveness and power production of both the gas turbine and combined cycle are directly influenced by the efficiency of the turbine. A more effective turbine makes it possible to collect more energy from the expanding gases, increasing mechanical power and net electricity output. The key to attaining the best performance in combined cycle is designing a turbine with a high efficiency. Trade-offs between turbine efficiency, materials, cost, and cycle efficiency must be taken into account by engineers. The layout of the whole system, the operating conditions, and the total capability for energy conversion are all impacted by the turbine design. In conclusion, the effectiveness, output, and overall performance of combined power cycle are significantly influenced by turbine efficiency. Engineers may increase the efficiency of both the gas turbine and ORC cycles by increasing turbine efficiency, creating a more effective and productive combined power plant. Achieving the

required outcomes requires careful consideration of turbine design and its influence on cycle performance.

Figure 4.19 shows the effect of turbine efficiency on the total efficiency of the system, as the increase in the turbine efficiency increase the efficiency of the system, and therefore the turbine efficiency value of 70% was the worst case, as the energy efficiency reached 28.5%, while the best efficiency reached is at turbine efficiency is 90%, as the efficiency reached 42.5%.

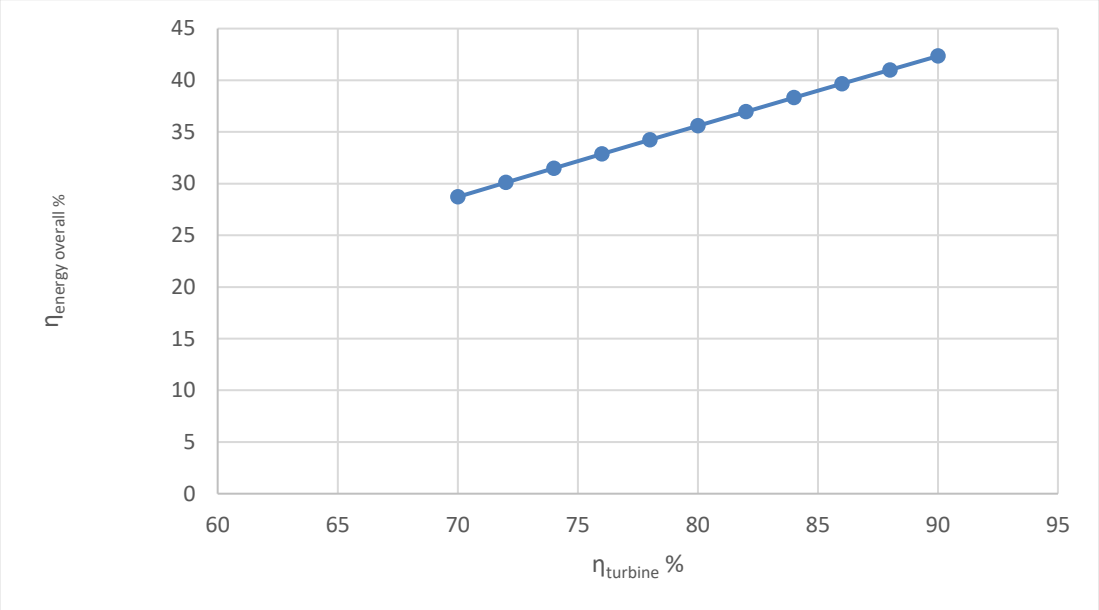

Figure 4.19. Variation of η_{energy} overall with turbine efficiency.

Figure 4.20 shows the effect of turbine efficiency on the exergy of the system, where the increase in the turbine efficiency increases the exergy of the system, and therefore the turbine efficiency value of 70% was the worst case, as the exergy reached 27.5%, while the best exergy was reached at turbine efficiency 90%, where the efficiency reached 41%.

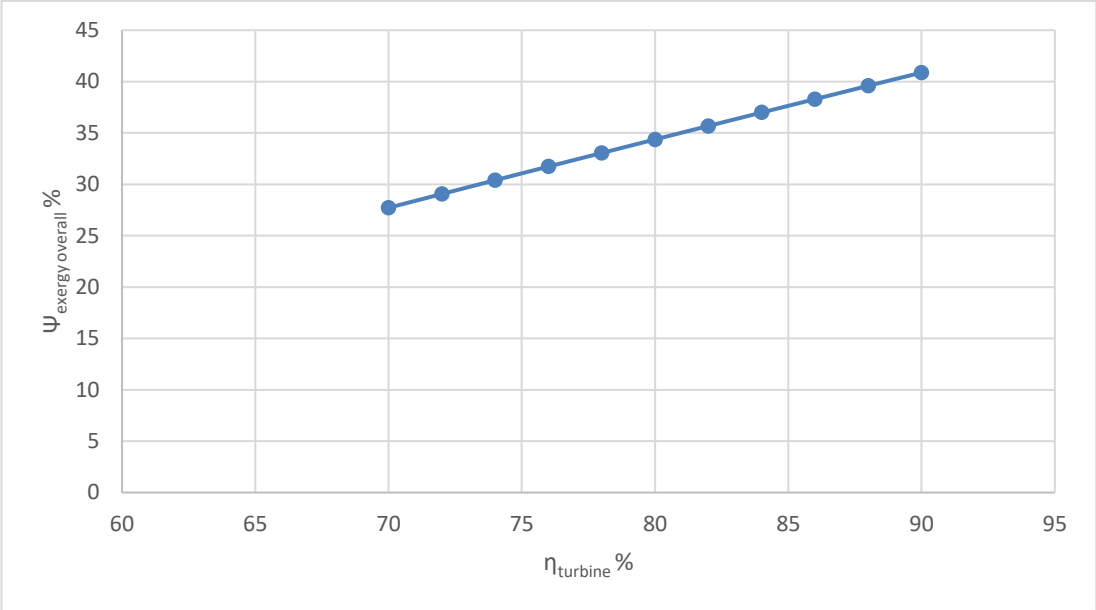

Figure 4.20. Variation of Ψ_{exergy} overall with turbine efficiency.

Figure 4.21 shows the effect of turbine efficiency on the cycle work net, as the increase in the turbine efficiency increase the cycle work net, and therefore the turbine efficiency 70% was the worst case, as the total work net reached 40 kJ, while the best work reached is at the 90%, where the total work was 58 kJ.

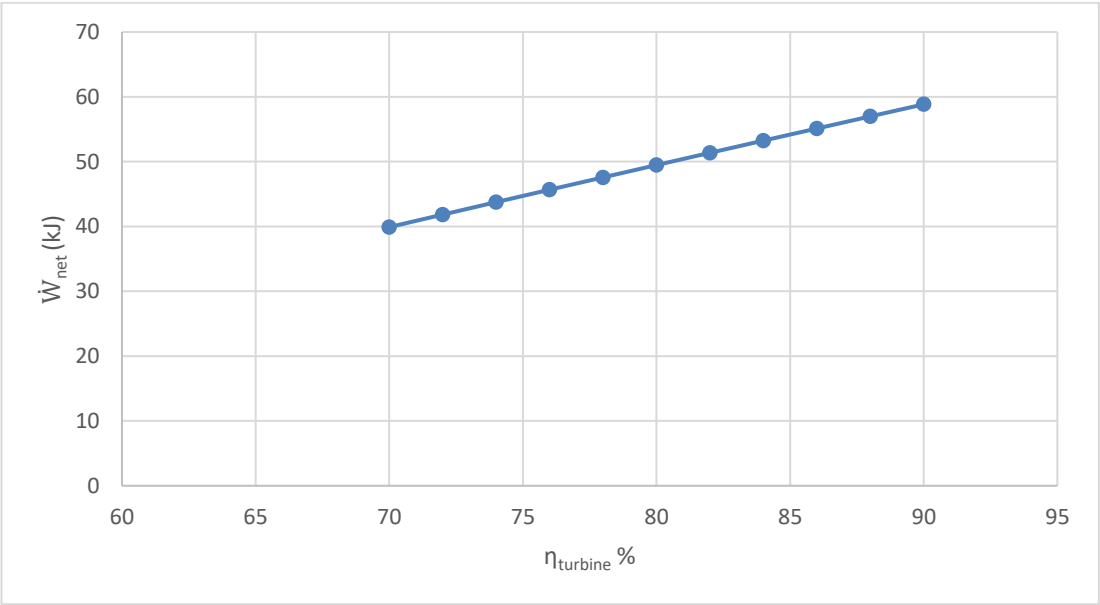

Figure 4.21. Variation of $\dot{W}_{net}$ with turbine efficiency.

Figure 4.22 shows the effect of turbine efficiency on the work of the gas turbine cycle, as the increase in the turbine efficiency increase the work of the gas turbine cycle. Therefore, the turbine efficiency value of 70 % was the worst case, as the total work BC reached 22.5 kJ, while the best work of the gas turbine cycle was reached. It is at a turbine efficiency of 90 %, where the gas turbine cycle work reached 45 kJ.

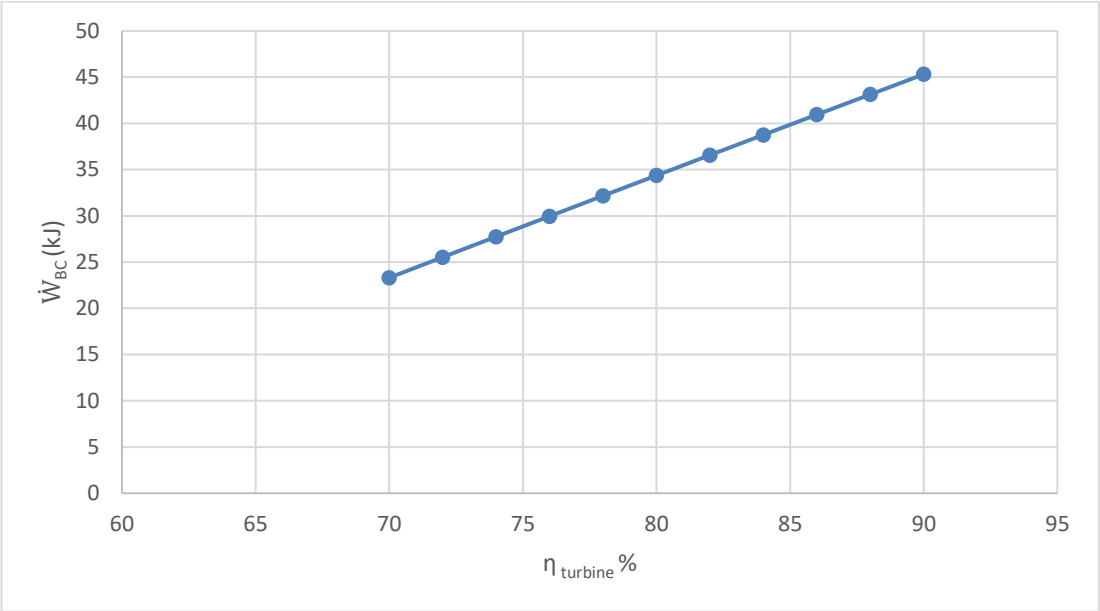

Figure 4.22. Variation of $\dot{W}_{BC}$ with turbine efficiency.

Figure 4.23 shows the effect of turbine efficiency on the cost of electric energy, as the increase in turbine efficiency increases the cost of electrical energy. Therefore, the turbine efficiency value of 90% was the worst case, as the cost of electrical energy reached 3.1 USD/MWh, while the best cost of electrical energy was It is reached at a turbine efficiency 75%, where the cost of electric energy reached 1.6 USD/MWh.

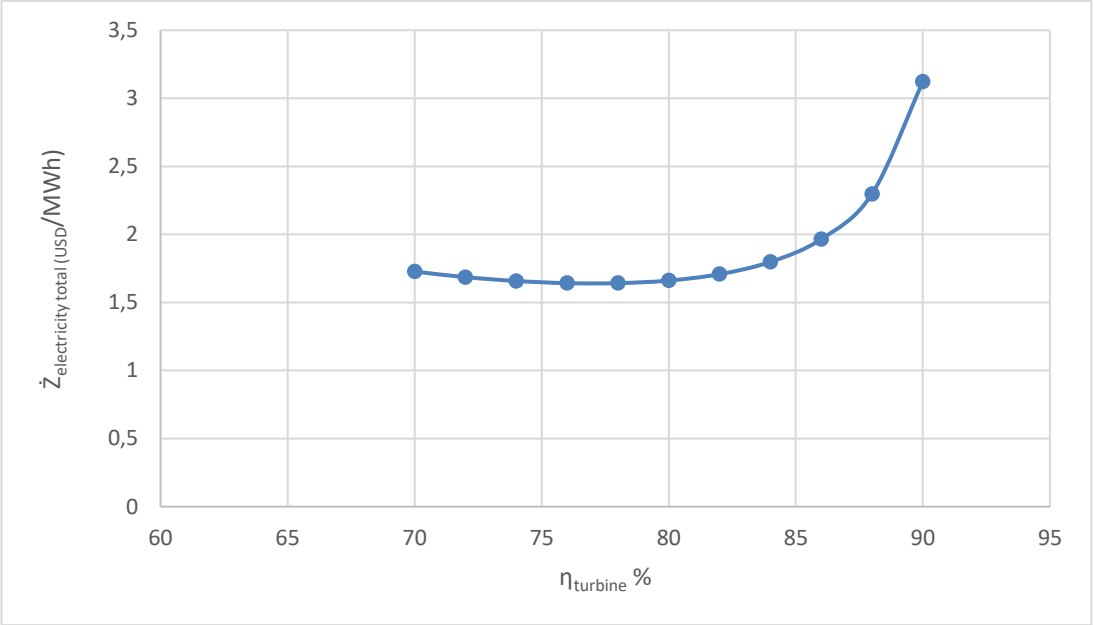

Figure 4.23. Variation of Ż electricity total with turbine efficiency.

4.6. EFFECT THE TEMPERATURE OF EXHAUST ON COMBINED CYCLE PERFORMANCE

The performance of the system as a whole is significantly impacted by the temperature of the exhaust gases in a combined power cycle, which contains both Organic Rankine cycle (ORC) units and gas turbine cycles (GTC). The efficiency and potential for energy recovery of both the gas turbine and ORC cycles are directly correlated with the exhaust gas temperature. The efficiency and output of the cycle are significantly influenced by the temperature of the exhaust gases that are released from the combustion chamber of the gas turbine. The thermal energy in the exhaust gases increases as the exhaust gas temperature rises. As a result of a greater temperature differential between the combustion gases and the surrounding air during expansion in the turbine, this may boost efficiency but also raise the possibility of higher NOx emissions. The comparatively hot exhaust gases from the gas turbine may be utilized as a heat source for the ORC devices. higher exhaust gas temperatures increase the amount of heat that is accessible for the ORC cycle, improving heat recovery and increasing ORC efficiency. As a result, the ORC units generate more power. The quantity of waste heat that is accessible to the ORC units directly depends on the temperature of the gas turbine's exhaust gas. The ORC cycle may transfer more heat

energy when the exhaust gas temperature is higher. The synergistic interaction between the ORC cycle and gas turbine results in improved overall efficiency and power production when they are combined. The combined cycle's total efficiency and power production are directly influenced by the temperature of the exhaust gas. The thermal efficiency of the gas turbine and ORC Cycle may both be improved via properly adjusting the exhaust gas temperature, increasing net power output. Higher exhaust gas temperatures have the potential to boost cycle efficiency but also emissions, especially of nitrogen oxides (NOx). When altering exhaust gas temperatures, it is important to carefully balance the trade-offs between efficiency improvements and environmental effects. higher exhaust gas temperatures may put more thermal strain on system parts like heat exchangers and turbine blades. For the longevity and dependability of the system, it is essential to make sure the materials utilized in these components can endure the high temperatures. in conclusion, the efficiency, power production, and environmental effect of combined power cycles are greatly influenced by the exhaust gas temperature. to balance efficiency benefits and pollution concerns while guaranteeing the system's long-term dependability, engineers must carefully adjust this parameter. a combined power plant's design and operation may be influenced by the evaluation of the impact of various exhaust gas temperatures on the cycle's overall performance using simulation tools and comprehensive analysis.

Figure 4.24 shows the effect of temperature of exhaust on the total efficiency of the system, as the increase in the temperature of exhaust reduce the efficiency of the system, and therefore the temperature of exhaust value of 300 ℃ was the worst case, as the energy efficiency reached 39.65%, while the best efficiency reached is at temperature of exhaust is 210 ℃, as the efficiency reached 40.9%.

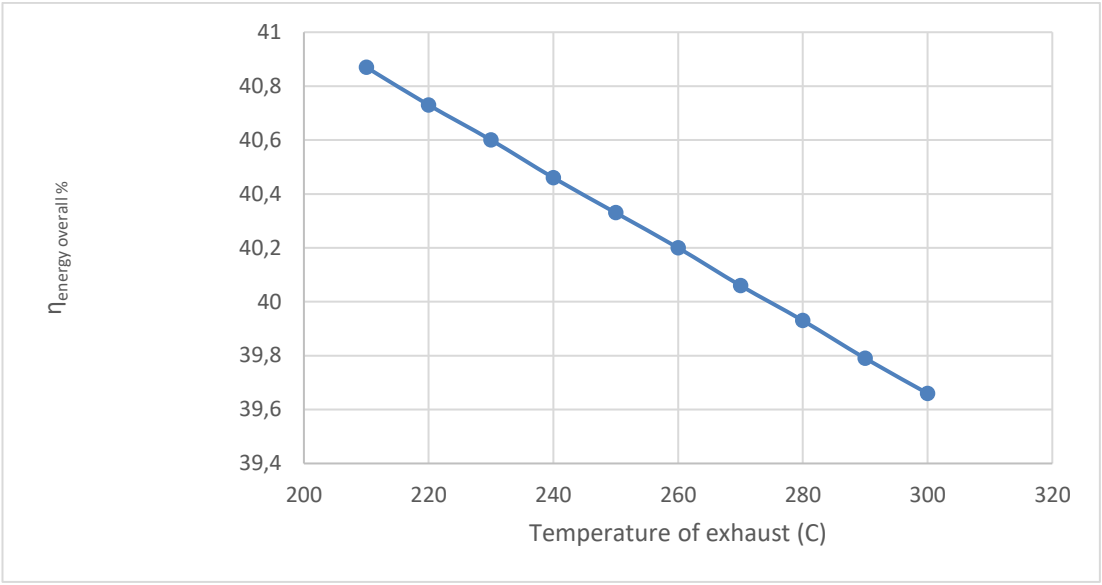

Figure 4.24. Variation of η_{energy} overall with temperature of exhaust.

Figure 4.25 shows the effect of temperature of exhaust on the exergy of the system, where the increase in the temperature of exhaust reduces the exergy of the system, and therefore the temperature of exhaust value of 300 ℃ was the worst case, as the exergy reached 38.3%, while the best exergy was reached at temperature of exhaust 210 ℃, where the efficiency reached 39.5%.

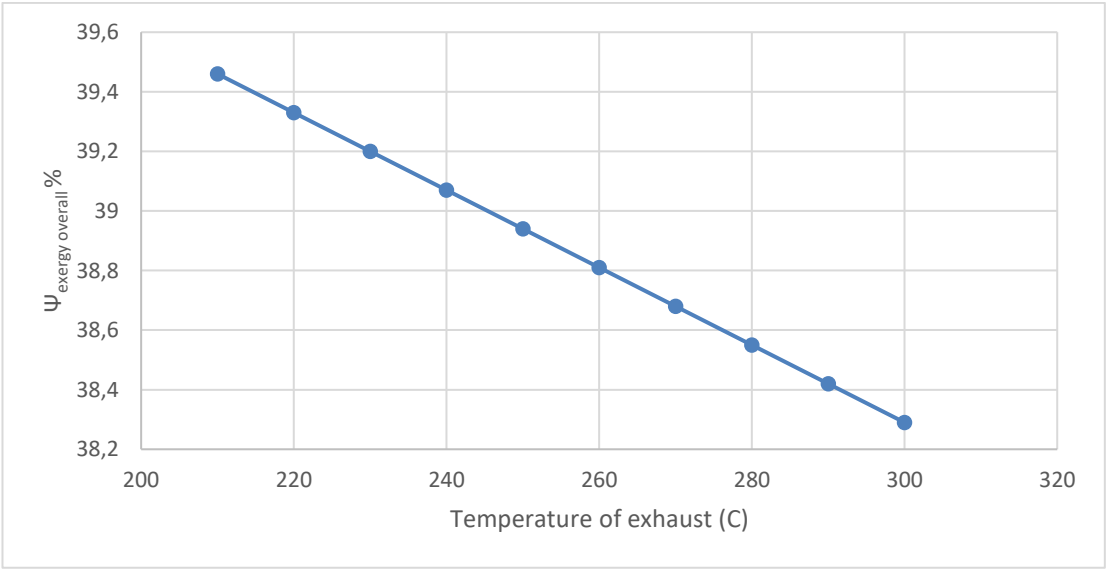

Figure 4.25. Variation of Ψ_{exergy} overall with temperature of exhaust.

Figure 4.26 shows the effect of temperature of exhaust on the cycle work net, as the increase in the temperature of exhaust reduces the cycle work net, and therefore the

temperature of exhaust 300 ℃ was the worst case, as the total work net reached 55.1 kJ, while the best work reached is at the 210 ℃, where the total work was 56.8 kJ.

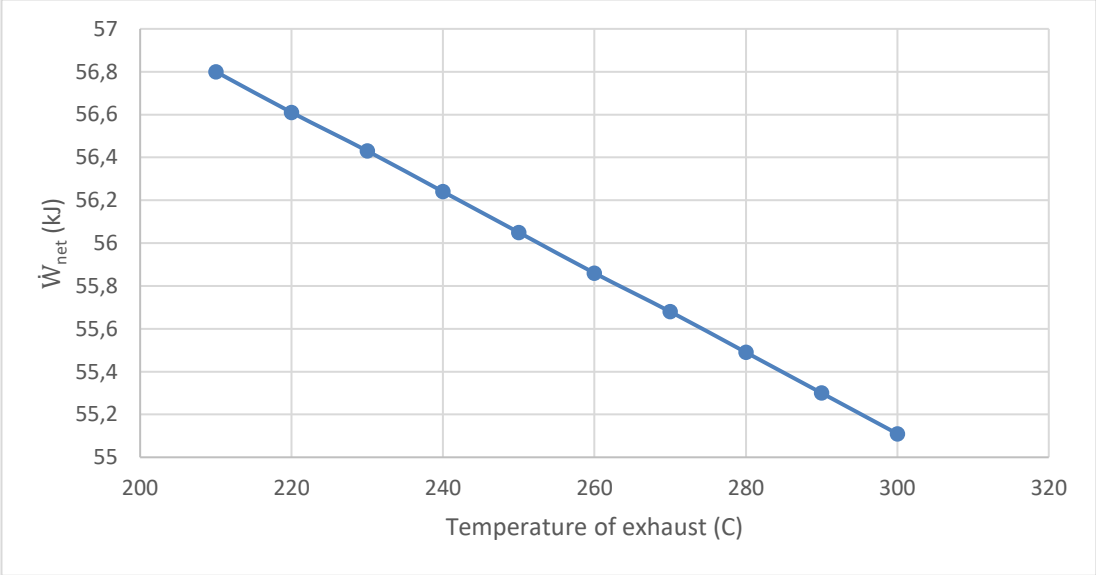

Figure 4.26. Variation of $\dot{W}_{net}$ with temperature of exhaust.

Figure 4.27 shows the effect of temperature of exhaust on the work of the gas turbine cycle, as the increase in the temperature of exhaust constant the work of the gas turbine cycle. Therefore, the temperature of exhaust all value was the total work BC reached 40.1 kJ

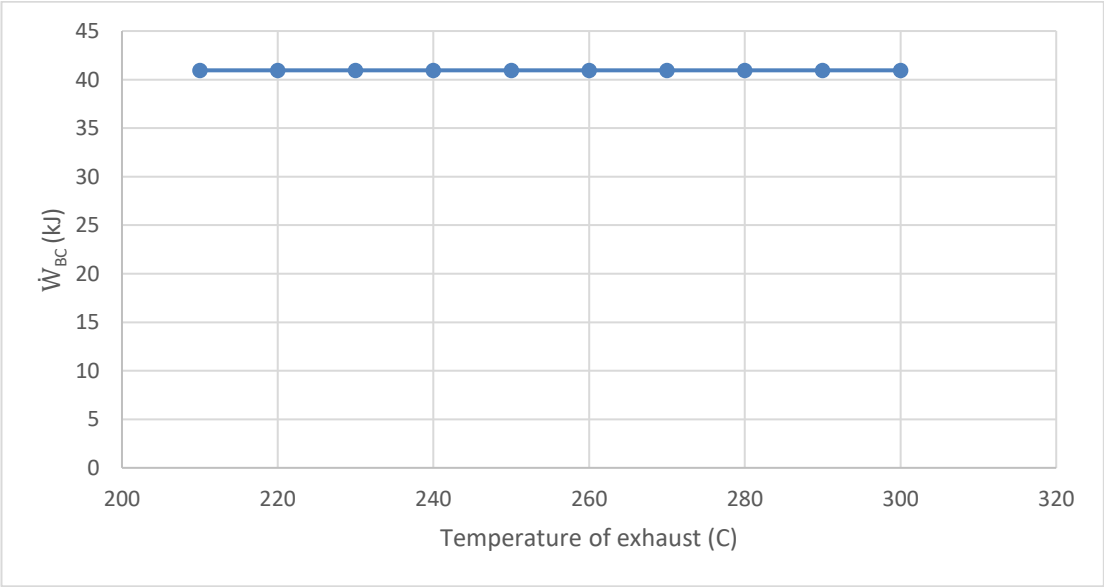

Figure 4.27. Variation of $\dot{W}_{BC}$ with temperature of exhaust.

Figure 4.28 shows the effect of temperature of exhaust on the cost of electric energy, as the increase in temperature of exhaust increases the cost of electrical energy. Therefore, the temperature of exhaust value of 300 ℃ was the worst case, as the cost of electrical energy reached 1.965 USD/MWh, while the best cost of electrical energy was It is reached at a temperature of exhaust 210 ℃, where the cost of electric energy reached 1.899 USD/MWh.

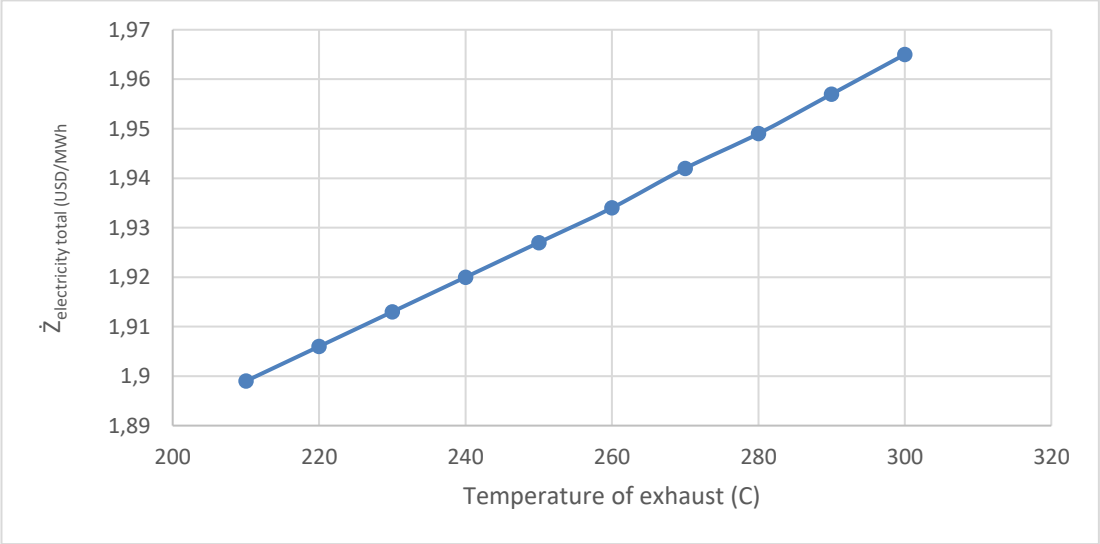

Figure 4.28. Variation of $\dot{Z}_{electricity}$ total with temperature of exhaust.

4.7. COMBINED POWER PLANE CYCLE PERFORMANCE

The performance of the Gulf CC cycle is discussed in this part along with the results of thermodynamic and economic modeling. In order to increase system efficiency and optimize the exploitation of heat losses, three ORC bottom cycles are added to the gas turbine cycle in the heat and power combined cycle system suggested for this study. The released gases are then delivered to the ORC evaporator. The suggested model's thermodynamic characteristics, including mass flow rates, enthalpies, entropies, and external energy flow rates for each situation, are listed in Table 4.1.

Table 4.1. Properties for each state for the combine power plane model at the optimum condition.

State	m (kg/s)	Pressure (kPa)	Temperature (K)	Entropy (kJ/kg. K)	Enthalpy (KJ/kg)	Exergy (MW)
1	142.6	101.3	324	67.73	5.933	0
2	142.6	1216	738.8	507.6	6.077	56.58
3	2.636	101.3	288	-4672	11.53	136.7
4	145.2	1155	1450	127.1	8.235	148.2
5	145.2	98.46	906.9	-556.1	8.385	41.87
6	145.2	95.51	500	-1024	7.712	5.625
7	145.2	98.37	400	-1132	7.462	1.668
8	145.2	101.3	300	-1239	7.188	-0.9436
9	122.8	800	306.4	235	1.119	0.07796
10	122.8	800	504	562.9	1.966	9.349
11	122.8	800	894.9	1033	2.617	43.26
12	122.8	121.6	836.8	949.3	2.627	32.59
13	122.8	121.6	306.1	402.8	1.669	0.5655
14	122.8	121.6	306.1	234.4	1.119	0.01973
15	27.43	121.6	324	3835	12.88	0
16	27.43	121.6	329	4212	14.03	0.08072
17	53.45	800	306.4	235	1.119	0.03394
18	53.45	800	363.1	297	1.303	0.4076
19	53.45	800	488	547.6	1.935	3.736
20	53.45	121.6	436.3	506.1	1.946	1.349
21	53.45	121.6	306.1	402.8	1.669	0.2462
22	53.45	121.6	306.1	234.4	1.119	0.008592
23	11.94	121.6	324	3835	12.88	0
24	11.94	121.6	329	4212	14.03	0.03515
25	63.45	800	306.4	235	1.119	0.04029
26	63.45	800	319.1	248.3	1.161	0.08312
27	63.45	800	388	455.7	1.727	2.538
28	63.45	121.6	336.2	425	1.737	0.4007
29	63.45	121.6	306.1	402.8	1.669	0.2922
30	63.45	121.6	306.1	234.4	1.119	0.0102
31	14.18	121.6	324	3835	12.88	0
32	14.18	121.6	329	4212	14.03	0.04172

PART 5

CONCLUSIONS AND RECOMMENDATION

5.1. CONCLUSIONS

1. The entry temperature has a significant impact on the efficiency and exergy of a system. The worst case is 51°C, with energy efficiency reaching 38.5%, while the best temperature is 15°C, with efficiency reaching 40.01%. The entry temperature also affects cycle occupancy, with the worst-case being 51°C, with total occupancy reaching 50.8 kJ. The gas turbine cycle occupancy is also affected, with the worst case being at 15°C, where occupancy reached 43.5 kJ. The entry temperature also affects the cost of electricity, with the worst-case being 51°C, with a cost of 2.14 USD/MWh, while the best is at 15°C, with a cost of 1.86 USD/MWh.
2. The pressure ratio plays a crucial role in determining the efficiency and exergy of a system. A high-pressure ratio results in a higher efficiency of 35.9%, while a low-pressure ratio leads to a lower efficiency of 34.6%. The cycle work net is also affected by the pressure ratio, with a high-pressure ratio reducing total work and a low-pressure ratio affecting the gas turbine cycle's work. The cost of electricity also increases with a high-pressure ratio, with a low value of 15 resulting in a higher cost of 2.4 USD/MWh, while a high-pressure ratio results in a lower cost of 1.25 USD/MWh.
3. Compressor efficiency significantly impacts the overall efficiency of a system. A compressor efficiency value of 70% is the worst case, with energy efficiency reaching 35.5%. The best efficiency is achieved at 90%, with exergy reaching 41%. The worst case is at 70%, with total work net reaching 45 kJ. The best work is at 90%, with total work reaching 48 kJ. The cost of electric energy also increases with compressor efficiency, with the worst case at 90% and the best at 75%.

4. The increase in turbine efficiency significantly impacts the total efficiency of a system. A 70% turbine efficiency is the worst case, with 28.5% energy efficiency, while the best efficiency is achieved at 90%, reaching 42.5%. The cycle work net also increases, with a 70% turbine efficiency being the worst case. The gas turbine cycle work is also affected, with a 90% turbine efficiency achieving 45 kJ of work. The cost of electricity also increases, with a 90% turbine efficiency being the worst case, with a cost of 3.1 USD/MWh, while the best is achieved at 75%, with a cost of 1.6 USD/MWh.
5. The temperature of exhaust significantly impacts the efficiency of a system. A 300 ℃ exhaust value is the worst case, with an energy efficiency of 39.65%. The best efficiency is achieved at 210 ℃, with an efficiency of 40.9%. The temperature of exhaust also affects the exergy of the system, with an exergy of 38.3%. The cycle work net is also affected, with a total work net of 55.1 kJ at 300 ℃. The cost of electrical energy is also affected, with a 300 ℃ exhaust value being the worst case, with a cost of 1.965 USD/MWh.
6. This dual-cycle power plant uses combustion heat more efficiently than single-cycle power plants using in iraq. combined cycle power plants are greener because they use less fuel and emit less greenhouse gas per unit of electricity. Operating flexibility and load-following are improved by combined cycle power plants. to match grid fluctuations, the gas turbine component can quickly adjust to electricity demand changes. The combined cycle power plant can produce more power with less fuel, making it a cost-effective and reliable solution for meeting varying electricity needs. Overall, combined cycle power generation offers increased efficiency, operational flexibility, and environmental benefits, making it a viable option for sustainable power generation.

5.2. RECOMMENDATION

In order to perform a thorough thermoeconomic analysis of combined cycle power plants in Iraq, it is advisable to begin by collecting precise information regarding the energy infrastructure, fuel sources, and operational parameters of the existing power plants in the area. during the initial phase, it is crucial to engage in collaboration with

local energy authorities, power plant operators, and pertinent governmental agencies to guarantee access to precise and current information. Furthermore, it is advantageous to take into account the precise climatic conditions in Iraq, as the ambient temperature and environmental factors can impact the performance and effectiveness of combined cycle power plants. Researchers can lay a strong groundwork for thermoeconomic analysis and draw relevant conclusions specific to the Iraqi context by gaining a comprehensive understanding of the current energy situation.

During the study, it is crucial to focus specifically on the economic facets of combined cycle power plants, which encompass capital expenditures, operational costs, and potential sources of income. an in-depth cost-benefit analysis can offer valuable insights into the economic feasibility and enduring viability of implementing combined cycle technology in Iraq. This analysis should encompass not only the direct financial consequences but also take into consideration the societal and ecological advantages linked to enhanced efficacy and diminished greenhouse gas emissions. Additionally, researchers should investigate possible funding mechanisms, incentives, and policy suggestions that could promote the implementation of combined cycle power plants in the energy sector of iraq.

To improve the significance and practicality of the study's results, it is advisable to participate in knowledge-sharing endeavors and collaborative endeavors with international organizations, research institutions, and industry experts. The collaborative approach facilitates the sharing of best practices, technological expertise, and policy recommendations, thereby enhancing the successful implementation of combined cycle power plants in Iraq. the research can provide a platform for dialogue and cooperation, serving as both an academic contribution and a practical guide for policymakers and industry stakeholders aiming to improve the efficiency and sustainability of Iraq's power generation infrastructure.

REFERENCES

1. Kalinowski, P., Hwang, Y., Radermacher, R., Al Hashimi, S., and Rodgers, P., "Application of waste heat powered absorption refrigeration system to the LNG recovery process", ***International Journal Of Refrigeration***, 32 (4): (2009).
2. Jurinak, J. J., Mitchell, J. W., and Beckman, W. A., "Open-cycle desiccant air conditioning as an alternative to vapor compression cooling in residential applications", ***Journal Of Solar Energy Engineering, Transactions Of The ASME***, 106 (3): (1984).
3. Li, H., Bu, X., Wang, L., Long, Z., and Lian, Y., "Hydrocarbon working fluids for a Rankine cycle powered vapor compression refrigeration system using low-grade thermal energy", ***Energy And Buildings***, 65: (2013).
4. Venkatarathnam, G. and Murthy, S. S., "Refrigerants for vapour compression refrigeration systems", ***Resonance***, 17 (2): (2012).
5. Gado, M. G., Ookawara, S., Nada, S., and El-Sharkawy, I. I., .
6. Darwish, N. A., Al-Hashimi, S. H., and Al-Mansoori, A. S., "Performance analysis and evaluation of a commercial absorption-refrigeration water-ammonia (ARWA) system", ***International Journal Of Refrigeration***, 31 (7): (2008).
7. Mohammed, Y. S., Mustafa, M. W., Bashir, N., and Mokhtar, A. S., .
8. Kaygusuz, K., .
9. Sawant, R. and Raut, A., "Study of Compressor Free Air Conditioning System for Solar Cooling", ***International Journal For Research In Applied Sciences And Biotechnology***, (2): (2015).
10. Basu, P., Butler, J., and Leon, M. A., "Biomass co-firing options on the emission reduction and electricity generation costs in coal-fired power plants", ***Renewable Energy***, 36 (1): (2011).
11. BIAN, Z., INYANG, H. I., DANIELS, J. L., OTTO, F., and STRUTHERS, S., "Environmental issues from coal mining and their solutions", ***Mining Science And Technology***, 20 (2): (2010).

12. Jayarama Reddy, P., "Clean Coal Technologies for Power Generation", Clean Coal Technologies for Power Generation, (2013).
13. Ahmadi, P. and Dincer, I., "Thermodynamic and exergoenvironmental analyses, and multi-objective optimization of a gas turbine power plant", ***Applied Thermal Engineering***, 31 (14–15): (2011).
14. Y. A. Çengel and M. A. Boles, "Thermodynamics: An Engineering Approach: McGraw-Hill Education", ***Angewandte Chemie International Edition, 6(11), 951–952.***, 13 (April): (2014).
15. Albring, "A. H. Shapiro, (Prof. am Massachusetts Institute of Technology). The Dynamics and Thermodynamics of Compressible Fluid Flow Bd I. XIII + 647 Seiten m. zahlr. Abb. New York 1953. The Ronald Press Company. Preis geb. 16 $", ***ZAMM - Journal Of Applied Mathematics And Mechanics / Zeitschrift Für Angewandte Mathematik Und Mechanik***, 34 (10–11): (1954).
16. Woodruf, E. B., Lammers, H. B., and Lammers, T. F., "Steam Plant Operation", ***Journal Of Chemical Information And Modeling***, 53 (9): (1981).
17. Elliot, J. R. and Lira, C. T., "Introductory Chemical Engineering Thermodynamics", ***Journal Of Materials Processing Technology***, 1 (1): (2012).
18. Woodruff, E. B., Lammers, H. B., and Lammers, T. F., "Steam Plant Operation", .
19. Saravanamuttoo, H. I. H., Rogers, G. F. C., and Cohen, H., "Gas Turbine Theory (5th Ed.)", ***Gas Turbine Theory (5th Ed.)***, (2001).
20. "Combined-cycle gas & steam turbine power plants", ***Choice Reviews Online***, 29 (04): (1991).
21. Boyce, M. P., "Gas Turbine Engineering Handbook", Gas Turbine Engineering Handbook, (2006).
22. Alobaid, F., Postler, R., Ströhle, J., Epple, B., and Kim, H. G., "Modeling and investigation start-up procedures of a combined cycle power plant", ***Applied Energy***, 85 (12): (2008).
23. Sakuma, A., Matsuura, T., and Kodama, H., "Steam turbine retrofits technology for improved performance and reliability", (2007).

24. Serth, R. W., "Process Heat Transfer: Principles, Applications and Rules of Thumb", Process Heat Transfer: Principles, Applications and Rules of Thumb, (2007).
25. Siddiqi, A. and Anadon, L. D., "The water-energy nexus in Middle East and North Africa", ***Energy Policy***, 39 (8): (2011).
26. Zamanabadi, A. N., .
27. Nye Jr, J. S., "US Power and Strategy after Iraq", ***Foreign Affairs***, 82 (4): (2003).
28. Tocci, L., Pal, T., Pesmazoglou, I., and Franchetti, B., .
29. Song, J., Gu, C. W., and Ren, X., "Parametric design and off-design analysis of organic Rankine cycle (ORC) system", ***Energy Conversion And Management***, 112: 157–165 (2016).
30. Lee, H. Y., Park, S. H., and Kim, K. H., "Comparative analysis of thermodynamic performance and optimization of organic flash cycle (OFC) and organic Rankine cycle (ORC)", ***Applied Thermal Engineering***, 100: 680–690 (2016).
31. Tumen Ozdil, N. F., Segmen, M. R., and Tantekin, A., "Thermodynamic analysis of an Organic Rankine Cycle (ORC) based on industrial data", ***Applied Thermal Engineering***, 91: 43–52 (2015).
32. Lecompte, S., Huisseune, H., Van Den Broek, M., Vanslambrouck, B., and De Paepe, M., .
33. Yu, G., Shu, G., Tian, H., Wei, H., and Liu, L., "Simulation and thermodynamic analysis of a bottoming Organic Rankine Cycle (ORC) of diesel engine (DE)", ***Energy***, 51: 281–290 (2013).
34. Wang, J., Yan, Z., Wang, M., Ma, S., and Dai, Y., "Thermodynamic analysis and optimization of an (organic Rankine cycle) ORC using low grade heat source", ***Energy***, 49 (1): 356–365 (2013).
35. Li, M., Wang, J., He, W., Gao, L., Wang, B., Ma, S., and Dai, Y., "Construction and preliminary test of a low-temperature regenerative Organic Rankine Cycle (ORC) using R123", ***Renewable Energy***, 57: 216–222 (2013).
36. Quoilin, S., Broek, M. Van Den, Declaye, S., Dewallef, P., and Lemort, V., .

37. Aghahosseini, S. and Dincer, I., "Comparative performance analysis of low-temperature Organic Rankine Cycle (ORC) using pure and zeotropic working fluids", ***Applied Thermal Engineering***, 54 (1): 35–42 (2013).
38. Wang, E. H., Zhang, H. G., Zhao, Y., Fan, B. Y., Wu, Y. T., and Mu, Q. H., "Performance analysis of a novel system combining a dual loop organic Rankine cycle (ORC) with a gasoline engine", ***Energy***, 43 (1): 385–395 (2012).
39. Wang, E. H., Zhang, H. G., Fan, B. Y., Ouyang, M. G., Zhao, Y., and Mu, Q. H., "Study of working fluid selection of organic Rankine cycle (ORC) for engine waste heat recovery", ***Energy***, 36 (5): 3406–3418 (2011).
40. Rayegan, R. and Tao, Y. X., "A procedure to select working fluids for Solar Organic Rankine Cycles (ORCs)", ***Renewable Energy***, 36 (2): 659–670 (2011).
41. Sun, J. and Li, W., "Operation optimization of an organic rankine cycle (ORC) heat recovery power plant", ***Applied Thermal Engineering***, 31 (11–12): 2032–2041 (2011).
42. Vaja, I. and Gambarotta, A., "Internal Combustion Engine (ICE) bottoming with Organic Rankine Cycles (ORCs)", ***Energy***, 35 (2): 1084–1093 (2010).
43. Delgado-Torres, A. M. and García-Rodríguez, L., "Analysis and optimization of the low-temperature solar organic Rankine cycle (ORC)", ***Energy Conversion And Management***, 51 (12): 2846–2856 (2010).
44. Dai, Y., Wang, J., and Gao, L., "Parametric optimization and comparative study of organic Rankine cycle (ORC) for low grade waste heat recovery", ***Energy Conversion And Management***, 50 (3): 576–582 (2009).
45. Wei, D., Lu, X., Lu, Z., and Gu, J., "Dynamic modeling and simulation of an Organic Rankine Cycle (ORC) system for waste heat recovery", ***Applied Thermal Engineering***, 28 (10): 1216–1224 (2008).
46. Wei, D., Lu, X., Lu, Z., and Gu, J., "Performance analysis and optimization of organic Rankine cycle (ORC) for waste heat recovery", ***Energy Conversion And Management***, 48 (4): 1113–1119 (2007).
47. Drescher, U. and Brüggemann, D., "Fluid selection for the Organic Rankine Cycle (ORC) in biomass power and heat plants", ***Applied Thermal Engineering***, 27 (1): 223–228 (2007).
48. Yamamoto, T., Furuhata, T., Arai, N., and Mori, K., "Design and testing of the Organic Rankine Cycle", (2001).

49. Angelino, G., Colonna, P., and Paliano, D. I., "MULTICOMPONENT WORKING FLUIDS FOR ORGANIC RANKINE CYCLES (ORCs)", (1998).
50. Wu, P., Ma, Y., Gao, C., Liu, W., Shan, J., Huang, Y., Wang, J., Zhang, D., and Ran, X., .
51. Yang, J., Yang, Z., and Duan, Y., "Part-load performance analysis and comparison of supercritical CO2 Brayton cycles", ***Energy Conversion And Management***, 214: (2020).
52. Chen, L., Shen, J., Ge, Y., Wu, Z., Wang, W., Zhu, F., and Feng, H., "Power and efficiency optimization of open Maisotsenko-Brayton cycle and performance comparison with traditional open regenerated Brayton cycle", ***Energy Conversion And Management***, 217: (2020).
53. Liu, Y., Wang, Y., and Huang, D., .
54. Mecheri, M. and Le Moullec, Y., "Supercritical CO2 Brayton cycles for coal-fired power plants", ***Energy***, 103: (2016).
55. Ho, C. K., Carlson, M., Garg, P., and Kumar, P., "Technoeconomic Analysis of Alternative Solarized s-CO2 Brayton Cycle Configurations", ***Journal Of Solar Energy Engineering, Transactions Of The ASME***, 138 (5): (2016).
56. Padilla, R. V., Soo Too, Y. C., Benito, R., and Stein, W., "Exergetic analysis of supercritical CO2 Brayton cycles integrated with solar central receivers", ***Applied Energy***, 148: (2015).
57. Al-Sulaiman, F. A. and Atif, M., "Performance comparison of different supercritical carbon dioxide Brayton cycles integrated with a solar power tower", ***Energy***, 82: (2015).
58. Ahn, Y. and Lee, J. I., "Study of various Brayton cycle designs for small modular sodium-cooled fast reactor", ***Nuclear Engineering And Design***, 276: (2014).
59. Le Roux, W. G., Bello-Ochende, T., and Meyer, J. P., .
60. Iverson, B. D., Conboy, T. M., Pasch, J. J., and Kruizenga, A. M., "Supercritical CO2 Brayton cycles for solar-thermal energy", ***Applied Energy***, 111: (2013).
61. Garg, P., Kumar, P., and Srinivasan, K., "Supercritical carbon dioxide Brayton cycle for concentrated solar power", ***Journal Of Supercritical Fluids***, 76: (2013).

62. Conboy, T., Wright, S., Pasch, J., Fleming, D., Rochau, G., and Fuller, R., "Performance characteristics of an operating supercritical CO 2 brayton cycle", ***Journal Of Engineering For Gas Turbines And Power***, 134 (11): (2012).
63. Sarkar, J., "Second law analysis of supercritical CO2 recompression Brayton cycle", ***Energy***, 34 (9): (2009).
64. Moisseytsev, A. and Sienicki, J. J., "Investigation of alternative layouts for the supercritical carbon dioxide Brayton cycle for a sodium-cooled fast reactor", ***Nuclear Engineering And Design***, 239 (7): (2009).
65. Zhang, W., Chen, L., and Sun, F., "Power and efficiency optimization for combined Brayton and inverse Brayton cycles", ***Applied Thermal Engineering***, 29 (14–15): (2009).
66. Pra, F., Tochon, P., Mauget, C., Fokkens, J., and Willemsen, S., "Promising designs of compact heat exchangers for modular HTRs using the Brayton cycle", ***Nuclear Engineering And Design***, 238 (11): (2008).
67. Alabdoadaim, M. A., Agnew, B., and Potts, I., "Performance analysis of combined Brayton and inverse Brayton cycles and developed configurations", ***Applied Thermal Engineering***, 26 (14–15): (2006).
68. Agnew, B., Anderson, A., Potts, I., Frost, T. H., and Alabdoadaim, M. A., "Simulation of combined Brayton and inverse Brayton cycles", ***Applied Thermal Engineering***, 23 (8): (2003).
69. Ibrahim, T. K., Mohammed, M. K., Awad, O. I., Abdalla, A. N., Basrawi, F., Mohammed, M. N., Najafi, G., and Mamat, R., .
70. Kotowicz, J. and Brzęczek, M., "Analysis of increasing efficiency of modern combined cycle power plant: A case study", ***Energy***, 153: (2018).
71. Ibrahim, T. k., Kamil, M., Awad, O. I., Rahman, M. M., Najafi, G., Basrawi, F., Abd Alla, A. N., and Mamat, R., .
72. Sabouhi, H., Abbaspour, A., Fotuhi-Firuzabad, M., and Dehghanian, P., "Reliability modeling and availability analysis of combined cycle power plants", ***International Journal Of Electrical Power And Energy Systems***, 79: (2016).
73. Kotowicz, J., Job, M., and Brzeczek, M., "The characteristics of ultramodern combined cycle power plants", ***Energy***, 92: (2015).

74. Tajik Mansouri, M., Ahmadi, P., Ganjeh Kaviri, A., and Jaafar, M. N. M., "Exergetic and economic evaluation of the effect of HRSG configurations on the performance of combined cycle power plants", ***Energy Conversion And Management***, 58: (2012).
75. Ersayin, E. and Ozgener, L., .
76. Ticâ, A., Guéguen, H., Dumur, D., Faille, D., and Davelaar, F., "Design of a combined cycle power plant model for optimization", ***Applied Energy***, 98: (2012).
77. Sarkar, J. and Bhattacharyya, S., "Application of graphene and graphene-based materials in clean energy-related devices Minghui", ***Archives Of Thermodynamics***, 33 (4): (2012).
78. Petrakopoulou, F., Tsatsaronis, G., Morosuk, T., and Carassai, A., "Conventional and advanced exergetic analyses applied to a combined cycle power plant", ***Energy***, 41 (1): (2012).
79. Ibrahim, T. K., Rahman, M. M., and Abdalla, A. N., "Optimum gas turbine configuration for improving the performance of combined cycle power plant", (2011).
80. Fraidenraich, N., Gordon, J. M., and Tiba, C., "Optimization of gas-turbine combined cycles for solar energy and alternative-fuel power generation", ***Solar Energy***, 48 (5): (1992).
81. Polyzakis, A. L., Koroneos, C., and Xydis, G., "Optimum gas turbine cycle for combined cycle power plant", ***Energy Conversion And Management***, 49 (4): 551–563 (2008).
82. Koch, C., Cziesla, F., and Tsatsaronis, G., "Optimization of combined cycle power plants using evolutionary algorithms", ***Chemical Engineering And Processing: Process Intensification***, 46 (11): (2007).
83. Cihan, A., Hacihafizoğlu, O., and Kahveci, K., "Energy-exergy analysis and modernization suggestions for a combined-cycle power plant", ***International Journal Of Energy Research***, 30 (2): (2006).
84. Hosseini, R., Soltani, M., and Valizadeh, G., "Technical and economic assessment of the integrated solar combined cycle power plants in Iran", ***Renewable Energy***, 30 (10): (2005).

85. Arrieta, F. R. P. and Lora, E. E. S., "Influence of ambient temperature on combined-cycle power-plant performance", ***Applied Energy***, 80 (3): (2005).
86. Franco, A. and Giannini, N., "Perspectives for the use of biomass as fuel in combined cycle power plants", ***International Journal Of Thermal Sciences***, 44 (2): (2005).
87. Chiesa, P. and Macchi, E., "A thermodynamic analysis of different options to break 60% electric efficiency in combined cycle power plants", ***Journal Of Engineering For Gas Turbines And Power***, 126 (4): (2004).
88. Franco, A. and Casarosa, C., "On some perspectives for increasing the efficiency of combined cycle power plants", ***Applied Thermal Engineering***, 22 (13): (2002).
89. Bolland, O. and Mathieu, P., .
90. Dubey*, K. K. and Mishra, R. S., "Statistical Analysis for Parametric Optimization of Gas Turbine-Steam Turbine Combined Power Cycle with Different Natural Gas Combustion", ***International Journal Of Recent Technology And Engineering (IJRTE)***, 8 (4): 4563–4570 (2019).
91. Cheng, K., Qin, J., Dang, C., Lv, C., Zhang, S., and Bao, W., "Thermodynamic analysis for high-power electricity generation systems based on closed-Brayton-cycle with finite cold source on hypersonic vehicles", ***International Journal Of Hydrogen Energy***, 43 (31): (2018).
92. Zhu, D. and Zheng, X., "Potential for energy and emissions of asymmetric twin-scroll turbocharged diesel engines combining inverse Brayton cycle system", ***Energy***, 179: (2019).
93. Report, F., Olaizola, M., Bridges, T., Flores, S., Sombardier, L., and Masutani, S. M., "Recovery and Sequestration of CO 2 from Stationary Combustion Systems by Photosynthesis of Microalgae", ***Carbon***, (April): (2005).
94. Chen, X. and Ray, A., "Deep Reinforcement Learning Control of a Boiling Water Reactor", ***IEEE Transactions On Nuclear Science***, 69 (8): (2022).
95. Ahmed, M. and Hassan, M., "Comparative Study On Modeling Of Gas Turbines In Combined Cycle Power Plants", (2010).
96. Kareem, A. F., Akroot, A., Abdul Wahhab, H. A., Talal, W., Ghazal, R. M., and Alfaris, A., "Exergo–Economic and Parametric Analysis of Waste Heat

Recovery from Taji Gas Turbines Power Plant Using Rankine Cycle and Organic Rankine Cycle", ***Sustainability (Switzerland)***, 15 (12): (2023).

APPENDIX A.

CODE

////GT/ORC CODE_15/10/2022////////
//////////////////Input data//////////////////////////////

     /////Brayton Cycle Model////
 Pr=12   /////Pressure ratio/////////
RH=0.36   ///Avarage RH in Bagdad////
 T_ambient=27 ///Avarage T in Bagdad////
T[1].=T_ambient+273
 T[4].=1450 [K]. /////Gas Turbine inlet temperature///////
eta_c= 0.80
eta_T= 0.86

m_dot_air=142.6[kg/s].

 T[6].=500
 T[7].=400
 T[8].=300/////Exhaust Temperature/////
eta_pump=0.8
eta_st=0.9

///%% Gases constant, (kJ/kmol•K)////
R_air= 0.2870 [kJ/kg-K].
R_N2=0.2968 [kJ/kg-K].
R_O2=0.2598 [kJ/kg-K].
R_H2O= 0.4615 [kJ/kg-K].
R_CO2= 0.1889 [kJ/kg-K].
R_CH4= 0.5182 [kJ/kg-K].
////Molecular weight of gases, kg/kmole///
MW_air= 28.97 [kg/kmol].
MW_N2= 28.013 [kg/kmol].
MW_O2= 31.999 [kg/kmol].
MW_H2O= 18.015 [kg/kmol].
MW_CO2= 44.01 [kg/kmol].
MW_CH4= 16.043 [kg/kmol].
////Chemical exergy of gases, kg/kmole///
ch_N2= 720 [kg/kmol].
ch_O2= 3970 [kg/kmol].
ch_H2O= 9500 [kg/kmol].
ch_CO2= 19870 [kg/kmol].
ch_H2O_L= 900 [kg/kmol].
ch_CH4= 831650 [kg/kmol].
                                                    ////Brayton Cycle Model//////
"State 1"
P[1].=101.325 [KPa].
RH=P_vap/P_g
P_g=**p_sat**(***Water***,***T***=T[1].)
Humidity=0.622*P_vap/(P[1].-P_vap)
Humidity=m_dot_v/m_dot_air
y_vap=Humidity
y_O2=0.21*(m_dot_air-m_dot_v)/m_dot_air
y_N2=0.79*(m_dot_air-m_dot_v)/m_dot_air
YY=y_N2+y_O2+y_vap
MW_in=y_O2*MW_O2+y_N2*MW_N2+y_vap*MW_H2O
h[1].=((1-y_vap)***enthalpy**(***Air***,***T***=T[1].)+y_vap***enthalpy**(***H2O***,***T***=T[1].))/MW_in
s[1].=((1-y_vap)***entropy**(***Air***,***T***=T[1].***P***=(1-
y_vap)*P[1].)+y_vap***entropy**(***H2O***,***T***=T[1].***P***=y_vap*P[1].))/MW_in
m_dot[1].=m_dot_air
Psi[1].=0 [MJ].
EX[1].=0 [MJ].

"State 2"
P[2]./P[1].=Pr
m_dot[2].=m_dot_air
"Air compressor Model"
s_2s=s[1].
T_2s=T[1].*(P[2]./P[1].)^((K1-1)/K1)
Cp1=(y_O2*cp(*O2*,*T*=T[1].)+y_N2*cp(*N2*,*T*=T[1].)+y_vap*cp(*H2O*,*T*=T[1].))/MW_in
Cv1=(y_O2*cv(*O2*,*T*=T[1].)+y_N2*cv(*N2*,*T*=T[1].)+y_vap*cv(*H2O*,*T*=T[1].))/MW_in
R_1=y_O2*R_O2+y_N2*R_N2+y_vap*R_H2O
K1=Cp1/(Cv1)
T[2].= T[1].+(T_2s-T[1].)/eta_c
h[2].=((1-y_vap)*enthalpy(*Air*,*T*=T[2].)+y_vap*enthalpy(*H2O*,*T*=T[2].))/MW_in
s[2].=((1-y_vap)*entropy(*Air*,*T*=T[2].*P*=(1-
y_vap)*P[2].)+y_vap*entropy(*H2O*,*T*=T[2].*P*=y_vap*P[2].))/MW_in
Cp2=(y_O2*cp(*O2*,*T*=T[2].)+y_N2*cp(*N2*,*T*=T[2].)+y_vap*cp(*H2O*,*T*=T[2].))/MW_in
EX[2].=m_dot_air*(h[2].-298*s[2].-(h[1].-298*s[1].))/1000
Psi[2].=h[2].-h[1].-T[1].*(s[2].-s[1].)
Cp_c=(Cp1+Cp2)/2
w_comp=m_dot_air*Cp_c*(T[2].-T[1].)/1000
"State 3"
T[3].=288 [K].
P[3].=P[1].
Q_out=0.02*LHV
LHV=50056 [kJ/kg].
s[3].=entropy(*CH4*,*T*=T[3].*P*=P[3].)/MW_CH4
h[3].=enthalpy(*CH4*,*T*=T[3].)/MW_CH4
EX[3].=m_dot_fuel*ch_CH4/MW_CH4/1000
m_dot[3].=m_dot_fuel
m_dot_air=m_dot_ex-m_dot_fuel
"State 4"
P[4].=P[2].-0.05*P[2].
Fuel$ = 'Propane (CH4)'
T_fuel = (25 + 273.15) "[K]."
P_fuel = 101.3 [kPa].
P_air = P[2].
T_air = T[2]. "[K]."
T_prod = T[4].
P_prod = P[4].
TsurrC = T[1].
T_surr = T[1].
2*A_th=1*2+2*1
Mw_moistair=y_N2*Mw_N2+y_O2*Mw_O2+y_vap*Mw_H2O
AF = (1+Ex)*A_th*(1+(y_N2/y_O2)+(y_vap/y_O2))*Mw_moistair/(1*Mw_CH4)
m_dot_air = m_dot_fuel * AF
HR = 1*(enthalpy(*CH4*, *T*=T_fuel))+
(1+Ex)*A_th*enthalpy(*O2*,*T*=T_air)+(1+Ex)*A_th*(y_N2/y_O2)*enthalpy(*N2*,*T*=T_air)+(1+E
x)*A_th*(y_vap/y_O2)*enthalpy(*H2O*,*T*=T_air)
HR= HP
HP=1*enthalpy(*CO2*,*T*=T_prod)+ (2+
(1+EX)*A_th*(y_vap/y_O2))*enthalpy(*H2O*,*T*=T_prod)+(1+Ex)*A_th*(y_N2/y_O2)*enthalpy(
N2,*T*=T_prod)+Ex*A_th*enthalpy(*O2*,T=T_prod)
DELTAE_cv = 0
n_react=1+(y_N2/y_O2)+(y_vap/y_O2)
P_O2_reac= 1/n_react*P_air
s_O2_reac=entropy(*O2*,*T*=T_air,*P*=P_O2_reac)
P_N2_reac= (y_N2/y_O2)/n_react*P_air
s_N2_reac=entropy(*N2*,*T*=T_air,*P*=P_N2_reac)
P_H2O_reac= (y_vap/y_O2)/n_react*P_air
s_H2O_reac=entropy(*H2O*,*T*=T_air,*P*=P_H2O_reac)

s_CH4_reac=**entropy**(***CH4***, ***T***=T_fuel,***P***=P_fuel)
SR = 1*s_CH4_reac + (1+Ex)*A_th*s_O2_reac + (1+Ex)*A_th* (y_N2/y_O2)*s_N2_reac+(1+Ex)*A_th* (y_vap/y_O2)*s_H2O_reac
N_prod = 1 + (2+ (1+EX)*A_th*(y_vap/y_O2)) + (1+Ex)*A_th*(y_N2/y_O2) + Ex*A_th
P_O2_prod = Ex*A_th/N_prod*P_prod
s_O2_prod=**entropy**(***O2***,***T***=T_prod,***P***=P_O2_prod)
P_N2_prod = (1+Ex)*A_th*(y_N2/y_O2) /N_prod*P_prod
s_N2_prod=**entropy**(***N2***,***T***=T_prod,***P***=P_N2_prod)
P_CO2_prod = 1/N_prod*P_prod
s_CO2_prod=**entropy**(***CO2***, ***T***=T_prod,***P***=P_CO2_prod)
P_H2O_prod =(2+ (1+EX)*A_th*(y_vap/y_O2))/N_prod*P_prod
s_H2O_prod=**entropy**(***H2O***, ***T***=T_prod,***P***=P_H2O_prod)
SP = 1*s_CO2_prod + (2+ (1+EX)*A_th*(y_vap/y_O2))*s_H2O_prod + (1+Ex)*A_th*(y_N2/y_O2)*s_N2_prod + Ex*A_th*s_O2_prod
S_dot_gen = (SP - SR)/(Mw_CH4)*m_dot_fuel
X_dot_dest = T_surr*S_dot_gen
y_N2_P= (1+Ex)*A_th*(y_N2/y_O2)/N_prod
y_O2_P=Ex*(A_th)/N_prod
y_H2O_P=(2+ (1+EX)*A_th*(y_vap/y_O2))/N_prod
y_CO2_P=1/N_prod
MW_P=y_O2_P*MW_O2+y_N2_P*MW_N2+ y_CO2_P*MW_CO2+y_H2O_P*MW_H2O
h[4].=(y_CO2_P***enthalpy**(***CO2***,***T***=T_prod)+y_H2O_P***enthalpy**(***H2O***,***T***=T_prod)+y_N2_P***enthalpy**(***N2***,***T***=T_prod)+y_O2_P***enthalpy**(***O2***,T=T_prod))/MW_P
Cp_4= (y_CO2_P***cp**(***CO2***,***T***=T[4].) +y_H2O_P***cp**(***H2O***,***T***=T[4].) +y_N2_P***cp**(***N2***,***T***=T[4].) +y_O2_P***cp**(***O2***, ***T***=T[4].))/MW_P
S[4]. = (y_CO2_P*s_CO2_prod + y_H2O_P*s_H2O_prod +y_N2_P*s_N2_prod + y_O2_P*s_O2_prod)/MW_P
y_P_dry=y_O2_P+y_N2_P+ y_CO2_P+y_H2O_v
P_v=3.1698 [KPa].
P_v=y_H2O_v/((y_O2_P+y_N2_P+ y_CO2_P)+y_H2O_v)*P[1].
y_H2O_L=y_H2O_P-y_H2O_v
y_N2_dry= y_N2_P/y_P_dry
y_O2_dry=y_O2_P/y_P_dry
y_H2O_dry=y_H2O_v/y_P_dry
y_CO2_dry=y_CO2_P/y_P_dry
h_4O=(y_CO2_P***enthalpy**(***CO2***,***T***=T[1].)+y_H2O_v***enthalpy**(***H2O***,***T***=T[1].)+y_N2_P***enthalpy**(***N2***,***T***=T[1].)+y_O2_P***enthalpy**(***O2***,T=T[1].)+y_H2O_L*(-285830))/MW_P
P_surr= P[1].
P_O2_surr = Ex*A_th/N_prod*P_surr
P_N2_surr = (1+Ex)*A_th*(y_N2/y_O2)/N_prod*P_surr
P_CO2_surr = 1/N_prod*P_surr
P_H2O_surr = (2+ (1+EX)*A_th*(y_vap/y_O2))/N_prod*P_surr
s_N2_ex=**entropy**(***N2***,***T***=T_surr,***P***=P_N2_surr)
s_CO2_ex=**entropy**(***CO2***, ***T***=T_surr,***P***=P_CO2_surr)
s_H2O_ex=**entropy**(***H2O***, ***T***=T_surr,***P***=P_H2O_surr)
s_O2_ex=**entropy**(***O2***,***T***=T_surr,***P***=P_O2_surr)
S_4O= (y_CO2_P*s_CO2_ex + y_H2O_v*s_H2O_ex +y_N2_P*s_N2_ex + y_O2_P*s_O2_ex+y_H2O_L*69.95)/ MW_P
Psi[4].=h[4].-h_4O-T[1].*(s[4].-s_4O)
e_ch_g=((y_CO2_dry*ch_CO2 + y_H2O_dry*ch_H2O +y_N2_dry*ch_N2+ y_O2_dry*ch_O2)+8.324*T[1].*(y_CO2_dry***ln**(y_CO2_dry)+ y_H2O_dry***ln**(y_H2O_dry) +y_N2_dry*ln(y_N2_dry) + y_O2_dry***ln**(y_O2_dry)))
e_ch=(e_ch_g+y_H2O_L*ch_H2O_L)/MW_P
EX[4].=(m_dot_air+m_dot_fuel)*(Psi[4].+e_ch)/1000
m_dot[4].=(m_dot_air+m_dot_fuel)
//// State 5/////
P[6].=P[5].-0.03*P[5].
R_P=y_O2_P*R_O2+y_N2_P*R_N2+ y_CO2_P*R_CO2+y_H2O_P*R_H2O
T_5s=T[4].*(P[5]./P[4].)^((K4-1)/K4)

K4=Cp_4/(Cp_4-R_P)
T[5].= T[4].-(T[4].-T_5s)*eta_t
h[5].=(y_CO2_P*enthalpy(*CO2*,*T*=T[5].)+y_H2O_P*enthalpy(*H2O*,*T*=T[5].)+y_N2_P*enthalpy(*N2*,*T*=T[5].)+y_O2_P*enthalpy(*O2*,T=T[5].))/MW_P
Cp_5= (y_CO2_P*cp(*CO2*,*T*=T[5].) +y_H2O_P*cp(*H2O*,*T*=T[5].) +y_N2_P*cp(*N2*,*T*=T[5].) + y_O2_P*cp(*O2*, *T*=T[5].))/MW_P
P_O2_5 = Ex*A_th/N_prod*P[5].
s_O2_5=entropy(*O2*,*T*=T[5].*P*=P_O2_5)
P_N2_5= (1+Ex)*A_th*3.76/N_prod*P[5].
s_N2_5=entropy(*N2*,*T*=T[5]. ,*P*=P_N2_5)
P_CO2_5= 1/N_prod*P[5].
s_CO2_5=entropy(*CO2*,*T*=T[5]. ,*P*=P_CO2_5)
P_H2O_5 = 2/N_prod*P[5].
s_H2O_5=entropy(*H2O*,*T*=T[5]. ,*P*=P_H2O_5)
S[5]. = (y_CO2_P*s_CO2_5+ y_H2O_P*s_H2O_5 +y_N2_P*s_N2_5+ y_O2_P*s_O2_5)/MW_P
Psi[5].=h[5].-h_4O-T[1].*(s[5].-s_4O)
EX[5].=(m_dot_air+m_dot_fuel)*(Psi[5].+e_ch)/1000
m_dot[5].=(m_dot_air+m_dot_fuel)
Cp_t=(Cp_5+Cp_4)/2
w_tt=m_dot[5].*Cp_t*(T[4].-T[5].)/1000
////State 6 //////
P[6].=P[7].-0.03*P[6].
h[6].=(y_CO2_P*enthalpy(*CO2*,*T*=T[6].)+y_H2O_P*enthalpy(*H2O*,*T*=T[6].)+y_N2_P*enthalpy(*N2*,*T*=T[6].)+y_O2_P*enthalpy(*O2*,T=T[6].))/MW_P
Cp_6= (y_CO2_P*cp(*CO2*,*T*=T[6].) +y_H2O_P*cp(*H2O*,*T*=T[6].) +y_N2_P*cp(*N2*,*T*=T[6].) + y_O2_P*cp(*O2*, *T*=T[6].))/MW_P
P_O2_6 = Ex*A_th/N_prod*P[6].
s_O2_6=entropy(*O2*,*T*=T[6].*P*=P_O2_6)
P_N2_6= (1+Ex)*A_th*3.77/N_prod*P[6].
s_N2_6=entropy(*N2*,*T*=T[6]. ,*P*=P_N2_6)
P_CO2_6= 1/N_prod*P[6].
s_CO2_6=entropy(*CO2*,*T*=T[6]. ,*P*=P_CO2_6)
P_H2O_6 = 2/N_prod*P[6].
s_H2O_6=entropy(*H2O*,*T*=T[6]. ,*P*=P_H2O_6)
S[6]. = (y_CO2_P*s_CO2_6+ y_H2O_P*s_H2O_6 +y_N2_P*s_N2_6+y_O2_P*s_O2_6)/MW_P
Psi[6].=h[6].-h_4O-T[1].*(s[6].-s_4O)
EX[6].=(m_dot_air+m_dot_fuel)*(Psi[6].+e_ch)/1000
m_dot[6].=(m_dot_air+m_dot_fuel)
Cp_56=(Cp_5+Cp_6)/2
////State 7 //////
P[7].=P[8].-0.03*P[7].
h[7].=(y_CO2_P*enthalpy(*CO2*,*T*=T[7].)+y_H2O_P*enthalpy(*H2O*,*T*=T[7].)+y_N2_P*enthalpy(*N2*,*T*=T[7].)+y_O2_P*enthalpy(*O2*,T=T[7].))/MW_P
Cp_7= (y_CO2_P*cp(*CO2*,*T*=T[7].) +y_H2O_P*cp(*H2O*,*T*=T[7].) +y_N2_P*cp(*N2*,*T*=T[7].) + y_O2_P*cp(*O2*, *T*=T[7].))/MW_P
P_O2_7 = Ex*A_th/N_prod*P[7].
s_O2_7=entropy(*O2*,*T*=T[7].*P*=P_O2_7)
P_N2_7= (1+Ex)*A_th*3.77/N_prod*P[7].
s_N2_7=entropy(*N2*,*T*=T[7]. ,*P*=P_N2_7)
P_CO2_7= 1/N_prod*P[7].
s_CO2_7=entropy(*CO2*,*T*=T[7]. ,*P*=P_CO2_7)
P_H2O_7 = 2/N_prod*P[7].
s_H2O_7=entropy(*H2O*,*T*=T[7]. ,*P*=P_H2O_7)
S[7]. = (y_CO2_P*s_CO2_7+ y_H2O_P*s_H2O_7 +y_N2_P*s_N2_7+y_O2_P*s_O2_7)/MW_P
Psi[7].=h[7].-h_4O-T[1].*(s[7].-s_4O)
EX[7].=(m_dot_air+m_dot_fuel)*(Psi[7].+e_ch)/1000

m_dot[7].=(m_dot_air+m_dot_fuel)
Cp_67=(Cp_6+Cp_7)/2
////State 8 //////
P[8].=P[1].
h[8].=(y_CO2_P*enthalpy(*CO2*,*T*=T[8].)+y_H2O_P*enthalpy(*H2O*,*T*=T[8].)+y_N2_P*enthalpy(*N2*,*T*=T[8].)+y_O2_P*enthalpy(*O2*,T=T[8].))/MW_P
Cp_8= (y_CO2_P*cp(*CO2*,*T*=T[8].) +y_H2O_P*cp(*H2O*,*T*=T[8].) +y_N2_P*cp(*N2*,*T*=T[8].) + y_O2_P*cp(*O2*, *T*=T[8].))/MW_P
P_O2_8 = Ex*A_th/N_prod*P[8].
s_O2_8=entropy(*O2*,*T*=T[8].*P*=P_O2_8)
P_N2_8= (1+Ex)*A_th*3.77/N_prod*P[8].
s_N2_8=entropy(*N2*,*T*=T[8]. ,*P*=P_N2_8)
P_CO2_8= 1/N_prod*P[8].
s_CO2_8=entropy(*CO2*,*T*=T[8]. ,*P*=P_CO2_8)
P_H2O_8 = 2/N_prod*P[8].
s_H2O_8=entropy(*H2O*,*T*=T[8]. ,*P*=P_H2O_8)
S[8]. = (y_CO2_P*s_CO2_8+ y_H2O_P*s_H2O_8 +y_N2_P*s_N2_8+y_O2_P*s_O2_7)/MW_P
Psi[8].=h[8].-h_4O-T[1].*(s[8].-s_4O)
EX[8].=(m_dot_air+m_dot_fuel)*(Psi[8].+e_ch)/1000
m_dot[8].=(m_dot_air+m_dot_fuel)
Cp_78=(Cp_7+Cp_8)/2
//////////////////////////
/////Organic Rankine Cycle Model////
Q_dot_EVAP1=m_dot[5].*(h[5].-h[6].)
Q_dot_EVAP1*0.85=m_dot[11].*(h[11].-h[10].)
Q_dot_EVAP2=m_dot[6].*(h[6].-h[7].)
Q_dot_EVAP2*0.85=m_dot[19].*(h[19].-h[18].)
Q_dot_EVAP3=m_dot[7].*(h[7].-h[8].)
Q_dot_EVAP3*0.85=m_dot[27].*(h[27].-h[26].)
Fluid$ = 'R123 '
MW=molarmass(Fluid$)

"state oo"
x_oo=0
T_oo=298 [K].
s_oo=entropy(Fluid$,*T*=T_oo,*x*=0)/ MW
h_oo=enthalpy(Fluid$,*T*=T_oo,*x*=0)/ MW
Psi_oo=0
////State 11/////
DEIT_T_2=12
T[11].=T[5].-DEIT_T_2
P[11].= 800 [kPa].
eta_OT=0.90
h_bar_11=enthalpy(Fluid$,*T*=T[11].*P*=P[11].)
s_bar_11=entropy(Fluid$,*T*=T[11].*P*=P[11].)
h[11].=h_bar_11/MW
s[11].=s_bar_11/MW
x[11].=quality(Fluid$,*P*=P[11].*T*=T[11].)
Psi[11].=h[11].-h_oo-298*(s[11].-s_oo)
EX[11].=m_dot[11].*(Psi[11].)/1000
////state 12/////
P[12].=1.2 *101.325 [kPa].
s12s=s_bar_11
h12s=enthalpy(Fluid$,*P*=P[12].*s*=s12s)
eta_st=(h_bar_11-h_bar_12)/(h_bar_11-h12s)
T[12].=temperature(Fluid$,*P*=P[12].*h*=h_bar_12)
x[12].=quality(Fluid$,*P*=P[12].*h*=h_bar_12)

s_bar_12=**entropy**(Fluid$,***P***=P[12].***T***=T[12].)
h[12].=h_bar_12/MW
s[12].=s_bar_12/MW
m_dot[12].=m_dot[11].
Psi[12].=h[12].-h_oo-298*(s[12].-s_oo)
EX[12].=m_dot[12].*(Psi[12].)/1000
"State 13"
P[13].= P[12].
x[13].=1
h_bar_13=**enthalpy**(Fluid$,***P***=P[13].***x***=x[13].)
S_bar_13=**entropy**(Fluid$,***P***=P[13].***x***=x[13].)
T[13].=**temperature**(Fluid$,***P***=P[13].***x***=x[13].)
h[13].=h_bar_13/MW
s[13].=s_bar_13/MW
m_dot[13].=m_dot[11].
Psi[13].=h[13].-h_oo-298*(s[13].-s_oo)
EX[13].=m_dot[13].*(Psi[13].)/1000
/////State 14/////
T[14].=**t_sat**(Fluid$,***P***=P[14].)
P[14].=P[13].
x[14].=0
h_bar_14=**enthalpy**(Fluid$,***T***=T[14].***x***=0)
s_bar_14=**entropy**(Fluid$,***T***=T[14].***x***=0)
h[14].=h_bar_14/MW
s[14].=s_bar_14/MW
Psi[14].=h[14].-h_oo-298*(s[14].-s_oo)
m_dot[14].=m_dot[11].
EX[14].=m_dot[14].*(Psi[14].)/1000
Q_dot_ORC1=m_dot[14].*(h[13].-h[14].)
s9s=s_bar_14
P[9].=P[11].
h9s=**enthalpy**(Fluid$,***P***=P[9].***s***=s9s)
eta_pump1=eta_pump
eta_pump1=(h9s-h_bar_14)/(h_bar_9-h_bar_14)
s_bar_9=**entropy**(Fluid$,***P***=P[9].***h***=h_bar_9)
x[9].=**quality**(Fluid$,***P***=P[9].***h***=h_bar_9)
T[9].=**temperature**(Fluid$,***P***=P[9].***h***=h_bar_9)
h[9].=h_bar_9/MW
s[9].=s_bar_9/MW
m_dot[9].=m_dot[11].
Psi[9].=h[9].-h_oo-298*(s[9].-s_oo)
EX[9].=m_dot[9].*(Psi[9].)/1000
" State 10"
P[10].=P[9].
T[10].=**temperature**(Fluid$,***P***=P[10].***h***=h_bar_10)
s_bar_10=**entropy**(Fluid$,***P***=P[10].***h***=h_bar_10)
h[10].=h_bar_10/MW
s[10].=s_bar_10/MW
(h[10].-h[9].) = epsilion*((h[12].-h[13].))
epsilion=0.6
Q_dot_HE1=(h[10].-h[9].)
m_dot[10].=m_dot[11].
Psi[10].=h[10].-h_oo-298*(s[10].-s_oo)
EX[10].=m_dot[10].*(Psi[10].)/1000
" State 15 and 16"
T[15].=T[1].
T[16].=T[15].+5
h[15].=**enthalpy**(***Water***,***T***=T[15]. ***x***=0)
h[16].=**enthalpy**(***Water***,***T***=T[16]. ***x***=0)

s[15].=**entropy**(***Water***,***T***=T[15]. ***x***=0)
s[16].=**entropy**(***Water***,***T***=T[16]. ***x***=0)
Q_dot_ORC1*0.5= m_dot[15].*(h[16].-h[15].)
psi[15].=h[15].-**enthalpy**(***Water***,***T***=T[1].***x***=0)-T[1].*(s[15].-**entropy**(***Water***,***T***=T[1].***x***=0))
EX[15].=m_dot[15].*psi[15]./1000
psi[16].=h[16].-**enthalpy**(***Water***,***T***=T[1].***x***=0)-T[1].*(s[16].-**entropy**(***Water***,***T***=T[1].***x***=0))
EX[16].=m_dot[16].*psi[16]./1000
m_dot[15].=m_dot[16].
////State 19/////
T[19].=T[6].-DEIT_T_2
P[19].= 800 [kPa].
h_bar_19=**enthalpy**(Fluid$,***T***=T[19].***P***=P[19].)
s_bar_19=**entropy**(Fluid$,***T***=T[19].***P***=P[19].)
h[19].=h_bar_19/MW
s[19].=s_bar_19/MW
x[19].=**quality**(Fluid$,***P***=P[19].***T***=T[19].)
Psi[19].=h[19].-h_oo-298*(s[19].-s_oo)
EX[19].=m_dot[19].*(Psi[19].)/1000
////state 20/////
P[20].=1.2 *101.325 [kPa].
s20s=s_bar_19
h20s=**enthalpy**(Fluid$,***P***=P[20].***s***=s20s)
eta_st=(h_bar_19-h_bar_20)/(h_bar_19-h20s)
T[20].=**temperature**(Fluid$,***P***=P[20].***h***=h_bar_20)
x[20].=**quality**(Fluid$,***P***=P[20].***h***=h_bar_20)
s_bar_20=**entropy**(Fluid$,***P***=P[20].***T***=T[20].)
h[20].=h_bar_20/MW
s[20].=s_bar_20/MW
m_dot[20].=m_dot[19].
Psi[20].=h[20].-h_oo-298*(s[20].-s_oo)
EX[20].=m_dot[20].*(Psi[20].)/1000
"State 21"
P[21].= P[20].
x[21].=1
h_bar_21=**enthalpy**(Fluid$,***P***=P[21].***x***=x[21].)
S_bar_21=**entropy**(Fluid$,***P***=P[21].***x***=x[21].)
T[21].=**temperature**(Fluid$,***P***=P[21].***x***=x[21].)
h[21].=h_bar_21/MW
s[21].=s_bar_21/MW
m_dot[21].=m_dot[19].
Psi[21].=h[21].-h_oo-298*(s[21].-s_oo)
EX[21].=m_dot[21].*(Psi[21].)/1000
/////State 22/////
T[22].=**t_sat**(Fluid$,***P***=P[22].)
P[22].=P[21].
x[22].=0
h_bar_22=**enthalpy**(Fluid$,***T***=T[22].***x***=0)
s_bar_22=**entropy**(Fluid$,***T***=T[22].***x***=0)
h[22].=h_bar_22/MW
s[22].=s_bar_22/MW
Psi[22].=h[22].-h_oo-298*(s[22].-s_oo)
m_dot[22].=m_dot[19].
EX[22].=m_dot[22].*(Psi[22].)/1000
Q_dot_ORC2=m_dot[22].*(h[21].-h[22].)
s17s=s_bar_22
P[17].=P[19].
h17s=**enthalpy**(Fluid$,***P***=P[17].***s***=s17s)
eta_pump2=eta_pump
eta_pump2=(h17s-h_bar_22)/(h_bar_17-h_bar_22)

s_bar_17=**entropy**(Fluid$,***P***=P[17].***h***=h_bar_17)
x[17].=**quality**(Fluid$,***P***=P[17].***h***=h_bar_17)
T[17].=**temperature**(Fluid$,***P***=P[17].***h***=h_bar_17)
h[17].=h_bar_17/MW
s[17].=s_bar_17/MW
m_dot[17].=m_dot[19].
Psi[17].=h[17].-h_oo-298*(s[17].-s_oo)
EX[17].=m_dot[17].*(Psi[17].)/1000
" State 18"
P[18].=P[17].
T[18].=**temperature**(Fluid$,***P***=P[18].***h***=h_bar_18)
s_bar_18=**entropy**(Fluid$,***P***=P[18].***h***=h_bar_18)
h[18].=h_bar_18/MW
s[18].=s_bar_18/MW
(h[18].-h[17].) = epsilion*((h[20].-h[21].))
Q_dot_HE2=(h[18].-h[17].)
m_dot[18].=m_dot[19].
Psi[18].=h[18].-h_oo-298*(s[18].-s_oo)
EX[18].=m_dot[18].*(Psi[18].)/1000
" State 23 and 24"
T[23].=T[1].
T[24].=T[23].+5
h[23].=**enthalpy**(***Water***,***T***=T[23]. ***x***=0)
h[24].=**enthalpy**(***Water***,***T***=T[24]. ***x***=0)
s[23].=**entropy**(***Water***,***T***=T[23]. ***x***=0)
s[24].=**entropy**(***Water***,***T***=T[24]. ***x***=0)
Q_dot_ORC2*0.5= m_dot[23].*(h[24].-h[23].)
psi[23].=h[23].-**enthalpy**(***Water***,***T***=T[1].***x***=0)-T[1].*(s[23].-**entropy**(***Water***,***T***=T[1].***x***=0))
EX[23].=m_dot[23].*psi[23]./1000
psi[24].=h[24].-**enthalpy**(***Water***,***T***=T[1].***x***=0)-T[1].*(s[24].-**entropy**(***Water***,***T***=T[1].***x***=0))
EX[24].=m_dot[24].*psi[24]./1000
m_dot[23].=m_dot[24].
//////////////////////////

////State 27/////
T[27].=T[7].-DEIT_T_2
P[27].= 800 [kPa].
h_bar_27=**enthalpy**(Fluid$,***T***=T[27].***P***=P[27].)
s_bar_27=**entropy**(Fluid$,***T***=T[27].***P***=P[27].)
h[27].=h_bar_27/MW
s[27].=s_bar_27/MW
x[27].=**quality**(Fluid$,***P***=P[27].***T***=T[27].)
Psi[27].=h[27].-h_oo-298*(s[27].-s_oo)
EX[27].=m_dot[27].*(Psi[27].)/1000
////state 28/////
P[28].=1.2 *101.325 [kPa].
s28s=s_bar_27
h28s=**enthalpy**(Fluid$,***P***=P[28].***s***=s28s)
eta_st=(h_bar_27-h_bar_28)/(h_bar_27-h28s)
T[28].=**temperature**(Fluid$,***P***=P[28].***h***=h_bar_28)
x[28].=**quality**(Fluid$,***P***=P[28].***h***=h_bar_28)
s_bar_28=**entropy**(Fluid$,***P***=P[28].***T***=T[28].)
h[28].=h_bar_28/MW
s[28].=s_bar_28/MW
m_dot[28].=m_dot[27].
Psi[28].=h[28].-h_oo-298*(s[28].-s_oo)
EX[28].=m_dot[28].*(Psi[28].)/1000
"State 29"
P[29].= P[28].

x[29].=1
h_bar_29=**enthalpy**(Fluid$,***P***=P[29].***x***=x[29].)
S_bar_29=**entropy**(Fluid$,***P***=P[29].***x***=x[29].)
T[29].=**temperature**(Fluid$,***P***=P[29].***x***=x[29].)
h[29].=h_bar_29/MW
s[29].=s_bar_29/MW
m_dot[29].=m_dot[27].
Psi[29].=h[29].-h_oo-298*(s[29].-s_oo)
EX[29].=m_dot[29].*(Psi[29].)/1000
/////State 30/////
T[30].=**t_sat**(Fluid$,***P***=P[30].)
P[30].=P[29].
x[30].=0
h_bar_30=**enthalpy**(Fluid$,***T***=T[30].***x***=0)
s_bar_30=**entropy**(Fluid$,***T***=T[30].***x***=0)
h[30].=h_bar_30/MW
s[30].=s_bar_30/MW
Psi[30].=h[30].-h_oo-298*(s[30].-s_oo)
m_dot[30].=m_dot[27].
EX[30].=m_dot[30].*(Psi[30].)/1000
Q_dot_ORC3=m_dot[30].*(h[29].-h[30].)
s25s=s_bar_30
P[25].=P[27].
h25s=**enthalpy**(Fluid$,***P***=P[25].***s***=s25s)
eta_pump3=eta_pump
eta_pump3=(h25s-h_bar_30)/(h_bar_25-h_bar_30)
s_bar_25=**entropy**(Fluid$,***P***=P[25].***h***=h_bar_25)
x[25].=**quality**(Fluid$,***P***=P[25].***h***=h_bar_25)
T[25].=**temperature**(Fluid$,***P***=P[25].***h***=h_bar_25)
h[25].=h_bar_25/MW
s[25].=s_bar_25/MW
m_dot[25].=m_dot[27].
Psi[25].=h[25].-h_oo-298*(s[25].-s_oo)
EX[25].=m_dot[25].*(Psi[25].)/1000
" State 26"
P[26].=P[25].
T[26].=**temperature**(Fluid$,***P***=P[26].***h***=h_bar_26)
s_bar_26=**entropy**(Fluid$,***P***=P[26].***h***=h_bar_26)
h[26].=h_bar_26/MW
s[26].=s_bar_26/MW
(h[26].-h[25].) = epsilion*((h[28].-h[29].))
Q_dot_HE3=(h[26].-h[25].)
m_dot[26].=m_dot[27].
Psi[26].=h[26].-h_oo-298*(s[26].-s_oo)
EX[26].=m_dot[26].*(Psi[26].)/1000
" State 31 and 32"
T[31].=T[1].
T[32].=T[31].+5
h[31].=**enthalpy**(***Water***,***T***=T[31]. ***x***=0)
h[32].=**enthalpy**(***Water***,***T***=T[32]. ***x***=0)
s[31].=**entropy**(***Water***,***T***=T[31]. ***x***=0)
s[32].=**entropy**(***Water***,***T***=T[32]. ***x***=0)
Q_dot_ORC3*0.5= m_dot[31].*(h[32].-h[31].)
psi[31].=h[31].-**enthalpy**(***Water***,***T***=T[1].***x***=0)-T[1].*(s[31].-**entropy**(***Water***,***T***=T[1].***x***=0))
EX[31].=m_dot[31].*psi[31]./1000
psi[32].=h[32].-**enthalpy**(***Water***,***T***=T[1].***x***=0)-T[1].*(s[32].-**entropy**(***Water***,***T***=T[1].***x***=0))
EX[32].=m_dot[32].*psi[32]./1000
m_dot[31].=m_dot[32].
///////Energy Analysis////////

////Brayton Cycle Performance////
W_dot_AC=m_dot_air*(h[2].-h[1].)
W_dot_GT=(m_dot_air+m_dot_fuel)*(h[4].-h[5].)
W_GT_net=W_dot_GT-W_dot_AC
W_dot_BC=W_GT_net/1000
Eta_BC=W_GT_net/(m_dot_fuel*LHV)*100
////Organic Rankine Cycle 1Performance////
W_ORT1=m_dot[12].*(h[11].-h[12].)
W_ORP1=m_dot[13].*(h[9].-h[14].)
W_ORC_net1=W_ORT1-W_ORP1
W_dot_ORC1=W_ORC_net1/1000
////Organic Rankine Cycle 2 Performance////
W_ORT2=m_dot[20].*(h[19].-h[20].)
W_ORP2=m_dot[21].*(h[17].-h[22].)
W_ORC_net2=W_ORT2-W_ORP2
W_dot_ORC2=W_ORC_net2/1000
////Organic Rankine Cycle 3 Performance////
W_ORT3=m_dot[28].*(h[27].-h[28].)
W_ORP3=m_dot[29].*(h[25].-h[30].)
W_ORC_net3=W_ORT(3.W_ORP3
W_dot_ORC3=W_ORC_net3/1000
///////System performance/////
W_dot_net=W_dot_BC+W_dot_ORC1+W_dot_ORC2+W_dot_ORC3
ETA_overall=(W_dot_net)/(m_dot_fuel*LHV/1000)*100
W_dot_net=W_net
Psi_in_fuel=m_dot_fuel*ch_CH4/MW_CH4/1000
Psi_overall=(W_net)/(Psi_in_fuel)*100
Psi_Bc=W_dot_BC/(Psi_in_fuel)*100
Psi_exergy2= (1-(Ed_total+EX[8].+EX[24].+EX[16].+EX[32].)/Psi_in_fuel)*100
///////Exergy Analysis////////
"compressor"
E_dot_F_AC=W_dot_AC/1000
E_dot_P_AC=(EX[2].-EX[1].)
Ed_AC=E_dot_F_AC-E_dot_P_AC
Epsilion_AC=E_dot_P_AC/E_dot_F_AC*100
"Combustion chamber"
E_dot_F_CC=(EX[2].+EX[3].)
E_dot_P_CC=EX[4].
Ed_CC=E_dot_F_CC-E_dot_P_CC
Epsilion_CC=E_dot_P_CC/E_dot_F_CC*100
"Gas turbine"
E_dot_F_GT= (EX[4].-EX[5].)
E_dot_P_GT=W_dot_GT/1000
Ed_GT=E_dot_F_GT-E_dot_P_GT
Epsilion_GT=E_dot_P_GT/E_dot_F_GT*100
/////ORC1////
"Evaporator"
E_dot_F_Evap1=(EX[5].-EX[6].)
E_dot_P_Evap1=(EX[11].-EX[10].)
Epsilion_Evap1=E_dot_P_Evap1/E_dot_F_Evap1*100
Ed_Evap1=E_dot_F_Evap1-E_dot_P_Evap1
"Recuperator"
E_dot_F_Recup1=(EX[12].-EX[13].)
E_dot_P_Recup1=(EX[10].-EX[9].)
Epsilion_Recup1=E_dot_P_Recup1/E_dot_F_Recup1*100
Ed_Recup1=E_dot_F_Recup1-E_dot_P_Recup1
"Pump1"
E_dot_P_P1=EX[9].-EX[14].
E_dot_F_P1=W_ORP1/1000

```
 Ed_P1=E_dot_F_P1-E_dot_P_P1
  Epsilion_P1=E_dot_P_P1/E_dot_F_P1*100
 "ORC turbine"
E_dot_F_ORCT1=EX[11].-EX[12].
E_dot_P_ORCT1=W_ORT1/1000
Ed_ORT1=E_dot_F_ORCT1-E_dot_P_ORCT1
Epsilion_ORT1=E_dot_P_ORCT1/E_dot_F_ORCT1*100
"Condenser1"
E_dot_F_cond1=(EX[13].-EX[14].)
E_dot_P_cond1=(EX[16].-EX[15].)
Epsilion_cond1=E_dot_P_cond1/E_dot_F_cond1*100
Ed_cond1=E_dot_F_cond1-E_dot_P_cond1
/////ORC2////
"Evaporator"
E_dot_F_Evap2=(EX[6].-EX[7].)
E_dot_P_Evap2=(EX[19].-EX[18].)
Epsilion_Evap2=E_dot_P_Evap2/E_dot_F_Evap2*100
Ed_Evap2=E_dot_F_Evap2-E_dot_P_Evap2
"Recuperator"
E_dot_F_Recup2=(EX[20].-EX[21].)
E_dot_P_Recup2=(EX[18].-EX[17].)
Epsilion_Recup2=E_dot_P_Recup2/E_dot_F_Recup2*100
Ed_Recup2=E_dot_F_Recup2-E_dot_P_Recup2
"Pump2"
E_dot_P_P2=EX[17].-EX[22].
E_dot_F_P2=W_ORP2/1000
 Ed_P2=E_dot_F_P2-E_dot_P_P2
  Epsilion_P2=E_dot_P_P2/E_dot_F_P2*100
 "ORC turbine"
E_dot_F_ORCT2=EX[19].-EX[20].
E_dot_P_ORCT2=W_ORT2/1000
Ed_ORT2=E_dot_F_ORCT2-E_dot_P_ORCT2
Epsilion_ORT2=E_dot_P_ORCT2/E_dot_F_ORCT2*100
"Condenser2"
E_dot_F_cond2=(EX[21].-EX[22].)
E_dot_P_cond2=(EX[24].-EX[23].)
Epsilion_cond2=E_dot_P_cond2/E_dot_F_cond2*100
Ed_cond2=E_dot_F_cond2-E_dot_P_cond2
/////ORC3////
"Evaporator"
E_dot_F_Evap3=(EX[7].-EX[8].)
E_dot_P_Evap3=(EX[27].-EX[26].)
Epsilion_Evap3=E_dot_P_Evap3/E_dot_F_Evap3*100
Ed_Evap3=E_dot_F_Evap(3.E_dot_P_Evap3
"Recuperator"
E_dot_F_Recup3=(EX[28].-EX[29].)
E_dot_P_Recup3=(EX[26].-EX[25].)
Epsilion_Recup3=E_dot_P_Recup3/E_dot_F_Recup3*100
Ed_Recup3=E_dot_F_Recup(3.E_dot_P_Recup3
"Pump3"
E_dot_P_P3=EX[25].-EX[30].
E_dot_F_P3=W_ORP3/1000
 Ed_P3=E_dot_F_P(3.E_dot_P_P3
  Epsilion_P3=E_dot_P_P3/E_dot_F_P3*100
 "ORC turbine"
E_dot_F_ORCT3=EX[27].-EX[28].
E_dot_P_ORCT3=W_ORT3/1000
Ed_ORT3=E_dot_F_ORCT(3.E_dot_P_ORCT3
Epsilion_ORT3=E_dot_P_ORCT3/E_dot_F_ORCT3*100
```

```
"Condenser3"
E_dot_F_cond3=(EX[29].-EX[30].)
E_dot_P_cond3=(EX[32].-EX[31].)
Epsilion_cond3=E_dot_P_cond3/E_dot_F_cond3*100
Ed_cond3=E_dot_F_cond(3.E_dot_P_cond3
//////Exergy destruction/////
Ed_total=                                    Ed_AC+Ed_CC+Ed_GT+Ed_Evap1+Ed_Recup1+
Ed_P1+Ed_cond1+Ed_ORT1+Ed_Evap2+Ed_Recup2+
Ed_P2+Ed_cond2+Ed_ORT2+Ed_Evap3+Ed_Recup3+ Ed_P3+Ed_cond3+Ed_ORT3
Ed_AC_%=Ed_AC/Ed_total*100
Ed_CC_%=Ed_CC/Ed_total*100
Ed_GT_%=Ed_GT/Ed_total*100
Ed_Evap_1%=Ed_Evap1/Ed_total*100
Ed_Recup_1%=Ed_Recup1/Ed_total*100
Ed_P1_%=Ed_P1/Ed_total*100
Ed_cond1_%=Ed_cond1/Ed_total*100
Ed_ORT_1%=Ed_ORT1/Ed_total*100
Ed_Evap_2%=Ed_Evap2/Ed_total*100
Ed_Recup_2%=Ed_Recup2/Ed_total*100
Ed_P2_%=Ed_P2/Ed_total*100
Ed_cond2_%=Ed_cond2/Ed_total*100
Ed_ORT_2%=Ed_ORT2/Ed_total*100
Ed_Evap_3%=Ed_Evap3/Ed_total*100
Ed_Recup_3%=Ed_Recup3/Ed_total*100
Ed_P3_%=Ed_P3/Ed_total*100
Ed_cond3_%=Ed_cond3/Ed_total*100
Ed_ORT_3%=Ed_ORT3/Ed_total*100
Ed_total_%=                Ed_AC_%+Ed_CC_%+Ed_GT_%+Ed_Evap_1%+Ed_Recup_1%+
Ed_P1_%+Ed_cond1_%+Ed_ORT_1%+Ed_Evap_2%+Ed_Recup_2%+
Ed_P2_%+Ed_cond2_%+Ed_ORT_2%+Ed_Evap_3%+Ed_Recup_3%+
Ed_P3_%+Ed_cond3_%+Ed_ORT_3%
//////////Cost Analysis//////////
n_year=20
i_eff = 0.10
tau=8000*3600
phi=1.06
CRF= (i_eff *(1+ i_eff)^n_year)/(((1+ i_eff)^n_year)-1)
"Brayton Cycle"
"Capital investment cost for eac component"
////Air compressor/////
PEC_AC=(71.1*m_dot[2]./(0.92-eta_c))*(P[2]./P[1].)*ln(P[2]./P[1].)
Z_dot_c=(CRF*phi/tau)*PEC_AC*3600
////Combustion chamber////
PEC_CC=(46.08*m_dot[4]./(0.995-(P[4]./P[2].)))*(1+exp(0.018*T[4].-26.4))
Z_dot_CC=(CRF*phi/tau)*PEC_CC*3600
////Gas turbine////
PEC_GT=(479.34*m_dot[4]./(0.9(3.eta_T))*ln(P[4]./P[5].)*(1+exp(0.036*T[4].-54.4))
 Z_dot_t=(CRF*phi/tau)*PEC_GT*3600
//////////
////Organic Steam turbine1////
PEC_ORST1=(479.3*m_dot[11]./(0.9(3.eta_T))*ln(P[11]./P[12].)*(1+exp(0.036*T[11].-54.4))
 Z_dot_ORST1=(CRF*phi/tau)*PEC_ORST1*3600
////Organic Pump///
PEC_O_Pump1=2100*(W_ORP1*1000/10)^(0.26)*((1-eta_pump1)/eta_pump1)^(0.5)
 Z_dot_O_Pump1=(CRF*phi/tau)*PEC_O_Pump1*3600
////Organic Condenser////
PEC_O_cond1=1773*(m_dot[13].)
 Z_dot_O_cond1=(CRF*phi/tau)*PEC_O_cond1*3600
////Organic Evaporaterr////
```

```
PEC_O_Evap1=235*(Q_dot_EVAP1)^(0.75)
 Z_dot_O_Evap1=(CRF*phi/tau)*PEC_O_Evap1*3600
////Organic Heat exchanger////
PEC_O_HE1=235*(Q_dot_HE1)^(0.75)
 Z_dot_O_HE1=(CRF*phi/tau)*PEC_O_HE1*3600
//////////////////////
////Organic Steam turbine2////
PEC_ORST2=(479.3*m_dot[19]./(0.9(3.eta_T))*ln(P[19]./P[20].)*(1+exp(0.036*T[19].-54.4))
 Z_dot_ORST2=(CRF*phi/tau)*PEC_ORST2*3600
////Organic Pump///
PEC_O_Pump2=2100*(W_ORP2*1000/10)^(0.26)*((1-eta_pump2)/eta_pump2)^(0.5)
 Z_dot_O_Pump2=(CRF*phi/tau)*PEC_O_Pump2*3600
////Organic Condenser////
PEC_O_cond2=1773*(m_dot[21].)
 Z_dot_O_cond2=(CRF*phi/tau)*PEC_O_cond2*3600
////Organic Evaporaterr////
PEC_O_Evap2=235*(Q_dot_EVAP2)^(0.75)
 Z_dot_O_Evap2=(CRF*phi/tau)*PEC_O_Evap2*3600
////Organic Heat exchanger////
PEC_O_HE2=235*(Q_dot_HE2)^(0.75)
 Z_dot_O_HE2=(CRF*phi/tau)*PEC_O_HE2*3600
//////////////////////
////Organic Steam turbine3////
PEC_ORST3=(479.3*m_dot[27]./(0.9(3.eta_T))*ln(P[27]./P[28].)*(1+exp(0.036*T[27].-54.4))
 Z_dot_ORST3=(CRF*phi/tau)*PEC_ORST3*3600
////Organic Pump///
PEC_O_Pump3=2100*(W_ORP3*1000/10)^(0.26)*((1-eta_pump3)/eta_pump3)^(0.5)
 Z_dot_O_Pump3=(CRF*phi/tau)*PEC_O_Pump3*3600
////Organic Condenser////
PEC_O_cond3=1773*(m_dot[29].)
 Z_dot_O_cond3=(CRF*phi/tau)*PEC_O_cond3*3600
////Organic Evaporaterr////
PEC_O_Evap3=235*(Q_dot_EVAP3)^(0.75)
 Z_dot_O_Evap3=(CRF*phi/tau)*PEC_O_Evap3*3600
////Organic Heat exchanger////
PEC_O_HE3=235*(Q_dot_HE3)^(0.75)
 Z_dot_O_HE3=(CRF*phi/tau)*PEC_O_HE3*3600
//////Cost performance/////
Z_dot_total_BC=Z_dot_c+Z_dot_CC+Z_dot_t
Z_electricity_BC=Z_dot_total_BC/W_dot_BC

Z_dot_total_ORC1=  Z_dot_ORST1+  Z_dot_O_cond1+Z_dot_O_Pump1+Z_dot_O_Evap1+
Z_dot_O_HE1
Z_electricity_ORC1=Z_dot_total_ORC1/(W_dot_ORC1)
Z_dot_total_ORC2=  Z_dot_ORST2+  Z_dot_O_cond2+Z_dot_O_Pump2+Z_dot_O_Evap2+
Z_dot_O_HE2
Z_electricity_ORC2=Z_dot_total_ORC2/(W_dot_ORC2)
Z_dot_total_ORC3=  Z_dot_ORST3+  Z_dot_O_cond3+Z_dot_O_Pump3+Z_dot_O_Evap3+
Z_dot_O_HE3
Z_electricity_ORC3=Z_dot_total_ORC3/(W_dot_ORC3)

    /////Total cost/////
Z_dot_electricity_total=((Z_dot_total_BC+Z_electricity_ORC1+Z_electricity_ORC2+Z_electri
city_ORC3)/((W_dot_net)))
```

RESUME

Bashar Mohameed MAJEED, graduated from the Department of machinery and Refrigeration and air conditioning eng department, Alrafdian University 2011, and is currently a master's student at Karabuk University.